INFORMATION TO USERS

This manuscript has been reproduced from the microfilm master. UMI films the text directly from the original or copy submitted. Thus, some thesis and dissertation copies are in typewriter face, while others may be from any type of computer printer.

The quality of this reproduction is dependent upon the quality of the copy submitted. Broken or indistinct print, colored or poor quality illustrations and photographs, print bleedthrough, substandard margins, and improper alignment can adversely affect reproduction.

In the unlikely event that the author did not send UMI a complete manuscript and there are missing pages, these will be noted. Also, if unauthorized copyright material had to be removed, a note will indicate the deletion.

Oversize materials (e.g., maps, drawings, charts) are reproduced by sectioning the original, beginning at the upper left-hand corner and continuing from left to right in equal sections with small overlaps.

Photographs included in the original manuscript have been reproduced xerographically in this copy. Higher quality 6" x 9" black and white photographic prints are available for any photographs or illustrations appearing in this copy for an additional charge. Contact UMI directly to order.

ProQuest Information and Learning
300 North Zeeb Road, Ann Arbor, MI 48106-1346 USA
800-521-0600

UMI®

DISSERTATION

MECHANICS OF LAYERED CYLINDRICAL ELASTIC WAVEGUIDES

Submitted by

Richard R. Laverty

Department of Mechanical Engineering

In partial fulfillment of the requirements

for the degree of Doctor of Philosophy

Colorado State University

Fort Collins, Colorado

Summer 2001

ProQuest Information and Learning Company
300 North Zeeb Road
P.O. Box 1346
Ann Arbor, MI 48106-1346

Colorado State University

January 12, 2001

WE HEREBY RECOMMEND THAT THE DISSERTATION PREPARED UNDER OURT SUPERVISION BY RICHARD LAVERTY, ENTITLED "MECHANICS OF LAYERED CYLINDRICAL ELASTIC WAVEGUIDES," BE ACCEPTED AS FULFILLING IN PART REQUIREMENTS FOR THE DEGREE OF DOCTOR OF PHILOSOPHY.

Committee on Graduate work

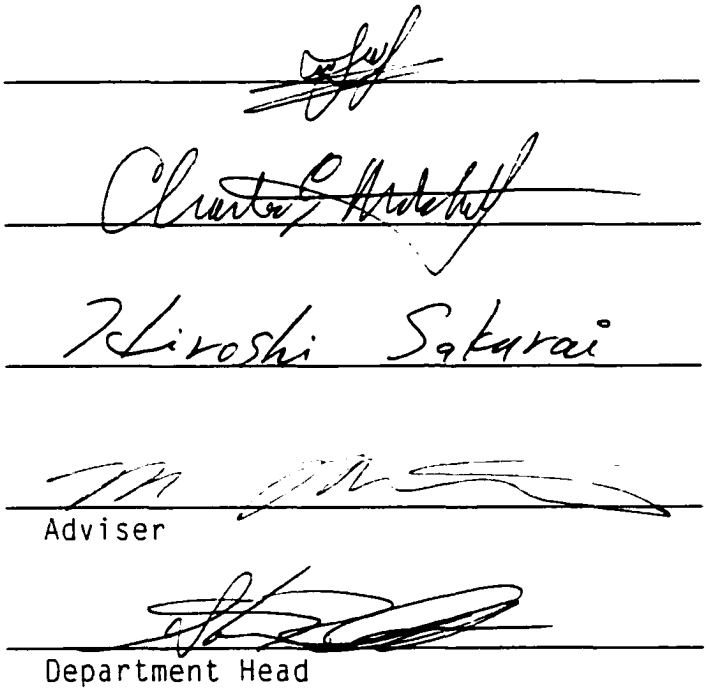

Adviser

Department Head

ABSTRACT OF DISSERTATION

MECHANICS OF LAYERED CYLINDRICAL ELASTIC WAVEGUIDES

This study provides an implementable method for constructing the dynamic response of a semi-infinite elastic cylinder. The cylinder is assumed to be composed of any number of homogeneous, transversely isotropic, coaxial layers. The source of the excitation is an axisymmetric normal pressure applied to the free end of the cylinder.

At each frequency, the propagating modes are retained and the evanescent modes are ignored, making the solution an approximation to the exact equations of elasticity. This approach yields a solution that is well suited for multiple mode waveguides in which the length of the waveguide is very large compared with its diameter.

Richard R. Laverty
Department of Mechanical Engineering
Colorado State University
Fort Collins, Colorado 80523
Summer 2001

TABLE OF CONTENTS

Chapter 1

INTRODUCTION

While the following research is primarily of a fundamental nature, it is important to note that a number of practical applications are of immediate relevance. Perhaps the most interesting and complex application is to the grading of small diameter timber for use in structural applications. Other investigators have also considered related problems with a view towards applications in areas such as inspection of composite materials and development of sensors for hostile and high temperature environments.

1.1 Motivation

Traditionally, the forest products industry in the United States has exhibited a preference for large diameter trees. Lumber and plywood mills were designed to process larger logs and small logs were sold as poles, fence posts, firewood and chips for pulp and manufactured wood product production. Little attention has been given to higher value end uses for material from small

diameter trees. A problem now exists with forest stands that are overgrown with small diameter trees. The small diameter timber resource presents potential problems in terms of the forest stand susceptibility to fire, insects and disease. One method of alleviating this problem is to remove the small diameter material from the forest. In order to make this a viable solution, new, higher value markets must be developed to provide economic incentive for its harvesting and use.

One potential use for small diameter timber (SDT) is in structural applications. Structural applications provide potential for adding value as well as demand for small diameter round timber. A major barrier to the structural use of this material is the limited knowledge of its engineering properties. While there is a fairly large database on the strength of full size round wood poles, conventional methods of deriving design stresses lack the rigor associated with the derivation of design stresses for stress graded lumber commonly used in engineered systems. In order to improve the image of round wood as a structural material, methods are needed to assign allowable stresses with greater accuracy than is currently obtained using visual inspection methods.

Wood is an anisotropic material that in the full round configuration is transversely isotropic. As a tree develops, the demands on the supporting structure of wood change from fast upward growth in order to compete for sunlight to lateral strength to resist horizontal wind forces. Mechanical properties in any one principle direction vary with location in the tree as a result of the growth from juvenile or crown wood to mature wood.

In order to determine the strength grade of a SDT the percentage of each type of wood which make up the cross section of the tree must be known.

When the SDT is excited by an external source of energy, the velocity and attenuation of elastic waves propagated in the material are related to the mechanical properties of the material. For many practical applications, the velocity in the material depends on the dimensions of the specimen and varies with the frequency of the signal. Phase and group velocity are well understood for isotropic, homogeneous materials, but are more complex for wood, or any other tranversely isotropic material. In order to reliably assess small diameter timber a better understanding of elastic waves in transversely isotropic materials is required.

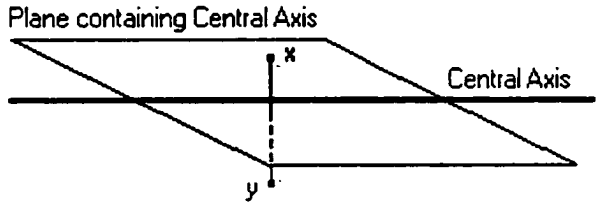

Figure 1.1: Transversely isotropic materials have symmetry about all planes containing the central axis

Dimension lumber that comes from larger trees is usually modeled as orthotropic. A small diameter timber section is a transversely isotropic cylinder. A transversely isotropic cylinder has symmetric properties in all directions from a central axis. This symmetry results from wood growth which occurs exclusively at the exterior of the tree. If the center of the tree is taken as the axis of symmetry, then the material properties of the tree are the same

in all of the radial directions from this central axis. Figure 1.1 illustrates this type of symmetry. In the figure the points x and y are reflections of each other over a plane containing the central axis. Thus, they have the same material properties.

In order to determine the behavior of waves through a SDT, the general behavior of longitudinal waves in tranversely isotropic cylinders must be established.

1.2 Background

With a historically rich area such as waves in cylindrical waveguides it is important that this proposed work be understood in the context of this long tradition. Theoretical work on the propagation of longitudinal waves in an isotropic cylinder is extensive. The original work on wave propagation in isotropic cylindrical waveguides was performed independently by two investigators, Pochhammer and Chree, late in the nineteenth century, [45, 6]. Later investigations were focused on theory and experiments related to the propagation of waves in a thin waveguide. Skalak, Miklowitz and Folk et al., [58, 37, 11]. Finally, less extensive investigations, primarily experimental, have considered thick waveguides for which the modes are separated in time. [35].

The solution presented by Pochhammer and Chree is a continuous wave result that is the basis for understanding waveguides. These original works showed the solution of the wave equation for this geometry, but it did not include calculations of the roots of the frequency equations. As described by

Love. p. 179 [32]. the characteristic (or frequency) equation can be easily obtained, although finding the roots of the equation is much more difficult.

Continuous wave results may be used to understand phase velocity, the propagation of modes and dispersion. Continuous waves consist of an infinite train of sinusoids. Most signals of interest are not in the form of a single sinusoid, but a pulse. Using a Fourier decomposition of a pulse, the response of the waveguide can be solved by first determining the response due to a single Fourier component of the pulse. This will be a single frequency sinusoid. Then, using the principle of superposition the sum of all of these single frequency responses is the response to the pulse. Using this method we may obtain the response to an arbitrary input which meets mild admissibility requirements.

The lowest branch roots of the frequency equation were first calculataed by Bancroft in 1941. [3]. Bancroft found the roots of the frequency equation for the first three modes. The numerical results from Bancroft's paper were verified by Davies in 1948. [7] Davies also performed experiments to test the results. In his experiments, the energy is propagated in the lowest mode of the waveguide. However, significant dispersion is evident in the received signal. Davies uses a summation of frequencies to calculate the dispersed signal. This approach is a physically intuitive way to address this relatively complicated calculation. The theoretical results show good correlation to experiments given the small number of frequencies that it was practical to include in his manual calculations.

Some of the later work on thin waveguides focused on the propagation of a pulse in a thin bar and examined the transient effects. Transient effects

may be ignored in many of the practical applications because of the distance that the pulse propagates from the excitation point. Multiple modes are generated in a waveguide when the waveguide is greater than approximately $1/20^{th}$ of a wavelength in diameter. Modes correspond to different shapes of the displacement across the diameter of the cylinder, and in general the modes travel at different group velocities and are dispersive. While the thin bar description (single mode waveguide) is commonly used to describe wave propagation, this description will not be employed so that the diameter-wavelength restriction may be avoided.

The subsequent work on waveguides that focused on transient effects for the propagation of a pulse in a thin bar was motivated by the split-Hopkinson bar experiment. It is important to understand the split-Hopkinson bar experiment because it remains a basic tool for high strain rate material measurements. The thin waveguide, in this context, may be considered less than one-quarter to one third of a wavelength in diameter. While only one mode propagates, dispersion is significant at the frequencies considered.

Among the work that considers modeling of the single mode dispersive waveguide are papers by Skalak, Miklowitz and Folk, [58, 37, 11]. While this research was concerned with a single mode propagating in the waveguide, the solutions are quite complicated because of the emphasis on transient behavior in a dispersive geometry. Experimental studies were also performed that support these theoretical investigations by Miklowitz and Nisewanger and Fox and Curtis, [38, 14]. These experimental studies use waveguides of approximately one-tenth of a wavelength in diameter. As in the theoretical work, dispersion of the first longitudinal mode is clearly evident.

Comparison of theory and experiment was done in the time domain with an emphasis placed on the prediction of the initial fast pressure rise seen in the split-Hopkinson bar tests. The assumptions which underlies all of this work is that the rise time at the leading edge of the wavefront contains a sufficiently small amount of high frequency energy so that the energy in the first waveguide mode greatly exceeds the energy in any other modes excited in the waveguide. This corresonds to the single dispersive mode that in the low frequency limit case results in the 1-D wave equation. This condition is satisfied if appropriate experimental conditions are met, however, in the most general case multiple modes are generated.

1.3 Multi-Mode Isotropic Cylinders

Experimental and theoretical models for a single mode waveguide were established in the late 1940's, with consideration of transient calculations continuing through the 1950's. However, complete exploration of the roots of the frequency equation for multi-mode waveguides did not occur until the numerical difficulties were overcome by Onoe et al. in 1972, [44]. Onoe and co-authors comprehensively explored both real and complex roots of the frequency equation.

A number of investigators have also made use of multi-mode waveguides to measure both the Young's modulus and shear modulus of materials in a single experiment, [35]. The experiments were typically described using a plane wave model which neglects dispersion. Discussion of multi-mode waveguides by experimental investigators continues to depend on a model

which disregards dispersion of the wave, [23, 28]. Experimental use of multi-mode waveguides is important since it provides the opportunity to obtain both the shear and longitudinal modulus from a single measurement. In addition, the opportunity exists for the modes which correspond to different displacements across the diameter of the cylinder to be used to inspect different portions of the cylinder. While experimentally important, analytical and numerical models continue to be developed. Although, in general, these models are computationally expensive and do not provide an appropriate tool for in-situ NDE without considerable modification, [42, 18].

Experimental investigators have been forced to avoid the limitations of the theoretical models by simply using plane wave descriptions of multi-mode wave propagation in solid cylinders. Alternatively, the 1-D waveguide model is used which is only applicable when the cylinder is very thin relative to the wavelength of the elastic wave. While the plane wave model used by experimental investigators becomes accurate in the limit of a large diameter waveguide, the effects of dispersion disappears only in the large diameter limit. A comprehensive approach is thus required which contains a sufficiently complete description of the waveform without requiring the use of computationally expensive modeling. The wave mechanics employed must be then in the form of an analytical or hybrid analytical-numerical solution.

1.4 Anisotropic Waveguides

Investigations of waves in anisotropic materials are considerably more difficult than the classical, and well understood, isotropic problem. As in the

isotropic case, anisotropic waves are governed by a hyperbolic system of second-order partial differential equations. However, the number of independent parameters, i.e. material constants, for anisotropic materials is much greater. Isotropic materials can be characterized by only two parameters, anisotropic materials can have from five to twenty-one independent material constants. In addition to the increased number of parameters, the geometry of the body and symmetry of the material may complicate analysis. In an isotropic solid, the behavior of the material is the same in all directions. Anisotropic solids show a preference to certain directions. Reconciling the geometry of the body with these preferred directions constitutes a large part of the analysis of many anisotropic problems.

A complete description of the response of an infinite anisotropic body responding to a localized disturbance was published by Duff in 1960. [8]. Duff's results for a homogeneous anisotropic solid describe the response of the solid in a Fourier transformed space. The study's conclusions were focused on characterizing the sheets of the different wave surfaces and their arrival at an arbitrary point in the medium.

Approximate theories, such as Mirsky's [39], are the most common approach to anisotropic waveguide problems. In a pair of articles, [40, 41], Mirsky compares his approximate theory with the results from the exact elasticity equations for a cylindrical shell. The comparison was made by examining the dispersion curves for the approximate and exact theories. For the exact theory, the dispersion curves were obtained via displacement potentials and the completeness of this solution is not clear. However, for lower frequencies the first four modes of the exact and approximate theories have

good agreement. At higher frequencies the dispersion curves for the approximate and exact theories do not agree.

Many other studies have been conducted on anisotropic waves with an interest towards testing composite materials. Investigations such as Spies, [59], are chiefly concerned with the more cartesian geometries of laminar composites. Nagy and Nayfeh, [43], investigate the layered cylindrical geometry of fibers in a fibrous composite, but only obtain the frequency equation and dispersion curves.

Chapter 2

WAVEGUIDE MODEL

The overall goal of this research is to construct an analytic solution to the response of a layered transversely isotropic cylinder to a pressure field being applied at one end of the cylinder. The primary focus for applications is on testing of small diameter timber. This application motivates the design of our model. The following model will be used throughout the remainder of the work.

The mathematical model of a cylindrical elastic waveguide is well established as presented by Love, [32]. The elastodynamic state of the body is described given the external stresses and body forces acting on the body. The coordinate system is chosen to be polar-cylindrical with the z-axis coinciding with the axis of the cylinder. In its simplest form this model would treat an infinite waveguide, i.e. the cylinder would occupy a region extending from $z = -\infty$ to $z = \infty$. A radially and time varying normal stress is applied to a cross-section of the waveguide. Thus, the model will extend from $z = c$, the location of the cross-section where the normal pressure is applied.

to $z = \infty$. For convenience, let $c = 0$.

2.1 The Homogeneous Shell

The first model is for a homogeneous shell. This is the basic component of the layered cylinder. Assume a normal pressure, σ_{zz}, is applied at $z = 0$. Let the radial displacement, u_r, vanish at$z = 0$. This is a mixed end condition since a stress anddisplacement are prescribed on the end. The condition $u_r = 0$ is an approximation of the more physically realistic pure end condition $\sigma_{zr} = 0$. However, it was shown by Kennedy and Jones, [26], that for large z the difference in the solution to the mixed and pure end condition problems becomes neglibible as z becomes large, i.e. the difference between the two solutions tends to zero as z approaches infinity. The remaining boundary conditions are that the inner and outer surfaces of the cylinder, $r = a$ and $r = b$, be traction free, i.e. $\sigma \bullet \mathbf{n} = 0$, where $\mathbf{n}$ is the outward unit normal to each surface.

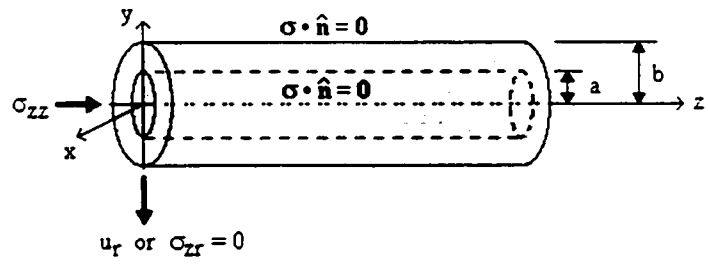

Figure 2.1: Picture of a cylindrical shell waveguide

Between $r = a$ and $r = b$ the elastic body must obey the equations of motion

$$\sigma_{ij,j} = \rho \ddot{u}_i \tag{2.1}$$

where σ_{ij} are the components of the stress tensor and u_i are the components of the displacement vector. Differentiation with respect to time is denoted by a dot and differentiation with respect to a spatial coordinate employs the comma notation convention. In eqn.(2.1) body forces are not included. In addition, the constitutive relation for isotropic or transversely isotropic solids and the linear strain-displacement relations are employed. For the constitutive laws the contracted notation for the components of the stress tensor, σ_{ij} and the components of the strain tensor, ϵ_{ij}, are used such that,

$$\begin{aligned}
\sigma_1 &= \sigma_{11}, \quad \epsilon_1 = \epsilon_{11} \\
\sigma_2 &= \sigma_{22}, \quad \epsilon_2 = \epsilon_{22} \\
\sigma_3 &= \sigma_{33}, \quad \epsilon_3 = \epsilon_{33} \\
\sigma_4 &= \sigma_{23}, \quad \epsilon_4 = \epsilon_{23} \\
\sigma_5 &= \sigma_{31}, \quad \epsilon_5 = \epsilon_{31} \\
\sigma_6 &= \sigma_{12}, \quad \epsilon_6 = \epsilon_{12}
\end{aligned}$$

The constitutive law for an isotropic solid is then shown in the matrix-vector equation as:

$$\begin{bmatrix} \sigma_1 \\ \sigma_2 \\ \sigma_3 \\ \sigma_4 \\ \sigma_5 \\ \sigma_6 \end{bmatrix} = \begin{bmatrix} \lambda+2\mu & \lambda & \lambda & 0 & 0 & 0 \\ \lambda & \lambda+2\mu & \lambda & 0 & 0 & 0 \\ \lambda & \lambda & \lambda+2\mu & 0 & 0 & 0 \\ 0 & 0 & 0 & \mu & 0 & 0 \\ 0 & 0 & 0 & 0 & \mu & 0 \\ 0 & 0 & 0 & 0 & 0 & \mu \end{bmatrix} \begin{bmatrix} \epsilon_1 \\ \epsilon_2 \\ \epsilon_3 \\ \epsilon_4 \\ \epsilon_5 \\ \epsilon_6 \end{bmatrix} \tag{2.2}$$

where λ and μ are the Lamé elastic constants. Using the same notation the constitutive law for the transversely isotropic solid is:

$$\begin{bmatrix} \sigma_1 \\ \sigma_2 \\ \sigma_3 \\ \sigma_4 \\ \sigma_5 \\ \sigma_6 \end{bmatrix} = \begin{bmatrix} c_{11} & c_{12} & c_{13} & 0 & 0 & 0 \\ c_{12} & c_{11} & c_{13} & 0 & 0 & 0 \\ c_{13} & c_{13} & c_{33} & 0 & 0 & 0 \\ 0 & 0 & 0 & c_{44} & 0 & 0 \\ 0 & 0 & 0 & 0 & c_{44} & 0 \\ 0 & 0 & 0 & 0 & 0 & \frac{1}{2}(c_{11}-c_{12}) \end{bmatrix} \begin{bmatrix} \epsilon_1 \\ \epsilon_2 \\ \epsilon_3 \\ \epsilon_4 \\ \epsilon_5 \\ \epsilon_6 \end{bmatrix} \tag{2.3}$$

The transversely isotropic solid has five independent constants while the isotropic has only two.

Theisotropiccase is the simple model which will be used for initial demonstration of the approach employed. The simple model will be used to describe several techniques for solving the problem of the shell response. However, application to areas such as testing of small diameter timber or carbon pan fibers requires more general material symmetry such as transverse isotropy.

A final assumption is made regarding the applied pressure field σ_{zz}. An axisymmetric applied stress field is assumed so that:

$$\sigma_{zz} = \sigma_{zz}(r, t). \tag{2.4}$$

This, along with the material symmetry which was imposed implies that the response of the cylinder will also be axisymmetric.

All of these assumptions leave us with a mathematical model of two coupled partial differential equations (PDE's) for the radial and axial dislplacements, u_r and u_z. The third equation in eqn.(2.1), involoving $u_3 = u_\theta$, will reduce to the trivial equation $0 = 0$ under the assumption of axisymmetry. For the isotropic case the analytical solution techniques can be found in [1, 11, 9, 15]. These are the Pochhammer-Chree solution, the double transform method and the method of eigenfunction expansions. The Pochhammer-Chree solution assumes a solution composed of a superposition of harmonic modes and derives a frequency equation based on this assumption. The double transform method uses a combination of Sine, Cosine and Fourier transforms to uncouple the PDE's and find a solution in the transformed space. The method of eigenfunction expansions assumes a series solution for each displacement, then obtains an eigenvalue problem for the unknown functions of the expansion. Each approach is examined in more detail in the Chapter 3, Alternative Methods.

2.2 The Layered Cylinder

Clearly, for many important applications a homogeneous waveguide cannot be assumed. A more complete waveguide model can be constructed which

consists of homogeneous coaxial layers. On the outer boundary of this cylinder the same boundary conditions exist as on the homogeneous shell.

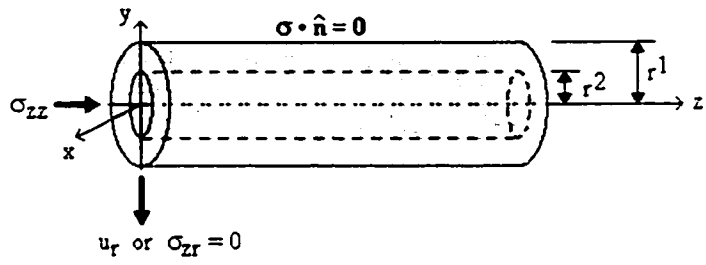

Figure 2.2: Picture of a two-layered cylinder, the outer and center layers have radii r^1 and r^2, respectively.

On the interior of the cylinder the equations of motion, constitutive and strain-displacement relations remain the same as in the shell. A discontinuity in material properties exist between the layers. Therefore, the governing differential equations take the same form except that the coefficients are defined piecewise.

Continuity of stresses and displacements across the layer interfaces allow a solution to be constructed from the solution to a single shell via transfer matrices. The transfer matrix method avoids the creation of a separate frequency equation for each layer and a single frequency equation is obtained for the entire cylinder.

Chapter 3

ALTERNATIVE METHODS

In principle, several alternatives exist for constructing an analytic solution to the waveguide problem. However, none of these approaches is sufficiently general to be used in all cases. This chapter is devoted to outlining some of these other methods. For simplicity in describing these techniques the material is assumed to be isotropic throughout this chapter. However, one of the reasons these methods are not employed for the more general case is that they do not lend themselves well to anisotropic problems. Each method does have some advantages in at least the class of application for which it was originally proposed. The suitable applications will be pointed out in each section.

3.1 Pochhammer-Chree Modes

The Pochhammer-Chree solution underlies all of the solution techniques which are used. These results are available in numerous references and are

included here for completeness, [1, 11, 9, 15]. The results motivate the form of the other approaches to constructing a solution to this problem. The first step is a Helmholtz decomposition of the displacement field. It is well known that any sufficiently 'well behaved' vector field, $\bar{u}$, may be decomposed into the sum of the gradient of a scalar potential, ϕ, and the curl of a solenoidal vector potential, $\bar{\psi}$, [2].

$$\bar{u} = \nabla\phi + \nabla \times \bar{\psi}, \text{ where } \nabla \cdot \bar{\psi} = 0. \tag{3.1}$$

The equations of motion for an isotropic elastic body may be written in invariant form as:

$$\mu\nabla^2\bar{u} + (\lambda + \mu)\nabla\nabla \cdot \bar{u} = \rho\ddot{\bar{u}} \tag{3.2}$$

Insertion of the decomposed form of $\bar{u}$, eqn.(3.1), into eqn.(3.2) yields the equation

$$\nabla\left[(\lambda + 2\mu)\nabla^2\phi - \rho\ddot{\phi}\right] + \nabla \times \left[\mu\nabla^2\bar{\psi} - \rho\ddot{\bar{\psi}}\right] = 0. \tag{3.3}$$

This equation is clearly satisfied if

$$\rho\ddot{\phi} = (\lambda + 2\mu)\nabla^2\phi \text{ and} \tag{3.4}$$

$$\rho\ddot{\bar{\psi}} = \mu\nabla^2\bar{\psi}. \tag{3.5}$$

It is clear that a solution to eqn.(3.4) and (3.5) will solve eqn.(3.3). What is not immediately clear is that all solutions of eqn.(3.3) must also be solutions

of eqn.(3.4) and (3.5). It is explained in Graff. p. 275-276, [19], that this is indeed the case. A simple wave equation for each of the displacement potentials is then produced. This approach is preferrable to attempting to evaluate the equations of motion in terms of displacements.

The solution to the wave equation,

$$\frac{1}{c^2}\ddot{f} = \nabla^2 f. \tag{3.6}$$

is a traveling wave of the form

$$f(\bar{p}\cdot\bar{x} - ct) \tag{3.7}$$

where $\bar{p}$ is the propagation direction, $\bar{x}$ is the spatial coordinate, c the velocity of propagation and t is time. In eqn.(3.4) the velocity of propagation is:

$$c = c_L = \sqrt{\frac{\lambda + 2\mu}{\rho}} \tag{3.8}$$

This is the velocity of longitudinal waves in an unbounded elastic medium. In eqn.(3.5) the velocity of propagation is:

$$c = c_T = \sqrt{\frac{\mu}{\rho}} \tag{3.9}$$

This is the velocity of transverse waves in an unbounded elastic medium.

Any reasonably smooth disturbance can also be represented as a sum of single frequency Fourier components. Due to the symmetry in the problem

the propagation is in the z-direction and the coefficient of any single Fourier component is a function of r alone. This leaves the following form for a single mode of the potentials.

$$\phi = \phi(r)e^{i(kz-\omega t)} \tag{3.10}$$

$$\psi_r = \psi_r(r)e^{i(kz-\omega t)} \tag{3.11}$$

$$\psi_\theta = \psi_\theta(r)e^{i(kz-\omega t)} \tag{3.12}$$

$$\psi_z = \psi_z(r)e^{i(kz-\omega t)} \tag{3.13}$$

The expression for ϕ can be put into eqn.(3.4). The resulting equation for $\phi(r)$ is the Bessel equation

$$\frac{1}{r}\frac{d}{dr}\left(r\frac{d\phi}{dr}\right) + \left(\frac{\omega^2}{c_L^2} - k^2\right)\phi = 0 \tag{3.14}$$

Therefore,

$$\phi(r) = AJ_0(pr) + BY_0(pr) \tag{3.15}$$

where J_0 and Y_0 are Bessel functions of order zero of the first and second kinds, respectively, $p^2 = \frac{\omega^2}{c_L^2} - k^2$, and A and B are arbitrary constants.

Now, consider the vector wave equation, eqn.(3.5). Writing out the components in cylindrical coordinates:

$$0 = \left[\nabla^2\psi_r - \frac{\psi_r}{r^2} - \frac{2}{r^2}\frac{\partial\psi_\theta}{\partial\theta} - \frac{\ddot{\psi}_r}{c_T^2}\right]\hat{e}_r \tag{3.16}$$

$$+ \left[\nabla^2\psi_\theta - \frac{\psi_\theta}{r^2} + \frac{2}{r^2}\frac{\partial\psi_r}{\partial\theta} - \frac{\ddot{\psi}_\theta}{c_T^2}\right]\hat{e}_\theta \tag{3.17}$$

$$+ \left[\nabla^2\psi_z - \frac{\ddot{\psi}_z}{c_T^2}\right]\hat{e}_z \tag{3.18}$$

First, note that for the right side of this equation to equal the zero vector, each component must vanish independently. Thus, eqn.(3.16), (3.17) and (3.18) represent three separate equations for the unknown components of $\bar{\psi}$. Second, notice that eqn.(3.18) is uncoupled from the other two. Therefore, it is the best place to start. Substituting eqn.(3.13) into eqn.(3.18) the following equation is obtained for $\psi_z(r)$.

$$\frac{1}{r}\frac{d}{dr}\left(r\frac{d\psi_z}{dr}\right) + \left(\frac{\omega^2}{c_T^2} - k^2\right)\psi_z = 0. \tag{3.19}$$

This equation is of the same form as eqn.(3.14). Thus, the solution is

$$\psi_z(r) = CJ_0(qr) + DY_0(qr). \tag{3.20}$$

The argument of the Bessel functions has changed to q where $q^2 = \frac{\omega^2}{c_T^2} - k^2$.

Now, the coupled PDE's, eqn.(3.16) and (3.17), need to be solved. In general, this is a very difficult problem. It is simplified somewhat by the fact that the solutions must be of the form in eqn.(3.11) and (3.12). Substitution of these forms for ψ_r and ψ_θ into eqn.(3.16) and (3.17) yields the uncoupled ODE's:

$$0 = \frac{1}{r}\frac{d}{dr}\left(r\frac{d\psi_r}{dr}\right) + \left[\left(\frac{\omega^2}{c_T^2} - k^2\right) - \frac{1}{r^2}\right]\psi_r \quad (3.21)$$

$$0 = \frac{1}{r}\frac{d}{dr}\left(r\frac{d\psi_\theta}{dr}\right) + \left[\left(\frac{\omega^2}{c_T^2} - k^2\right) - \frac{1}{r^2}\right]\psi_\theta \quad (3.22)$$

The solutions to these two equations are

$$\upsilon_r(r) = EJ_1(qr) + FY_1(qr) \text{ and} \quad (3.23)$$

$$\upsilon_\theta(r) = GJ_1(qr) + HY_1(qr). \quad (3.24)$$

The functions J_1 and Y_1 are Bessel functions of first order of the first and second kinds, respectively.

One more detail must be addressed in the Helmholtz decomposition of the displacement field. The vector potential, $\bar{\psi}$, is restricted to be solenoidal, i.e. $\nabla \cdot \bar{\psi} = 0$. With expressions for all of the components of $\bar{\psi}$ the exact consequence of this requirement is evident. In cylindrical coordinates

$$\nabla \cdot \bar{\psi} = \frac{1}{r}\frac{\partial}{\partial r}(r\psi_r) + \frac{1}{r}\frac{\partial \psi_\theta}{\partial \theta} + \frac{\partial \psi_z}{\partial z} \quad (3.25)$$

Using the solutions for the components of $\bar{\psi}$, $\nabla \cdot \bar{\psi} = 0$ implies

$$0 = \{q[EJ_0(qr) + FY_0(qr)] + ik[CJ_0(qr) + DY_0(qr)]\}e^{i(kz-\omega t)} \quad (3.26)$$

$$= [qEJ_0(qr) + qFY_0(qr)] + i[kCJ_0(qr) + kDY_0(qr)]. \quad (3.27)$$

Equating real and imaginary parts it may be concluded that $E = F = C = D = 0$ since J_0 and Y_0 are linearly independent. Therefore, for axisymmetric modes of an isotropic cylindrical shell the displacement potentials are

$$\phi = [AJ_0(pr) + BY_0(pr)]\, e^{i(kz-\omega t)} \tag{3.28}$$

$$\psi_r = 0 \tag{3.29}$$

$$\psi_\theta = [GJ_1(qr) + HY_1(qr)]\, e^{i(kz-\omega t)} \tag{3.30}$$

$$\psi_z = 0. \tag{3.31}$$

A technical remark can also be made regarding eqn.(3.27). It is possible for q to take on complex values. However, when this occurs q will be purely imaginary. The series expansion for Bessel functions of order zero contain only even powers of their argument. Therefore, although the arguments may be imaginary, Bessel functions of order zero (or any even order) will have real values. This justifies equating real and imaginary parts of eqn.(3.27). It should be kept in mind, however, that Bessel functions of odd order, first order in particular, will not have real values when their arguments are imaginary.

For a general decomposition of the form in eqn.(3.1) the components of displacement are related to the potentials by

$$u_r = \frac{\partial \phi}{\partial r} + \frac{1}{r}\frac{\partial \psi_z}{\partial \theta} - \frac{\partial \psi_\theta}{\partial z} \tag{3.32}$$

$$u_\theta = \frac{1}{r}\frac{\partial \phi}{\partial \theta} + \frac{\partial \psi_r}{\partial z} - \frac{\partial \psi_z}{\partial r} \tag{3.33}$$

$$u_z = \frac{\partial \phi}{\partial z} + \frac{1}{r}\frac{\partial}{\partial r}(r\psi_\theta) - \frac{1}{r}\frac{\partial \psi_r}{\partial \theta}. \tag{3.34}$$

Using what has been presented thus far,

$$u_r = -[pAJ_1(pr) + pBY_1(pr) + ikGJ_1(qr) + ikHY_1(qr)]\, e^{i(kz-\omega t)} \quad (3.35)$$

$$u_\theta = 0 \quad (3.36)$$

$$u_z = [ikAJ_0(pr) + ikBY_0(pr) + qGJ_0(qr) + qHY_0(qr)]\, e^{i(kz-\omega t)} \quad (3.37)$$

From this result the form of the modes of the isotropic shell have been established. The cross-sectional displacements are a linear combination of Bessel functions of the first and second kinds of two different arguments multiplied by a factor $e^{i(kz-\omega t)}$. Later, when the form of a solution is specified this result is the major justification for the 'guess.' A very similar form will also be used for the transversely isotropic shell. The difference will be in the arguments of the Bessel functions, the form will otherwise be the same.

3.2 Double Transform Method

The double transform method is one method that has been successful in generating formal analytic solutions to the semi-infinite cylinder. This method uses a combination of Fourier and Fourier sine and cosine transforms to simplify the equations of motion. In the z-variable a Fourier sine or cosine transform is used and the Fourier transform is used to transform t. The transforms of a quantity f are defined by: (Superscripts denote transformed quantities.)

$$f^F(r,z,\omega) = \int_0^\infty f(r,z,t)e^{i\omega t}dt \tag{3.38}$$

$$f^S(r,\gamma,t) = \int_0^\infty f(r,z,t)\sin(\gamma z)dz \tag{3.39}$$

$$f^C(r,\gamma,t) = \int_0^\infty f(r,z,t)\cos(\gamma z)dz \tag{3.40}$$

The method can be used to find the solution, in the transformed space, to the displacements in a semi-infinite isotropic shell subject to mixed end conditions. This requires only a minor modification of the procedure described in [11], where a solid cylinder is considered. While the double transform method has significant advantages, a significant barrier also exists to practical implementation as well.

To apply the method the effect of the transforms on derivatives needs to be established.

$$\left(\frac{\partial f}{\partial t}\right)^F = f(t=0) - i\omega f^F \tag{3.41}$$

$$\left(\frac{\partial f}{\partial z}\right)^C = -f(z=0) + \gamma f^S \tag{3.42}$$

$$\left(\frac{\partial f}{\partial z}\right)^S = -\gamma f^C \tag{3.43}$$

Under axisymmetry the equations of motion may be written as:

$$\ddot{u} = c_L^2\frac{\partial \Delta}{\partial r} + 2c_T^2\frac{\partial \Omega}{\partial z} \tag{3.44}$$

$$\ddot{w} = c_L^2\frac{\partial \Delta}{\partial z} + \frac{2}{r}c_T^2\frac{\partial (r\Omega)}{\partial r} \tag{3.45}$$

Where u and w are the radial and axial displacements, c_L and c_T are the velocity of longitudinal and transverse waves in unbounded media, and Δ and Ω are the dilatation and non-vanishing component of rotation.

First, a Fourier sine, then a Fourier transform of eqn.(3.44) is taken. Noting that the cylinder is initially at rest, $u(t=0) = \dot{u}(t=0) = 0$:

$$-\omega^2 u^{SF} = c_L^2 \frac{\partial \Delta^{SF}}{\partial r} - 2C_T^2 \gamma \Omega^{CF} \tag{3.46}$$

For eqn.(3.45), a Fourier cosine, then a Fourier transform are taken. Again, note that the cylinder is initially at rest.

$$-\omega^2 w^{CF} = -c_L^2 \Delta^F(z=0) + c_L^2 \gamma \Delta^{SF} - 2c_T^2 \frac{1}{r} \frac{\partial \left(r\Omega^{CF}\right)}{\partial r} \tag{3.47}$$

To continue, a more convenient form for the term $\Delta^F(z=0)$ is needed. Recall that this is the mixed end condition problem, therefore, $u\,|_{z=0} = 0$, and

$$\Delta(z=0) = \Delta\,|_{z=0} = \frac{1}{r}\frac{\partial(ru)}{\partial r}|_{z=0} + \frac{\partial w}{\partial z}\,|_{z=0} = \frac{\partial w}{\partial z}\,|_{z=0} \tag{3.48}$$

The other end condition is to specify the normal stress at $z=0$. For now consider a time varying end stress and denote it by:

$$\sigma_{zz}\,|_{z=0} = P(t) \tag{3.49}$$

Then, using the constitutive law for isotropic solids

$$\sigma_{zz}|_{z=0} = \lambda\Delta|_{z=0} + 2\mu\frac{\partial w}{\partial z}|_{z=0} = (\lambda + 2\mu)\frac{\partial w}{\partial z}|_{z=0} = \rho c_L^2 \frac{\partial w}{\partial z}|_{z=0} \qquad (3.50)$$

Therefore,

$$P(t) = \rho c_L^2 \frac{\partial w}{\partial z}|_{z=0} \qquad (3.51)$$

Combining eqn.(3.48) and (3.51), it can be concluded that

$$\Delta(z=0) = \frac{P(t)}{\rho c_L^2}. \qquad (3.52)$$

Take a Fourier transform of eqn.(3.52) and replace $\Delta^F(z=0)$ in eqn.(3.47) to obtain a final equation for the axial displacement in the transformed space.

$$-\omega^2 w^{CF} = -\frac{P^F}{\rho} + c_L^2 \gamma \Delta^{SF} - 2c_T^2 \frac{1}{r}\frac{\partial\left(r\Omega^{CF}\right)}{\partial r} \qquad (3.53)$$

So far the method has yielded two ODE's for the transforms of the dilatation and the rotation, eqn.(3.46) and (3.53). Before solving these equations they must be uncoupled. This is accomplished by first noting

$$\Delta^{SF} = \frac{1}{r}\frac{\partial(ru^{SF})}{\partial r} - \gamma w^{CF} \text{ and} \qquad (3.54)$$

$$\Omega^{CF} = \frac{1}{2}\left(\gamma u^{SF} - \frac{\partial w^{CF}}{\partial r}\right). \qquad (3.55)$$

Taking the appropriate combinations of the ODE's, eqn(3.46) and (3.53), the left hand sides will contain the quantities Δ^{SF} and Ω^{CF} and the equations will be uncoupled.

$$0 = \frac{1}{r}\frac{\partial}{\partial r}\left[r\frac{\partial \Delta^{SF}}{\partial r}\right] + \left(\frac{\omega^2}{c_L^2} - \gamma^2\right)\Delta^{SF} + \frac{\gamma}{\rho c_L^2}P^F \tag{3.56}$$

$$0 = \frac{\partial}{\partial r}\left[\frac{1}{r}\frac{\partial(r\Omega^{CF})}{\partial r}\right] + \left(\frac{\omega^2}{c_T^2} - \gamma^2\right)\Omega^{CF} \tag{3.57}$$

These are Bessel equations and can be solved easily. The equation for Δ^{SF} contains the non-homogeneous term $\frac{\gamma}{\rho c_L^2}P^F$. If the applied pressure has a radial dependence then this must be dealt with at this stage. However, as it is, this term is constant with respect to r and the solutions are:

$$\Delta^{SF} = AJ_0(pr) + BY_0(pr) + \frac{\gamma P^F}{\rho(\gamma^2 c_L^2 - \omega^2)} \tag{3.58}$$

$$\Omega^{CF} = CJ_1(qr) + DY_1(qr) \tag{3.59}$$

where J_i and Y_i are Bessel functions of the first and second kind, respectively. A, B, C and D are constants with respect to r and

$$p^2 = \frac{\omega^2}{c_L^2} - \gamma^2 \tag{3.60}$$

$$q^2 = \frac{\omega^2}{c_T^2} - \gamma^2. \tag{3.61}$$

Ignoring the possibility of a radial dependence in the applied pressure, P, is a large physical restriction. To include the possibility of P depending on r introduces the complication that the non-homogeneous term in eqn.(3.56) is non-constant. This is not an oversight, but a simplification for the purpose of brevity.

The boundary conditions on the curved surfaces of the shell are used to determine the arbitrary constants in eqn.(3.58) and (3.59). Expressions

for the transforms of the displacements are needed. This is accomplished by using the coupled ODE's. eqn.(3.46) and (3.53), and inserting the expressions for Δ^{SF} and Ω^{CF} from eqn.(3.58) and (3.59).

$$u^{SF} = \frac{2c_T^2\gamma}{\omega^2}\left[CJ_1(qr) + DY_1(qr)\right] + \frac{c_L^2 p}{\omega^2}\left[AJ_1(pr) + BY_1(pr)\right] \tag{3.62}$$

$$\begin{aligned} w^{CF} &= \left[1 - \frac{c_L^2\gamma^2}{\gamma^2 c_L^2 - \omega^2}\right]\frac{P^F}{\rho\omega^2} - \frac{c_L^2\gamma}{\omega^2}\left[AJ_0(pr) + BY_0(pr)\right] \\ &+ \frac{2c_T^2 q}{\omega^2}\left[CJ_0(qr) + DY_0(qr)\right] \end{aligned} \tag{3.63}$$

The equations that will determine the constants are the traction free lateral surface conditions. Since there exist two non-trivial stresses, σ_{rr} and σ_{zr}, this will provide four equations, two at the inner and two at the outer radius.

The transformed stresses are

$$\sigma_{rr}^{SF} = \rho(c_L^2 - 2c_T^2)\Delta^{SF} + 2\rho c_T^2\frac{\partial u^{SF}}{\partial r} \text{ and} \tag{3.64}$$

$$\sigma_{zr}^{CF} = \rho c_T^2\left(\gamma u^{SF} + \frac{\partial w^{CF}}{\partial r}\right). \tag{3.65}$$

The undetermined constants are now found by solving the following equations.

$$\sigma_{rr}^{SF} = 0 \text{ at } r = a \tag{3.66}$$

$$\sigma_{rr}^{SF} = 0 \text{ at } r = b \tag{3.67}$$

$$\sigma_{zr}^{CF} = 0 \text{ at } r = a \tag{3.68}$$

$$\sigma_{zr}^{CF} = 0 \text{ at } r = b \tag{3.69}$$

where a is the inner radius and b is the outer radius.

After determining the constants the solutions to the radial displacements and the axial displacements in the transformed space are complete. From these any desired quantity can be found, provided the inversion of the transforms is practical.

The double transform method was first used by Folk, Fox, Curtis and Shook, [11], to find the sum of the strains, $\epsilon_{zz} + \epsilon_{\theta\theta}$. However, the method is equally well suited for finding any of the components of displacement, stress or strain. Upon finding the transform of any desired quantity the only remaining step in finding the solution is inverting the transforms. This is a very non-trivial procedure and a large obstacle in practical implementation. In [11, 26, 18] the Fourier sine and cosine transforms were inverted asymptotically, and in [30] an exact inversion via the residue calculus is shown to be impossible. Therefore, these existing analytic approximations are difficult to obtain and only valid for large z.

The method has successfully been extended to several cases of interest. First, Kennedy and Jones, [26], were able to apply the method to the case where the applied normal stress varies radially on the free end. They were also able to show that the asymptotic solution is a good approximation at distances greater than 20 diameters down the axis of the cylinder. In an extension by Goldberg and Folk, [18], the pure end condition problem is treated by splitting the pure end condition into the sum of 2 mixed end conditions. Lastly, in Laverty and Peterson [30], an explicit method is given for extending the double transorm solution of the response to a pressure step to any time varying pressure. This keeps inversion of the fourier transform

relatively simple by avoiding a complicated P^F.

3.3 Eigenfunction Expansions

The method of eigenfunction expansions is used to generate a series solution for any combination of boundary and initial conditions on the shell. To apply the method a series solution is sought for all displacements and stresses of the form:

$$f(r,z,t) = \sum_n a_n f_n(r) e^{i(k_n z - \omega t)}$$

This sum is a superposition of modes of constant frequency and varying wavenumber. The functions $f_n(r)$ are called the radial eigenfunctions. Substituting these sums into the equations of motion yields an eigenvalue problem involving the radial eigenfunctions, f_n, and the eigenvalues, k_n. All quantities have the same coefficients, a_n, which are determined using a bi-orhtogonality relation and the boundary data. They key to implementing the method is solving the eigenvalue problem then discovering the bi-orthogonality relation and applying it properly.

Power and Childs, [46], were the first to use the method. They found series solutions for displacement potentials of semi-infinite cylinders, then combined solutions of 2 semi-infinite cylinders to obtain a solution to a finite cylinder. Later, Fama, [9], used the technique on the equations of equilibrium and found a most general bi-orthogonality relation for isotropic shells that could be used on any combination of stresses and displacements in the

boundary data. This paper also established the completeness of the radial eigenfunctions for most cases and at least conjectures the completeness for all cases. In a short note, Fraser, [15], extended the exact approach in [9] to find the bi-orthogonality relation for the dynamic case. All of these papers, [46, 9, 15], were concerned with isotropic cylinders with circular cross-sections. In two papers Robert and Keer, [54, 55], used this method to solve for the axisymmetric and asymmetric response of both semi-infinite and finite cyliders for many different combinations of boundary data.

Gregory, [20], showed that a general bi-orthogonality relation exists for cylinders of general cross-sectional shape and anisotropic materials providing that the planes $z = constant$ are planes of elastic symmetry. This even more general relation is merely a consequence of the dynamic recirocal identity, and need not be derived for each case from the differential equations.

With a slight variation, Folk and Herczinski, [12, 13], used the method of eigenfunction expansions to produce a generalization of Sturm-Liouville theory to a set of non self-adjoint operators, then applied their method within the context of dynamic elasticity to check the results against a previous solution, [11], obtained by the double transform method.

3.3.1 Governing Differential Equations

Now, the method will be outlined using an isotropic cylindrical shell with traction free lateral surfaces. The equations of motion in terms of displacements are given by:

$$\ddot{u} = c_L^2 \frac{\partial}{\partial r}\left[\frac{1}{r}\frac{\partial (ru)}{\partial r} + \frac{\partial w}{\partial z}\right] + c_T^2 \frac{\partial}{\partial z}\left[\frac{\partial u}{\partial z} - \frac{\partial w}{\partial r}\right] \tag{3.70}$$

$$\ddot{w} = c_L^2 \frac{\partial}{\partial z}\left[\frac{1}{r}\frac{\partial (ru)}{\partial r} + \frac{\partial w}{\partial z}\right] - \frac{c_T^2}{r}\frac{\partial}{\partial r}\left[r\left(\frac{\partial u}{\partial z} - \frac{\partial w}{\partial r}\right)\right] \tag{3.71}$$

First, apply the proposed displacements to eqn.(3.70) and (3.71).

$$u = \sum_n a_n u_n(r) e^{i(k_n z - \omega t)} \tag{3.72}$$

$$w = \sum_n a_n w_n(r) e^{i(k_n z - \omega t)} \tag{3.73}$$

After substituting the expressions for u and w into the equations of motion, the ODE's for the radial eigenfunctions u_n and w_n are obtained.

$$0 = \frac{d}{dr}\left[\frac{1}{r}\frac{d(ru_n)}{dr}\right] + \left(\frac{\omega^2}{c_L^2} - c^2 k_n^2\right) u_n + ik_n(1 - c^2)\frac{dw_n}{dr} \tag{3.74}$$

$$0 = \frac{1}{r}\frac{d}{dr}\left[r\frac{dw_n}{dr}\right] + \left(\frac{\omega^2}{c_L^2} - k_n^2\right) w_n + ik_n(1 - c^2)\frac{1}{r}\frac{d(ru_n)}{dr} \tag{3.75}$$

These equations contain the complication that the eigenvalue, k_n, appears both linearly and squared in each equation. To remedy this, assume an eigenfunction expansion for the dilatation and rotation.

$$\Delta = \sum_n a_n \Delta_n(r) e^{i(k_n z - \omega t)} \tag{3.76}$$

$$\Omega = \sum_n a_n \Omega_n(r) e^{i(k_n z - \omega t)} \tag{3.77}$$

In terms of displacements these quantities are:

$$\Delta = \frac{1}{r}\frac{\partial(ru)}{\partial r} + \frac{\partial w}{\partial z} \tag{3.78}$$

$$\Omega = \frac{1}{2}\left[\frac{\partial u}{\partial z} - \frac{\partial w}{\partial r}\right] \tag{3.79}$$

The radial eigenfunctions for each of these quantities is related by the equations:

$$\Delta_n = \frac{1}{r}\frac{d(ru_n)}{dr} + ik_n w_n \tag{3.80}$$

$$\Omega_n = \frac{1}{2}\left[ik_n u_n - \frac{dw_n}{dr}\right] \tag{3.81}$$

Differentiating eqn.(3.80), solving for $ik_n\frac{dw_n}{dr}$ and substituting into eqn.(3.74) yeilds eqn.(3.82). This equation contains the eigenvalue squared only. Similarly, an expression for $ik_n\frac{1}{r}\frac{d(ru_n)}{dr}$ can be obtained from eqn.(3.81) then substituted into eqn.(3.75). This results in eqn.(3.83), which also contains the eigenvalue squared. These two resulting ODE's, eqn.(3.82) and (3.83), now contain four unknown radial eigenfunctions, but only the square of the eigenvalue k_n.

$$0 = \frac{d}{dr}\left[\frac{1}{r}\frac{d(ru_n)}{dr}\right] + \left(\frac{\omega^2}{c_L^2} - c^2k_n^2\right)u_n + (1-c^2)\left[\frac{d\Delta_n}{dr} - \frac{d}{dr}\left[\frac{1}{r}\frac{d(ru_n)}{dr}\right]\right] \tag{3.82}$$

$$0 = \frac{1}{r}\frac{d}{dr}\left[r\frac{dw_n}{dr}\right] + \left(\frac{\omega^2}{c_L^2} - k_n^2\right)w_n + (1-c^2)\left[\frac{2}{r}\frac{d(r\Omega_n)}{dr} + \frac{1}{r}\frac{d(rw_n}{dr}\right] \tag{3.83}$$

Two more equations involving the four radial eigenfunctions are needed. Consider the equations of motion in terms of the dilatation and rotation.

$$\ddot{u} = c_L^2 \frac{\partial \Delta}{\partial r} + 2c_T^2 \frac{\partial \Omega}{\partial z} \tag{3.84}$$

$$\ddot{w} = c_L^2 \frac{\partial \Delta}{\partial z} + \frac{2}{r} c_T^2 \frac{\partial (r\Omega)}{\partial r} \tag{3.85}$$

By differentiating, these two equations can be uncoupled into wave equations for the dilatation and rotation. First, perform the operations:

$$\frac{1}{r}\frac{\partial}{\partial r}[r(3.84)] + \frac{\partial}{\partial z}[(3.85)] \tag{3.86}$$

This will yield a wave equation for the dilatation:

$$\ddot{\Delta} = c_L^2 \left[\frac{1}{r}\frac{\partial}{\partial r}\left(r\frac{\partial \Delta}{\partial r} \right) + \frac{\partial^2 \Delta}{\partial z^2} \right] \tag{3.87}$$

Similarly,

$$\frac{\partial}{\partial z}[(3.84)] - \frac{\partial}{\partial r}[(3.85)] \tag{3.88}$$

will yield a wave equation for the rotation:

$$\ddot{\Omega} = c_T^2 \frac{\partial}{\partial r}\left[\frac{1}{r}\frac{\partial (r\Omega)}{\partial r} \right] + c_T^2 \frac{\partial^2 \Omega}{\partial z^2} \tag{3.89}$$

These equations agree with the intuition that the dilatation will travel with the speed of a longitudinal wave and the rotation will travel with the speed

of a shear wave. Applying the eigenfunction expansions for Δ and Ω to the wave equations for Δ and Ω, eqn.(3.76) and (3.77), two additional equations are obtained involving the square of the eigenvalue k_n.

$$0 = \frac{1}{r}\frac{d}{dr}\left[r\frac{d\Delta_n}{dr}\right] + \left(\frac{\omega^2}{c_L^2} - k_n^2\right)\Delta_n \tag{3.90}$$

$$0 = \frac{d}{dr}\left[\frac{1}{r}\frac{d}{dr}(r\Omega_n)\right] + \left(\frac{\omega^2}{c_T^2} - k_n^2\right)\Omega_n \tag{3.91}$$

3.3.2 Boundary Conditions

Determing the radial eigenfunctions and eigenvalues is now acheived by solving eqn.(3.82), (3.83), (3.90) and (3.91) along with the appropriate boundary conditions. The condition that the inner and outer surfaces of the shell remain traction free is written as:

$$\sigma_{rr} = 0 \text{ at } r = a, b \tag{3.92}$$

$$\sigma_{rz} = 0 \text{ at } r = a, b \tag{3.93}$$

where a and b are the inner and outer radii of the shell, respectively. The stresses in eqn.(3.92) and (3.93) can be expressed in terms of u, w, Δ and Ω.

$$\sigma_{rr} = 2\mu\left(\Omega + \frac{dw}{dz}\right) \tag{3.94}$$

$$\sigma_{rz} = \lambda\Delta + 2\mu\frac{du}{dr} \tag{3.95}$$

In terms of radial eigenfunctions these boundary conditions can be expressed as:

$$\Omega_n + \frac{dw_n}{dr} = 0 \text{ at } r = a, b \tag{3.96}$$

$$\lambda\Delta_n + 2\mu\frac{du_n}{dr} = 0 \text{ at } r = a, b \tag{3.97}$$

After solving these BVP's, what remains is finding the bi-orthogonality relationship and applying it to determine the constants, a_n. This relationship is found for the isotropic cylinder by directly manipulating the equations of motion, [9, 15]. However, dealing with each type of material symmetry separately by using the differential equations can be avoided by employing the dynamic reciprocal identity. Gregory, [20], derives the necessary bi-orthogonality relationship from the reciprocal identity for cylinders of any material that has the planes z=constant as planes of symmetry. His relationship is also applicable to cylinders of general cross-sectional shape, not just circular.

This method is very general. The bi-orthogonality relation has been shown to exist for very larger class of materials, but so far the method has been used only on isotropic problems. For anisotropic materials it is not clear how to include the eigenvalues, k_n, in only one form. For the isotropic case the governing differential equations were manipulated until the eigenvalues were squared in each equation. This is possible because the dilatation and rotation are uncoupled in isotropic materials. In general, for anisotropic materials, the dilatation and rotation are coupled, thus making it impossible to use the same approach.

Chapter 4

SUPERPOSITION OF PROPAGATING MODES

The method of superposition of propagating modes will be used to construct solutions to the fundamental problem of waves in a transversely isotropic shell. This solution can then be extended to include layered cylinders. This technique is consistent with the approach employed by Nagy and Nayfeh. [43]. However, it is repeated here to extend the method to obtain physically meaningful quantities such as displacements and stresses in the layered cylinder.

This method is a variation of the eigenfunction expansion method. In the eigenfunction expansion, a series solution is sought for any quantity of interest. In the present approach the advantage of a couple of physical insights is used. First, an input, a normal pressure σ_{zz} at a fixed frequency, will produce a response of the same frequency in the absence of non-linearities. The actual input will be assumed to be composed of a finite number of frequen-

cies. Therefore, the response will be a superposition of responses at the same frequencies. The assumption of a finite frequency input does not represent a significant limitation because even an infinite number of frequencies in the input can be combined with a Fourier decomposition to find the frequencies with the largest Fourier coefficients. The response of the shell to these frequencies will dominate the solution.

The second physical insight used to simplify the process is that at any given frequency, only a finite number of modes will propagate down the waveguide without attenuation. An infinite number of modes are generated in order to satisfy the end conditions, but those modes above the cutoff frequency will be evanescent and will decay exponentially. Because of the exponential decay along the length of the waveguide the contribution these modes make to the overall response will become negligible.

The advantage of this insight is that the response of the shell can be represented as a finite sum of propagating modes. One apparent disadvantage is that by ignoring all attenuating modes, the end conditions on the shell are only satisfied approximately. However, by selecting an appropriate inner product for the end condition and the modes, no limitations on the accuracy of the solution exist. In practice, a simplified inner product is usually used because of the complexity of the orthogonality relationship, [66].

4.1 Constructing Mode Shapes

The axisymmetric equations of motion, for any material symmetry, are given by:

$$\rho\frac{\partial^2 u}{\partial t^2} = \frac{1}{r}\frac{\partial}{\partial r}(r\sigma_{rr}) - \frac{\sigma_{\theta\theta}}{r} + \frac{\partial \sigma_{rz}}{\partial z} \tag{4.1}$$

$$\rho\frac{\partial^2 w}{\partial t^2} = \frac{1}{r}\frac{\partial}{\partial r}(r\sigma_{rz}) + \frac{\partial \sigma_{zz}}{\partial z}. \tag{4.2}$$

In these equations σ_{ij} are the components of stress, ρ is the density and u and w are the radial and axial components of displacement, respectively.

For a transversely isotropic solid the non-vanishing components of stress under axisymmetry may be written in terms of the displacements

$$\sigma_{rr} = c_{11}\frac{\partial u}{\partial r} + c_{12}\frac{u}{r} + c_{13}\frac{\partial w}{\partial z} \tag{4.3}$$

$$\sigma_{\theta\theta} = c_{12}\frac{\partial u}{\partial r} + c_{11}\frac{u}{r} + c_{13}\frac{\partial w}{\partial z} \tag{4.4}$$

$$\sigma_{zz} = c_{13}\frac{1}{r}\frac{\partial}{\partial r}(ru) + c_{33}\frac{\partial w}{\partial z} \tag{4.5}$$

$$\sigma_{rz} = c_{44}\left(\frac{\partial u}{\partial z} + \frac{\partial w}{\partial r}\right) \tag{4.6}$$

where c_{ij} refers to the contracted notation for the 4^{th} order constitutive tensor for a Hookean solid. Using these relationships between stress and displacment the equations of motion can be written as:

$$\rho\frac{\partial^2 u}{\partial t^2} = c_{11}\frac{\partial}{\partial r}\left[\frac{1}{r}\frac{\partial}{\partial r}(ru)\right] + (c_{13}+c_{44})\frac{\partial^2 w}{\partial r \partial z} + c_{44}\frac{\partial^2 u}{\partial z^2} \tag{4.7}$$

$$\rho\frac{\partial^2 w}{\partial t^2} = (c_{13}+c_{44})\frac{1}{r}\frac{\partial}{\partial r}\left(r\frac{\partial u}{\partial z}\right) + c_{44}\frac{1}{r}\frac{\partial}{\partial r}\left(r\frac{\partial w}{\partial r}\right) + c_{33}\frac{\partial^2 w}{\partial z^2} \tag{4.8}$$

The propagating modes of this solid are sought when it is excited by a normal pressure applied to the end at $z = 0$. This can be formulated as a part of the model through the application of the boundary condition

$$\sigma_{zz}\mid_{z=0} = P(r,t). \tag{4.9}$$

In addition, the curved surfaces at the inner and outer radius of the shell are to remain traction free. This implies that

$$\sigma_{rr}\mid_{r=a,b} = 0 \tag{4.10}$$

$$\sigma_{rz}\mid_{r=a,b} = 0. \tag{4.11}$$

Equations (4.7) through eqn.(4.11) compose a boundary value problem (BVP) for the displacements. The analysis of this problem is begun by attempting to solve these PDE's and then considering the consequences of the boundary conditions. For the case of an isotropic shell (see section 3.1) the displacements are a superposition of traveling waves of the form

$$u = \left[AJ_1(pr) + BJ_1(qr) + CY_1(pr) + DY_1(qr)\right] e^{i(kz-\omega t)} \tag{4.12}$$

$$w = \left[EJ_0(pr) + FJ_0(qr) + GY_0(pr) + HY_0(qr)\right] e^{i(kz-\omega t)} \tag{4.13}$$

where $p^2 = \frac{\omega^2}{c_L^2} - k^2$, $q^2 = \frac{\omega^2}{c_T^2} - k^2$ and c_L and c_T are material constants.

From this result it is reasonable to assume that the displacements in the transversely isotropic shell will be similar. Therefore, the modes are assumed to take the form

$$u = A\mathcal{B}_1(\gamma r)e^{i(kz-\omega t)} \tag{4.14}$$

$$w = B\mathcal{B}_0(\gamma r)e^{i(kz-\omega t)}. \tag{4.15}$$

The functions $\mathcal{B}_0$ and $\mathcal{B}_1$ are Bessel functions of order 0 and 1, respectively, and A and B are arbitrary constants. The Bessel functions may be of the first or second kind. In the isotropic shell Bessel functions of the first and second kind were present. The radial wavenumber γ has yet to be determined in eqn.(4.14) and (4.15). In the isotropic shell γ had two values, p and q, which depended on the frequency, ω, the material constants, c_L and c_T and the axial wavenumber, k. It is therefore reasonable to expect γ to depend on the corresponding quantities for the transversely isotropic shell. The frequency, ω, material constants, c_{ij} and axial wavenumber, k.

Upon substituting eqn.(4.14) and (4.15) into eqn.(4.7) and (4.8), a 2×2 system of linear algebraic equations is obtained for A and B.

$$\begin{bmatrix} \rho\omega^2 - c_{11}\gamma^2 - c_{44}k^2 & -ik\gamma(c_{13} + c_{44}) \\ ik\gamma(c_{13} + c_{44}) & \rho\omega^2 - c_{44}\gamma^2 - c_{33}k^2 \end{bmatrix} \begin{bmatrix} A \\ B \end{bmatrix} = \begin{bmatrix} 0 \\ 0 \end{bmatrix} \tag{4.16}$$

Existence of non-trivial solutions requires that the determinant of the coefficient matrix vanish. This gives a quadratic equation in γ^2.

$$0 = b_0 + b_1\gamma^2 + b_2\gamma^4 \tag{4.17}$$

Since the coefficients in this equation are expressions involving ω, k, ρ and the c_{ij}'s, the initial interpretation of the nature of γ is consistent with the isotropic cylinder.

If the two solutions to eqn.(4.17), viewed as a quadratic in γ^2, are given the labels γ_1^2 and γ_2^2, then solutions to the quartic equation are $\pm\gamma_1$ and $\pm\gamma_2$. This represents four solutions to the original differential equations. The

solution for a single mode should be a sum of these four solutions. However, $\mathcal{B}_0(-\gamma r) = \mathcal{B}_0(\gamma r)$ and $\mathcal{B}_1(-\gamma r) = -\mathcal{B}_1(\gamma r)$ so only γ_1 and γ_2 contribute linearly independent solutions. Thus, it is possible to let the contributions from $-\gamma_1$ and $-\gamma_2$ be absorbed into the solutions from γ_1 and γ_2.

One more piece of information can be obtained from the matrix equation for A and B. There exists a constant ξ such that $B = \xi A$. This constant will reduce the number of arbitrary constants in the general solution. It is easily shown that:

$$\xi_{1,2} = \frac{\rho\omega^2 - c_{11}\gamma_{1,2}^2 - c_{44}k^2}{ik\gamma_{1,2}(c_{13} + c_{44})}. \tag{4.18}$$

Assume that $\mathcal{B}_0 = J_0$ and $\mathcal{B}_1 = J_1$. Then the expression for the displacements would be a linear combination of the solutions corresponding to γ_1 and γ_2.

$$\begin{aligned} u &= [A_1 J_1(\gamma_1 r) + A_2 J_1(\gamma_2 r)]\, e^{i(kz-\omega t)} && (4.19)\\ w &= [B_1 J_0(\gamma_1 r) + B_2 J_0(\gamma_2 r)]\, e^{i(kz-\omega t)} && (4.20)\\ &= [A_1\xi_1 J_0(\gamma_1 r) + A_2\xi_2 J_0(\gamma_2 r)]\, e^{i(kz-\omega t)} \end{aligned}$$

If instead, $\mathcal{B}_0 = Y_0$ and $\mathcal{B}_1 = Y_1$. Then the displacements would be

$$\begin{aligned} u &= \left[\bar{A}_1 Y_1(\gamma_1 r) + \bar{A}_2 Y_1(\gamma_2 r)\right] e^{i(kz-\omega t)} && (4.21)\\ w &= \left[\bar{B}_1 Y_0(\gamma_1 r) + \bar{B}_2 Y_0(\gamma_2 r)\right] e^{i(kz-\omega t)} && (4.22)\\ &= \left[\bar{A}_1\xi_1 Y_0(\gamma_1 r) + \bar{A}_2\xi_2 Y_0(\gamma_2 r)\right] e^{i(kz-\omega t)}. \end{aligned}$$

These two possible solutions are linearly independent, therefore, a full solution must be a linear combination of the two. Since the constants are already arbitrary the solution is the sum of the two solutions.

$$u = \left[A_1 J_1(\gamma_1 r) + A_2 J_1(\gamma_2 r) + \bar{A}_1 Y_1(\gamma_1 r) + \bar{A}_2 Y_1(\gamma_2 r)\right] e^{i(kz-\omega t)} \qquad (4.23)$$

$$w = \left[A_1 \xi_1 J_0(\gamma_1 r) + A_2 \xi_2 J_0(\gamma_2 r) + \bar{A}_1 \xi_1 Y_0(\gamma_1 r) + \bar{A}_2 \xi_2 Y_0(\gamma_2 r)\right] e^{i(kz-\omega t)} \qquad (4.24)$$

4.2 The Stresses

The next step is to consider the stresses that correspond to the displacements constructed in the previous section. These expressions will be used in the following section to derive a frequency equation. The number of modes that propagate in the shell without attenuation will be determined by finding the roots of the frequency equation. The expression for the stress applied at the end of the shell, σ_{zz}, can then be represented as an expansion over all modes to find the amplitudes of the propagating modes.

For compactness of notation, the common term of $e^{i(kz-\omega t)}$ will be suppressed. The stresses are then:

$$
\begin{aligned}
\sigma_{rr} &= c_{11}\frac{\partial u}{\partial r} + c_{12}\frac{u}{r} + c_{13}\frac{\partial w}{\partial z} \qquad (4.25)\\
&= \left[(c_{11}\gamma_1 + ikc_{13}\xi_1)J_0(\gamma_1 r) + (c_{12}-c_{11})\frac{1}{r}J_1(\gamma_1 r)\right] A_1\\
&+ \left[(c_{11}\gamma_1 + ikc_{13}\xi_1)Y_0(\gamma_1 r) + (c_{12}-c_{11})\frac{1}{r}Y_1(\gamma_1 r)\right] \bar{A}_1\\
&+ \left[(c_{11}\gamma_2 + ikc_{13}\xi_2)J_0(\gamma_2 r) + (c_{12}-c_{11})\frac{1}{r}J_1(\gamma_2 r)\right] A_2\\
&+ \left[(c_{11}\gamma_2 + ikc_{13}\xi_2)Y_0(\gamma_2 r) + (c_{12}-c_{11})\frac{1}{r}Y_1(\gamma_2 r)\right] \bar{A}_2
\end{aligned}
$$

$$
\begin{aligned}
\sigma_{zz} &= c_{13}\frac{1}{r}\frac{\partial}{\partial r}(ru) + c_{33}\frac{\partial w}{\partial z} \qquad (4.26)\\
&= \left[(c_{13}\gamma_1 + ikc_{33}\xi_1)J_0(\gamma_1 r)\right] A_1\\
&+ \left[(c_{13}\gamma_1 + ikc_{33}\xi_1)Y_0(\gamma_1 r)\right] \bar{A}_1\\
&+ \left[(c_{13}\gamma_2 + ikc_{33}\xi_2)J_0(\gamma_2 r)\right] A_2\\
&+ \left[(c_{13}\gamma_2 + ikc_{33}\xi_2)Y_0(\gamma_2 r)\right] \bar{A}_2
\end{aligned}
$$

$$
\begin{aligned}
\sigma_{rz} &= c_{44}\left(\frac{\partial u}{\partial z} + \frac{\partial w}{\partial r}\right) \qquad (4.27)\\
&= \left[c_{44}(ik - \gamma_1\xi_1)J_1(\gamma_1 r)\right] A_1\\
&+ \left[c_{44}(ik - \gamma_1\xi_1)Y_1(\gamma_1 r)\right] \bar{A}_1\\
&+ \left[c_{44}(ik - \gamma_2\xi_2)J_1(\gamma_2 r)\right] A_2\\
&+ \left[c_{44}(ik - \gamma_2\xi_2)Y_1(\gamma_2 r)\right] \bar{A}_2
\end{aligned}
$$

4.3 The Frequency Equation

The frequency equation is derived from the traction free conditions on the inner and outer surface of the shell. The equation relates the frequency, ω, and the axial wave number, k. In general, for multi-mode waveguides it is of the form

$$F(\omega, k) = 0. \tag{4.28}$$

If we consider ω as being fixed the k's that satisfy eqn.(4.28) form a discrete set, $\{k_1, k_2, \ldots\}$. For each of these k's there is an admissible mode in the shell that should be considered.

The displacements for a fixed frequency response are of the form:

$$u = u(r, z, t; k) \tag{4.29}$$

$$w = w(r, z, t; k). \tag{4.30}$$

It is well established that there may be more than one admissible value of k for any single frequency. Thus, using the priciple of superposition, the displacements must be a sum of these admissible modes.

$$u = \sum_j u(r, z, t; k_{(j)}) \tag{4.31}$$

$$w = \sum_j w(r, z, t; k_{(j)}) \tag{4.32}$$

Similarly, the stresses in the shell will be a sum over a set of admissible modes. In the final analysis only a finite number of the k's are retained.

The resulting sums are finite. The finite number of k terms also keeps the analysis relatively simple and makes the use of limit operations, such as differentiation, justified.

In order to obtain the frequency equation consider a single mode traveling down the length of the shell. At the inner and outer curved surfaces of the shell the stresses σ_{rr} and σ_{rz} are zero. Evaluating the expressions in eqn.(4.25) and (4.27) at $r = a$ and $r = b$ four equations are obtained for the four constants A_1, $\bar{A}_1$, A_2 and $\bar{A}_2$.

$$\begin{bmatrix} M_{11} & \cdots & M_{14} \\ \vdots & \ddots & \vdots \\ M_{41} & \cdots & M_{44} \end{bmatrix} \begin{bmatrix} A_1 \\ \bar{A}_1 \\ A_2 \\ \bar{A}_2 \end{bmatrix} = \begin{bmatrix} 0 \\ 0 \\ 0 \\ 0 \end{bmatrix} \tag{4.33}$$

The entries in the coefficient matrix are

$$
\begin{aligned}
M_{11} &= (c_{11}\gamma_1 + ikc_{13}\xi_1)J_0(\gamma_1 a) + (c_{12} - c_{11})\frac{1}{a}J_1(\gamma_1 a) \\
M_{12} &= (c_{11}\gamma_1 + ikc_{13}\xi_1)Y_0(\gamma_1 a) + (c_{12} - c_{11})\frac{1}{a}Y_1(\gamma_1 a) \\
M_{13} &= (c_{11}\gamma_2 + ikc_{13}\xi_2)J_0(\gamma_2 a) + (c_{12} - c_{11})\frac{1}{a}J_1(\gamma_2 a) \\
M_{14} &= (c_{11}\gamma_2 + ikc_{13}\xi_2)Y_0(\gamma_2 a) + (c_{12} - c_{11})\frac{1}{a}Y_1(\gamma_2 a) \\
M_{21} &= (c_{11}\gamma_1 + ikc_{13}\xi_1)J_0(\gamma_1 b) + (c_{12} - c_{11})\frac{1}{b}J_1(\gamma_1 b) \\
M_{22} &= (c_{11}\gamma_1 + ikc_{13}\xi_1)Y_0(\gamma_1 b) + (c_{12} - c_{11})\frac{1}{b}Y_1(\gamma_1 b) \\
M_{23} &= (c_{11}\gamma_2 + ikc_{13}\xi_2)J_0(\gamma_2 b) + (c_{12} - c_{11})\frac{1}{b}J_1(\gamma_2 b) \\
M_{24} &= (c_{11}\gamma_2 + ikc_{13}\xi_2)Y_0(\gamma_2 b) + (c_{12} - c_{11})\frac{1}{b}Y_1(\gamma_2 b) \\
M_{31} &= \frac{c_{44}}{2}(ik - \gamma_1\xi_1)J_1(\gamma_1 a) \\
M_{32} &= \frac{c_{44}}{2}(ik - \gamma_1\xi_1)Y_1(\gamma_1 a) \\
M_{33} &= \frac{c_{44}}{2}(ik - \gamma_2\xi_2)J_1(\gamma_2 a) \\
M_{34} &= \frac{c_{44}}{2}(ik - \gamma_2\xi_2)Y_1(\gamma_2 a) \\
M_{41} &= \frac{c_{44}}{2}(ik - \gamma_1\xi_1)J_1(\gamma_1 b) \\
M_{42} &= \frac{c_{44}}{2}(ik - \gamma_1\xi_1)Y_1(\gamma_1 b) \\
M_{43} &= \frac{c_{44}}{2}(ik - \gamma_2\xi_2)J_1(\gamma_2 b) \\
M_{44} &= \frac{c_{44}}{2}(ik - \gamma_2\xi_2)Y_1(\gamma_2 b).
\end{aligned}
$$

The determinant of the coefficient matrix must vanish for non-trivial solutions to exist. The evaluation of the determinant of the coefficient matrix results in the frequency equation that relates ω and k. For the transversely isotropic shell the resulting expression is quite complicated. The values of

k that satisfy the equation may be ootained by a numerical method. In Appendix A, a copy of the Matlab code to find the roots of the frequency equation is shown.

4.4 The Modal Coefficients

In addition to the wavenumbers, it is neccessary to determine the amplitudes of the modes. It is assumed in this discussion that the k values that satisfy the frequency equation have been obtained. In fact, to actually meet all of the conditions at $z = 0$ all of the modes are required. However, in order to determine the amplitudes it is not neccessaary to have all of the modes, since a simple inner product can be used to find the amplitudes of any single mode, independent from the others. It is useful to note the independence of these calculations since in the end only a finite number of modes will be used.

All of the analysis assumes a single frequency excitation and response. The applied stress can then be written as:

$$\sigma_{zz} \mid_{z=0} = f_\omega(r) e^{-\imath\omega t} \tag{4.34}$$

Assume that $\{k_1, \ldots, k_K\}$ are the wavenumbers that are kept. Then, summing over these modes in eqn.(4.26) and equating to eqn.(4.34), an expression for $f_\omega(r)$ may be obtained.

$$
\begin{aligned}
f_\omega(r) &= \sum_{j=1}^{K} \left[(c_{13}\gamma_{1(j)} + ik_{(j)}c_{33}\xi_{1(j)}) J_0(\gamma_{1(j)}r) \right] A_{1(j)} \qquad (4.35) \\
&+ \sum_{j=1}^{K} \left[(c_{13}\gamma_{1(j)} + ik_{(j)}c_{33}\xi_{1(j)}) Y_0(\gamma_{1(j)}r) \right] \bar{A}_{1(j)} \\
&+ \sum_{j=1}^{K} \left[(c_{13}\gamma_{2(j)} + ik_{(j)}c_{33}\xi_{2(j)}) J_0(\gamma_{2(j)}r) \right] A_{2(j)} \\
&+ \sum_{j=1}^{K} \left[(c_{13}\gamma_{2(j)} + ik_{(j)}c_{33}\xi_{2(j)}) Y_0(\gamma_{2(j)}r) \right] \bar{A}_{2(j)}.
\end{aligned}
$$

To determine coefficients $A_{1(m)}$, $\bar{A}_{1(m)}$, $A_{2(m)}$ and $\bar{A}_{2(m)}$, $m = 1, \ldots, K$, several inner products must be taken on both sides of this equation. First, eqn.(4.35) is multiplied by $J_0(\gamma_{1(m)}r)$ and integrated from a to b. The integration may be passed inside the sums with since they are finite. The index m is varied from 1 to K, yielding K equations of the form:

$$
\begin{aligned}
\int_a^b J_0(\gamma_{1(m)}r) f_\omega(r) dr &= \sum_{j=1}^{K} \left[(c_{13}\gamma_{1(j)} + ik_{(j)}c_{33}\xi_{1(j)}) \int_a^b J_0(\gamma_{1(m)}r) J_0(\gamma_{1(j)}r) dr \right] A_{1(j)} \\
&+ \sum_{j=1}^{K} \left[(c_{13}\gamma_{1(j)} + ik_{(j)}c_{33}\xi_{1(j)}) \int_a^b J_0(\gamma_{1(m)}r) Y_0(\gamma_{1(j)}r) dr \right] \bar{A}_{1(j)} \\
&+ \sum_{j=1}^{K} \left[(c_{13}\gamma_{2(j)} + ik_{(j)}c_{33}\xi_{2(j)}) \int_a^b J_0(\gamma_{1(m)}r) J_0(\gamma_{2(j)}r) dr \right] A_{2(j)} \\
&+ \sum_{j=1}^{K} \left[(c_{13}\gamma_{2(j)} + ik_{(j)}c_{33}\xi_{2(j)}) \int_a^b J_0(\gamma_{1(m)}r) Y_0(\gamma_{2(j)}r) dr \right] \bar{A}_{2(j)} \\
m &= 1, \ldots, K.
\end{aligned}
$$

This process is repeated three more times, each time resulting in K more

equations. Equation(4.35) is multiplied by $Y_0(\gamma_{1(m)}r)$, $m = 1, \ldots, K$, and integrated from a to b. Next, multiply eqn.(4.35) by $J_0(\gamma_{2(m)}r)$, $m = 1, \ldots, K$, and integrate. Last, multiply by $Y_0(\gamma_{2(m)}r)$, $m = 1, \ldots, K$, and integrate. Through this process a $4K \times 4K$ system of equations is obtained for the coefficients.

The system is of the form:

$$SA = F \tag{4.36}$$

where S is the coefficient matrix, A is the vector of unknown modal coefficients and F is a vector of inner products involving the input fucntion $f_\omega(r)$. The components of the vectors A and F are given by:

$$A = \begin{bmatrix} A_{1(1)} \\ \vdots \\ A_{1(K)} \\ \bar{A}_{1(1)} \\ \vdots \\ \bar{A}_{1(K)} \\ A_{2(1)} \\ \vdots \\ A_{2(K)} \\ \bar{A}_{2(1)} \\ \vdots \\ \bar{A}_{2(K)} \end{bmatrix}, \qquad F = \begin{bmatrix} \int_a^b J_0(\gamma_{1(1)}r) f_\omega(r) dr \\ \vdots \\ \int_a^b J_0(\gamma_{1(K)}r) f_\omega(r) dr \\ \int_a^b Y_0(\gamma_{1(1)}r) f_\omega(r) dr \\ \vdots \\ \int_a^b Y_0(\gamma_{1(K)}r) f_\omega(r) dr \\ \int_a^b J_0(\gamma_{2(1)}r) f_\omega(r) dr \\ \vdots \\ \int_a^b J_0(\gamma_{2(K)}r) f_\omega(r) dr \\ \int_a^b Y_0(\gamma_{2(1)}r) f_\omega(r) dr \\ \vdots \\ \int_a^b Y_0(\gamma_{2(K)}r) f_\omega(r) dr \end{bmatrix} \tag{4.37}$$

The components of the matrix S may be obtained in the following way:

Rows $1, \ldots, K$: These coefficients are obtained from the inner product of eqn.(4.35) with $J_0(\gamma_{1(m)}r)$, $m = 1, \ldots, K$.

Rows $K+1, \ldots, 2K$: These coefficients are obtained from the inner product of eqn.(4.35) with $Y_0(\gamma_{1(m)}r)$, $m = 1, \ldots, K$.

Rows $2K+1, \ldots, 3K$: These coefficients are obtained from the inner product of eqn.(4.35) with $J_0(\gamma_{2(m)}r)$, $m = 1, \ldots, K$.

Rows $3K+1, \ldots, 4K$: These coefficients are obtained from the inner product of eqn.(4.35) with $Y_0(\gamma_{2(m)}r)$, $m = 1, \ldots, K$.

Another issue that should be addressed is the orthogonality of the Bessel functions. From basic Sturm-Liouville theory it is true that within the proper inner product space the solutions of eqn.(4.7) and (4.8), of the form in eqn.(4.14) and (4.15), should be orthogonal. Using the inner product from the appropriate space on eqn.(4.35), instead of the one used, would lead to a diagonal system of equations for the amplitudes, i.e. the matrix S would be diagonal. This would greatly reduce the overall number of calculations necessary to construct the response of the shell. However, the appropriate inner product to use is unclear. The simple inner product chosen, was selected for sufficiency and simplicity. The Bessel functions are at least linearly independent in this space, therefore, this choice is sufficient in that it leads to a non-singular matrix S.

4.5 Example

In this section, the method described in this chapter is applied to a specific transversely isotropic shell. The process begins by obtaining the dispersion curves from the frequency equation, which was found to be the determinant of the coefficient matrix M in eqn.(4.33). Using the information in the dispersion curves the admissible values of k corresponding to a single frequency are obtained. These k values are then used in expressions such as eqn.(4.17) and (4.18) to obtain the constants γ_1, γ_2, ξ_1 and ξ_2. These will be applied to evaluate the elements of the matrix M and solve the system in eqn.(4.33) to get the amplitudes of each mode. Once all of this is done eqn.(4.23) and (4.24) may be combined with eqn.(4.31) and (4.32) to yield explicit expressions for the displacements.

The shell being considered has an outer radius of 20cm and an inner radius of 10 cm. The shell will be subject to an harmonic normal pressure on the end, $\sigma_{zz} = fe^{-i\omega t}$ where f is constant across the cross section of the cylinder. The following material properties are typical values for Douglas Fir and were taken from Ritter, [53].

Using these material constants dispersion curves were found using the Matlab script *dispcurves.m*, found in Appendix A. The dispersion curves are shown in Fig.4.1.

For a single test case of a frequency of 6kHz, $\omega = (2\pi)6 \times 10^3$. From Fig.4.1 three real values of k are obtained at this frequency.

It is interesting to note that the shell, like a plate, has a non-dispersive mode. This contrasts with a homogeneous cylinder for which the lowest

c_{11}	4.07 GPa
c_{12}	2.69 GPa
c_{13}	0.24 GPa
c_{33}	6.89 GPa
c_{44}	0.49 GPa
ρ	800 kg/m^3
b	0.20 m
a	0.10 m

Table 4.1: Material Constants for Douglas Fir.

k_1	12.52
k_2	11.36
k_3	4.90

Table 4.2: Axial wavenumbers corresponding to $\omega = (2\pi)6 \times 10^3$.

mode is non-dispersive only in the low frequency limit. The phase velocity of any mode is $\frac{\omega}{k}$. The first mode is a straight line starting at the origin. Therefore, the ratio of ω to k is a constant for this mode, making the mode non-dispersive.

For each of the above values of k, γ and ξ are obtained by solving eqn.(4.17) for γ_1 and γ_2 and substituting these values into eqn.(4.18) to obtain ξ_1 and xi_2.

For each mode the system in eqn.(4.36) is solved to obtain the amplitudes.

These constants is all that is needed to construct the response of the shell

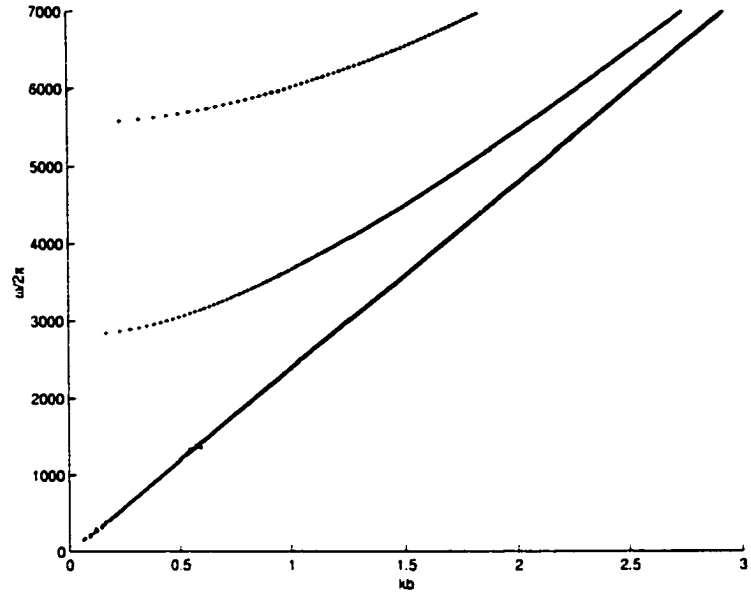

Figure 4.1: Dispersion curves for shell composed of Douglas Fir.

to the excitation at the frequency $\omega = (2\pi)6 \times 10^3$. At the outer surface of the shell, r=20cm, at a distance of 2m from the end where the normal pressure is applied, z=2m, the radial displacements look like:

The radial displacements of each mode have varying wavelengths, as can bee seen here. The higher modes, having lower axial wavenumbers, have the longer wavelengths.

The cross-sectional shape of axial displacements for each of the propagating modes look like:

These cross-sectional shapes don't have the regular structure such as in the modes traveling in a plate, [19]. However, it was shown by Simmons, [57], that the cross sectional shapes for anisotropic shells don't have the symmetry

$\gamma_{1(1)}$	19.22	$\xi_{1(1)}$	$3.44i$
$\gamma_{1(2)}$	32.49	$\xi_{1(2)}$	$17.77i$
$\gamma_{1(3)}$	63.01	$\xi_{1(3)}$	$100.29i$
$\gamma_{2(1)}$	12.99	$\xi_{2(1)}$	$-522.77i$
$\gamma_{2(2)}$	16.17	$\xi_{2(2)}$	$-48.42i$
$\gamma_{2(3)}$	16.67	$\xi_{2(3)}$	$-4.39i$

$A_{1(1)}$	0.005	$\bar{A}_{1(1)}$	-0.040	$A_{2(1)}$	0.030	$\bar{A}_{2(1)}$	0.008
$A_{1(2)}$	-0.0002	$\bar{A}_{1(2)}$	0.0	$A_{2(2)}$	-1.44	$\bar{A}_{2(2)}$	0.31
$A_{1(3)}$	0.0	$\bar{A}_{1(3)}$	0.0	$A_{2(3)}$	8.77	$\bar{A}_{2(3)}$	-5.26

Table 4.3: Modal coefficients, all quantities $\times 10^{-9}$.

often found in isotropic materials. It is also apparent, from the few modes plotted here, that the axial displacements become more concentrated near the outer radius of the shell with higher modes.

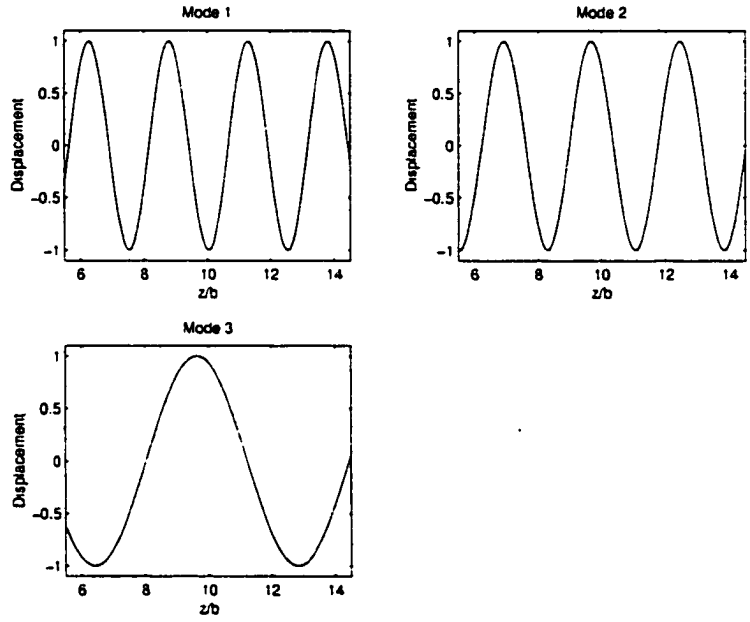

Figure 4.2: Radial displacements at r=0.2m.

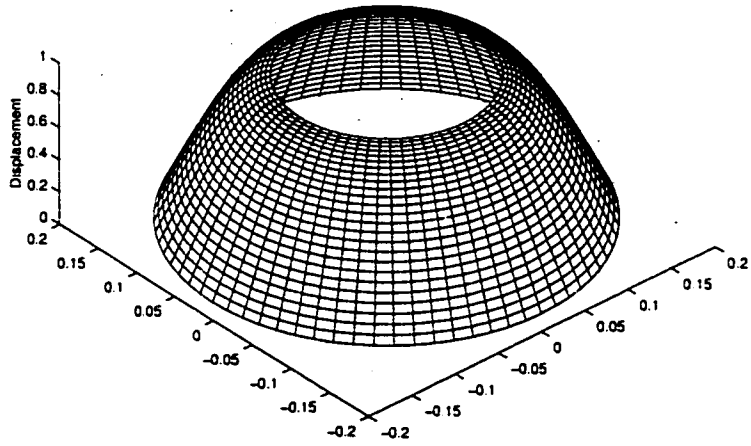

Figure 4.3: Shape of mode 1 axial displacements

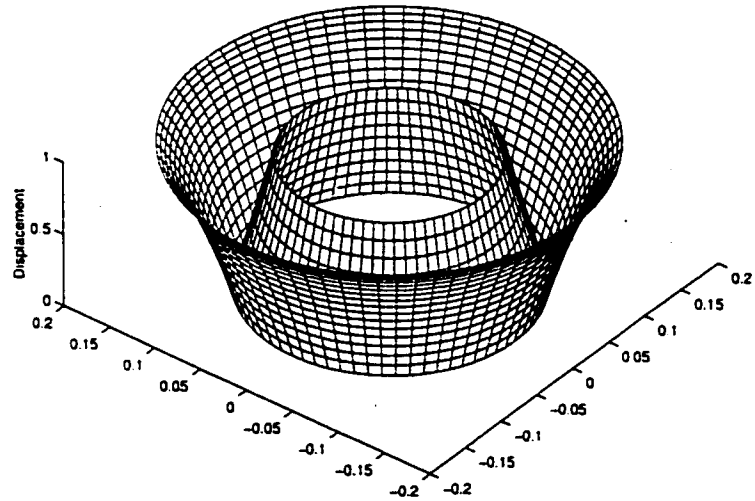

Figure 4.4: Shape of mode 2 axial displacements

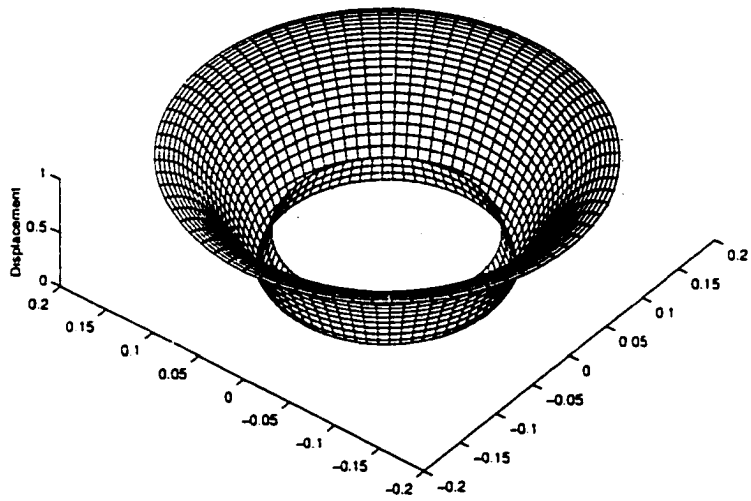

Figure 4.5: Shape of mode 3 axial displacements

Chapter 5

EXTENSION TO LAYERED CYLINDERS

5.1 The General Case

Very little literature exists concerning the dynamics of a layered cylinder because of the complexity of the problem. Numerical approaches have existed for some time, [21], but there is a nearly complete absence of analytic solutions to which numerical results may be compared.

One of the main references is a review tutorial directed at experimentalists by Thurston, [60]. The focus of the paper by Thurston is on the determination of dispersion relations for clad rods. Thurston also addresses the conditions under which Stonely waves can be generated at an interface between two layers of differing material properties. Nagy and Nayfeh, [43], treat the case of a layered transversely isotropic cylinder by using transfer matrices, a technique used extensively in cartesian geometries. The general

technique of the transfer matrices will be applied to extend the solution of the single cylindrical shell to that of a layered cylinder.

5.1.1 Local Transfer Matrix

Consider the response of a layered, transversely isotropic cylinder to a fixed frequency excitation. The construction is based on the results for a single shell. The first step is to formally construct a local transfer matrix. This transfer matrix relates the displacements and stresses within a single layer.

To set up the notation, consider a cylinder composed of homogeneous layers of a transversely isotropic material. All of the quantities are labeled by layer with a superscript. The outermost layer, layer 1, occupies the region between $r = r^1$ and $r = r^2$. The next outer layer, layer 2, lies between $r = r^2$ and $r = r^3$. This method of numbering the layers continues to the innermost layer, layer p. Layer p extends from $r = 0$ to $r = r^p$. A cross section of the cylinder is shown in Fig.5.1.

From the solution to the transversely isotropic shell the displacements in a single layer are:

$$u^l = \sum_j \left[A^l_{1(j)} J_1(\gamma^l_{1(j)} r) + \bar{A}^l_{1(j)} Y_1(\gamma^l_{1(j)} r) + A^l_{2(j)} J_1(\gamma^l_{2(j)} r) + \bar{A}^l_{2(j)} Y_1(\gamma^l_{2(j)} r)\right] \tag{5.1}$$

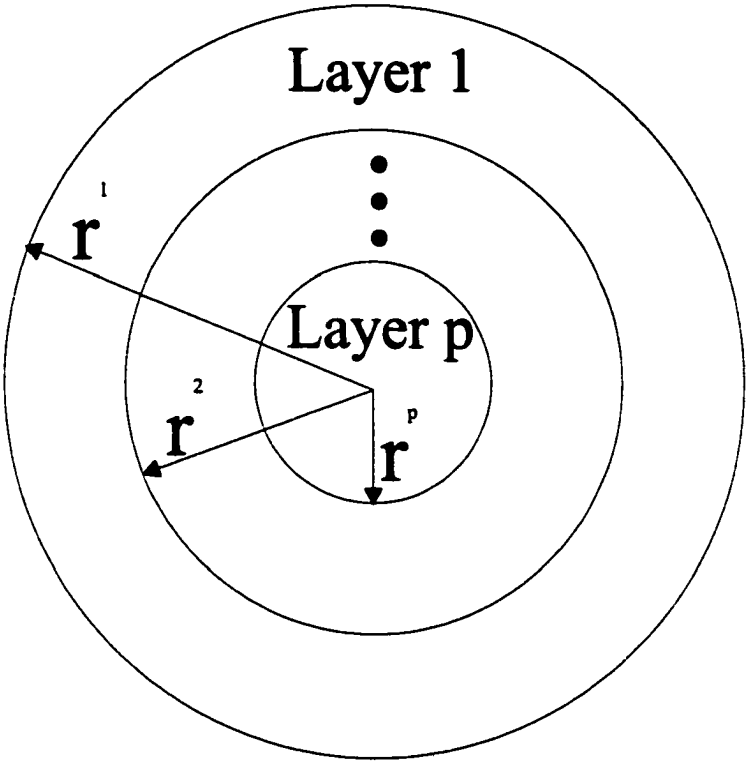

Figure 5.1: Labeling of the cylinder layers

$$
\begin{aligned}
w^l &= \sum_j \left[A^l_{1(j)}\xi^l_{1(j)}J_0(\gamma^l_{1(j)}r) + \bar{A}^l_{1(j)}\xi^l_{1(j)}Y_0(\gamma^l_{1(j)}r)\right] \qquad (5.2)\\
&+ \sum_j \left[A^l_{2(j)}\xi^l_{2(j)}J_1(\gamma^l_{2(j)}r) + \bar{A}^l_{2(j)}\xi^l_{1(j)}Y_0(\gamma^l_{2(j)}r)\right]
\end{aligned}
$$

where the sum over j is a sum over the modes and the term $e^{i(k_{(j)}z-\omega t)}$ is suppressed and the superscript l denotes the layer number. Similarly, the stresses may be written

$$\sigma^l_{rr} = \sum_j \left[(c^l_{11}\gamma^l_{1(j)} + ik^l_{(j)}c^l_{13}\gamma^l_{1(j)})J_0(\gamma^l_{1(j)}r) + (c^l_{12} - c^l_{11})\frac{1}{r}J_1(\gamma^l_{1(j)}r)\right] A^l_{1(j)} \quad (5.3)$$

$$+ \sum_j \left[(c^l_{11}\gamma^l_{1(j)} + ik^l_{(j)}c^l_{13}\gamma^l_{1(j)})Y_0(\gamma^l_{1(j)}r) + (c^l_{12} - c^l_{11})\frac{1}{r}Y_1(\gamma^l_{1(j)}r)\right] \bar{A}^l_{1(j)}$$

$$+ \sum_j \left[(c^l_{11}\gamma^l_{2(j)} + ik^l_{(j)}c^l_{13}\gamma^l_{2(j)})J_0(\gamma^l_{2(j)}r) + (c^l_{12} - c^l_{11})\frac{1}{r}J_1(\gamma^l_{2(j)}r)\right] A^l_{2(j)}$$

$$+ \sum_j \left[(c^l_{11}\gamma^l_{2(j)} + ik^l_{(j)}c^l_{13}\gamma^l_{2(j)})Y_0(\gamma^l_{2(j)}r) + (c^l_{12} - c^l_{11})\frac{1}{r}Y_1(\gamma^l_{2(j)}r)\right] \bar{A}^l_{2(j)}$$

$$\sigma^l_{rz} = \sum_j \left[c^l_{44}(ik^l_{(j)} - \gamma^l_{1(j)}\xi^l_{1(j)})J_1(\gamma^l_{1(j)}r)\right] A^l_{1(j)} \quad (5.4)$$

$$+ \sum_j \left[c^l_{44}(ik^l_{(j)} - \gamma^l_{1(j)}\xi^l_{1(j)})Y_1(\gamma^l_{1(j)}r)\right] \bar{A}^l_{1(j)}$$

$$+ \sum_j \left[c^l_{44}(ik^l_{(j)} - \gamma^l_{2(j)}\xi^l_{2(j)})J_1(\gamma^l_{2(j)}r)\right] A^l_{2(j)}$$

$$+ \sum_j \left[c^l_{44}(ik^l_{(j)} - \gamma^l_{2(j)}\xi^l_{2(j)})Y_1(\gamma^l_{2(j)}r)\right] \bar{A}^l_{2(j)}$$

The expression for the four quantities in layer l can be written in matrix-vector form as

$$\sum_j \begin{bmatrix} u^l_{(j)} \\ w^l_{(j)} \\ \sigma^l_{rr(j)} \\ \sigma^l_{rz(j)} \end{bmatrix} = \sum_j X^l_{(j)} \begin{bmatrix} A^l_{1(j)} \\ \bar{A}^l_{1(j)} \\ A^l_{2(j)} \\ \bar{A}^l_{2(j)} \end{bmatrix} \quad (5.5)$$

where, for example, $u^l_{(j)}$ is the j^{th} mode in the l^{th} layer of the radial displacement. The symbol $X^l_{(j)}$ represents a coefficient matrix. The components of this matrix may be found by examining the equations for the displacements and stresses.

If the following notations are used in the solution,

$$U^l_{(j)} = \begin{bmatrix} u^l_{(j)} \\ w^l_{(j)} \\ \sigma^l_{rr(j)} \\ \sigma^l_{rz(j)} \end{bmatrix} \text{ and} \tag{5.6}$$

$$A^l_{(j)} = \begin{bmatrix} A^l_{1(j)} \\ \bar{A}^l_{1(j)} \\ A^l_{2(j)} \\ \bar{A}^l_{2(j)} \end{bmatrix} \tag{5.7}$$

the expression which relates the displacements and stresses in a single layer can then be written compactly as:

$$\sum_j U^l_{(j)} = \sum_j X^l_{(j)} A^l_{(j)} \tag{5.8}$$

Equating coefficients of the suppressed $e^{i(k_{(j)}z-\omega t)}$.

$$U^l_{(j)} = X^l_{(j)} A^l_{(j)}. \tag{5.9}$$

Noting that the components of $U^l_{(j)} = U^l_{(j)}(r)$ and $X^l_{(j)} = X^l_{(j)}(r)$ are functions of r the notation is further extended as:

$$U^{l(inner,outer)}_{(j)} = U^l_{(j)}(r^{l+1}, r^l) \text{ and} \tag{5.10}$$

$$X^{l(inner,outer)}_{(j)} = X^l_{(j)}(r^{l+1}, r^l) \tag{5.11}$$

Using the two equations,

$$U_{(j)}^{l(inner)} = X_{(j)}^{l(inner)} A_{(j)}^{l} \text{ and} \tag{5.12}$$

$$U_{(j)}^{l(outer)} = X_{(j)}^{l(outer)} A_{(j)}^{l}, \tag{5.13}$$

the *inner* and *outer* solutions for the l^{th} layer can by related as:

$$U_{(j)}^{l(outer)} = X_{(j)}^{l(outer)} (X_{(j)}^{l(inner)})^{-1} U_{(j)}^{l(inner)} \tag{5.14}$$

Let $N_{(j)}^{l} = X_{(j)}^{l(outer)} (X_{(j)}^{l(inner)})^{-1}$ be defined as the local transfer matrix. The local transfer matrix relates properties of the *inner* and *outer* surface of a single layer.

5.1.2 Modes of the Composite Cylinder

The objective is to relate the properties between the layers. The properties can be related by the global transfer matrix. Before formally deriving the matrix, it is necessary to address some issues regarding modes that do not arise when considering a single layer.

Consider two adjoining layers in the cylinder. The layers are labeled as layer l and layer $l+1$. The outside surface of layer $l+1$ is in contact with the inside surface of layer l. To demonstrate the concept, consider the radial displacements.

$$u^l = \sum_j u^l_{(j)} = \sum_j g^l_{(j)}(r) e^{i(k^l_{(j)} z - \omega t)} \tag{5.15}$$

$$u^{l+1} = \sum_j u^{l+1}_{(j)} = \sum_j g^{l+1}_{(j)}(r) e^{i(k^{l+1}_{(j)} z - \omega t)} \tag{5.16}$$

$g_{(j)}(r)^m$ is shorthand for the radial dependence of each mode. More completely,

$$g^m_{(j)} = A^m_{1(j)} J_1(\gamma^m_{1(j)} r) + \bar{A}^m_{1(j)} Y_1(\gamma^m_{1(j)} r) + A^m_{2(j)} J_1(\gamma^m_{2(j)} r) + \bar{A}^m_{2(j)} Y_1(\gamma^m_{2(j)} r). \tag{5.17}$$

where the two shells meet, the radial displacements will be set equal. The difficulty lies in the fact that the $k^m_{(j)}$, the j^{th} wavenumber in layer m, is entirely dependent on the material properties of layer m alone. Therefore the sets $\{k^l_{(1)}, k^l_{(2)}, \dots\}$ and $\{k^{l+1}_{(1)}, k^{l+1}_{(2)} \dots\}$ might have no elements in common. This doesn't just create a computational difficulty in dealing with the entire sums for u^l and u^{l+1}. It creates a physical problem whose resolution will give us the justification for simplifying the computations.

The wavenumber and phase velocity of a single mode are related by

$$c = \frac{\omega}{k} \tag{5.18}$$

where c is the phase velocity. If there is a wavenumber $k^{l+1}_{(n)}$ that is not in the set $\{k^l_{(1)}, k^l_{(2)}, \dots\}$ then a disturbance will occur at the outer boundary of layer $l+1$ and travel with velocity $c^{l+1}_{(n)} = \frac{\omega}{k^{l+1}_{(n)}}$. It is impossible that this disturbance can occur in layer $l+1$ completely independent of what

happens in layer l, see Fig.5.2. This would contradict the assumption that displacements and stresses are continuous across layer boundaries. Therefore, the disturbance with velocity $c_{(n)}^{l+1}$ in layer $l+1$ will create a disturbance with the same velocity, and therefore the same wavenumber, in layer l. Thus, it is necessary to add $k_{(n)}^{l+1}$ to the set of wavenumbers in layer l.

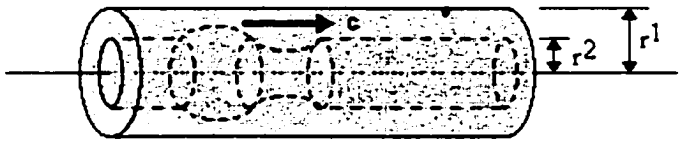

Figure 5.2: Disturbance in layer $l+1$

Using this same argument it is apparent that a global set of wavenumbers is required, $\{k_{(1)}, k_{(2)}, \dots\}$, that contains all the wavenumbers from each layer.

$$\{k_{(1)}, k_{(2)}, \dots\} = \bigcup_{l=1}^{p} \{k_{(1)}^{l}, k_{(2)}^{l}, \dots\} \tag{5.19}$$

Therefore, the layer label on the wavenumbers may be omitted. However, the layer label is still required on the γ's, ξ's and A's. All of these quantites have a dependence on the material properties of their respective layers.

There are two large advantages to using this 'global' set of wavenumbers. First, equality of any physical quantity, like a displacement or a stress, will

reduce to mode-wise equality. Thus, when performing any operations on the sums may be dropped. Second, there will be only one frequency equation. Considering the layered cylinder as p independent shells yields p different frequency equations, each with their own set of dispersion curves. Treating the layered cylinder as a whole, each layer affecting and being affected by every other layer, only one set of wavenumbers is generated from one frequency equation.

5.1.3 Global Transfer Matrix

Now, it is necessary to construct the relationship that exists between the solutions at the very outer edge of the cylinder and the very center. This is accomplished with the global transfer matrix. The global transfer matrix will also provide the means to obtain the single frequency equation for the layered cylinder.

Consider the solution at the outer edge of the cylinder.

$$\begin{aligned} U_{(j)}^{1(outer)} &= N_{(j)}^{1} U_{(j)}^{1(inner)} \\ &= N_{(j)}^{1} U_{(j)}^{2(outer)} \\ &= N_{(j)}^{1} N_{(j)}^{2} U_{(j)}^{2(inner)} \\ &\vdots \\ &= N_{(j)}^{1} N_{(j)}^{2} \cdots N_{(j)}^{p} U_{(j)}^{p(inner)} \\ &= Q_{(j)} U_{(j)}^{p(inner)} \end{aligned} \tag{5.20}$$

The matrices $N_{(j)}^{1}, N_{(j)}^{2}, \ldots, N_{(j)}^{p}$ are the local transfer matrices and the ma-

trix $Q_{(j)} = N^1_{(j)} N^2_{(j)} \cdots N^p_{(j)}$ is called the global transfer matrix.

To derive the frequency equation, recall eqn.(5.12).

$$\begin{aligned} U^{1(outer)}_{(j)} &= Q_{(j)} U^{p(inner)}_{(j)} \\ &= Q_{(j)} X^{p(inner)}_{(j)} A^p_{(j)} \end{aligned} \tag{5.21}$$

There exists information in the boundary conditions concerning $U^{1(outer)}_{(j)}$. Information about $U^{p(inner)}_{(j)}$ also exits in the requirement that physical quantities remain finite. First, the outside surface of the cylinder is traction free.

$$U^{1(outer)}_{(j)} = \begin{bmatrix} u^{1(outer)}_{(j)} \\ w^{1(outer)}_{(j)} \\ 0 \\ 0 \end{bmatrix} \tag{5.22}$$

Second, at the center of the cylinder all physical quantities must remain finite. Therefore, at $r = 0$ there can be no Bessel functions of the second kind. A typical element of $U^{p(inner)}_{(j)}$, the solution at the center of the cylinder, is of the form:

$$u^{p(inner)}_{(j)} = A^p_{1(j)} J_1(0) + \bar{A}^p_{1(j)} Y_1(0) + A^p_{2(j)} J_1(0) + \bar{A}^p_{2(j)} Y_1(0) \tag{5.23}$$

For this to be finite $\bar{A}^p_{1(j)}$ and $\bar{A}^p_{2(j)}$ must vanish. Therefore, the vector $A^p_{(j)}$ is of the form:

$$A^p_{(j)} = \begin{bmatrix} A^p_{1(j)} \\ 0 \\ A^p_{2(j)} \\ 0 \end{bmatrix} \tag{5.24}$$

Note that eqn.(5.24) gives the amplitudes for layer p only.

The expression in eqn.(5.21) may now be written as:

$$\begin{bmatrix} u^{1(outer)}_{(j)} \\ w^{1(outer)}_{(j)} \\ 0 \\ 0 \end{bmatrix} = \begin{bmatrix} Q'_{11(j)} & \cdots & Q'_{41(j)} \\ \vdots & \ddots & \vdots \\ Q'_{41(j)} & \cdots & Q'_{44(j)} \end{bmatrix} \begin{bmatrix} A^p_{1(j)} \\ 0 \\ A^p_{2(j)} \\ 0 \end{bmatrix} \tag{5.25}$$

where the product $Q_{(j)}.X^{p(inner)}_{(j)}$ is denoted by $Q'_{(j)}$. Writing out the 2×2 system corresponding to the third and fourth equations of eqn.(5.25) yields:

$$\begin{bmatrix} 0 \\ 0 \end{bmatrix} = \begin{bmatrix} Q'_{31(j)} & Q'_{33(j)} \\ Q'_{41(j)} & Q'_{43(j)} \end{bmatrix} \begin{bmatrix} A^p_{1(j)} \\ A^p_{2(j)} \end{bmatrix} \tag{5.26}$$

In order for non-trivial solutions to exist the determinant of the coefficient matrix in eqn.(5.26) must vanish. This generates a relationship between the frequency ω and the wavenumber k that is the frequency equation for the layered cylinder.

$$0 = Q'_{31(j)}Q'_{43(j)} - Q'_{33(j)}Q'_{41(j)} \tag{5.27}$$

The roots of this equation represent the modes that travel in the composite cylinder.

5.1.4 Amplitudes

The amplitudes of each component of each mode still need to be determined. If the set $\{k_1, k_2, \ldots, k_K\}$ is kept as the set of significant wavenumbers, then for an arbitrary layer l the displacements are of the form:

$$u^l = \sum_{j=1}^{K} \left[A^l_{1(j)} J_1(\gamma^l_{1(j)} r) + \bar{A}^l_{1(j)} Y_1(\gamma^l_{1(j)} r)\right] \tag{5.28}$$
$$+ \sum_{j=1}^{K} \left[A^l_{2(j)} J_1(\gamma^l_{2(j)} r) + \bar{A}^l_{2(j)} Y_1(\gamma^l_{2(j)} r)\right]$$

$$w^l = \sum_{j=1}^{K} \left[A^l_{1(j)} \xi^l_{1(j)} J_0(\gamma^l_{1(j)} r) + \bar{A}^l_{1(j)} \xi^l_{1(j)} Y_0(\gamma^l_{1(j)} r)\right] \tag{5.29}$$
$$+ \sum_{j=1}^{K} \left[A^l_{2(j)} \xi^l_{(2(j)} J_0(\gamma^l_{2(j)} r) + \bar{A}^l_{2(j)} \xi^l_{2(J)} Y_0(\gamma^l_{2(j)} r)\right].$$

The normal axial stress in layer l, σ^l_{zz}, may be written as:

$$\sigma^l_{zz} = c^l_{13} \frac{1}{r} \frac{\partial}{\partial r}(r u^l) + c^l_{33} \frac{\partial w^l}{\partial z} \tag{5.30}$$

$$= \sum_{j=1}^{K} \left[D^l_{1(j)} J_0(\gamma^l_{1(j)} r) A^l_{1(j)} + D^l_{1(j)} Y_0(\gamma^l_{1(j)} r) \bar{A}^l_{1(j)}\right] \tag{5.31}$$
$$+ \sum_{j=1}^{K} \left[D^l_{2(j)} J_0(\gamma^l_{2(j)} r) A^l_{2(j)} + D^l_{2(j)} Y_0(\gamma^l_{2(j)} r) \bar{A}^l_{2(j)}\right],$$

where $D^l_{s(j)} = c^l_{13} \gamma^l_{s(j)} + i k_{(j)} c^l_{33} \xi^l_{s(j)}$ for $s = 1, 2$.

The end stress, σ_{zz} at $z = 0$, will be used to determine the unknown amplitudes. Let the applied stress, at frequency ω, be expressed, as in eqn.(4.36)

$$\sigma_{zz} \mid_{z=0} = f_\omega(r)e^{-i\omega t}. \tag{5.32}$$

Denote the restriction of $f_\omega(r)$ to layer l by $f_\omega^l(r)$. Thus, $\sigma_{zz} \mid_{z=0}$ may be expressed as:

$$\sigma_{zz} \mid_{z=0} = \begin{cases} f_\omega^1(r) & \text{if } r^2 < r \leq r^1, \\ f_\omega^2(r) & \text{if } r^3 < r \leq r^2, \\ \vdots & \vdots \\ f_\omega^p(r) & \text{if } 0 \leq r \leq r^p. \end{cases} \tag{5.33}$$

Consider the coefficients in a two layer cylinder. The process of obtaining the coefficients is similar to the shell, but general enough to include all of the complications of any p-layer cylinder. To begin, equate the two expressions for σ_{zz}, eqn.(5.31) and (5.33), and take an appropriate inner product of both sides. This inner product must reflect the fact that the modes of the layered cylinder are coupled to eachother, so all of the layers should impact the inner product. For this reason the inner product of two functions, h and k, is chosen to be:

$$\langle h, k \rangle = \int_0^{r^1} h(r)k(r)dr \tag{5.34}$$

Thus, the inner product of the normal stress with any quantity h is:

$$\int_0^{r^1} \sigma_{zz}(r)h(r)dr = \int_{r^2}^{r^1} \sigma^1_{zz}(r)h^1(r)dr + \int_0^{r^2} \sigma^2_{zz}(r)^1h^2(r)dr \quad (5.35)$$
$$= \int_{r^2}^{r^1} f^1_\omega(r)^1h^1(r)dr + \int_0^{r^2} f^2_\omega(r)h^2(r)dr$$

where a superscript denotes the restriction of a quantity to a certain layer. Now, let $z = 0$, eliminate the common term of $e^{-i\omega t}$ when equating eqn.(5.31) and (5.33), and take the inner product of both sides with $J_0(\gamma^1_{1(1)}r)$.

$$\int_{r^2}^{r^1} f^1_\omega(r)J_0(\gamma^1_{1(1)}r)dr + \int_0^{r^2} f^2_\omega(r)J_0(\gamma^1_{1(1)}r)dr \quad (5.36)$$
$$= \sum_{j=1}^{K} D^1_{1(j)} \int_{r^2}^{r^1} J_0(\gamma^l_{1(j)}r)J_0(\gamma^1_{1(1)}r)dr A^l_{1(j)}$$
$$+ \sum_{j=1}^{K} D^l_{1(j)} \int_{r^2}^{r^1} Y_0(\gamma^l_{1(j)}r)J_0(\gamma^1_{1(1)}r)\bar{A}^l_{1(j)}dr$$
$$+ \sum_{j=1}^{K} D^l_{2(j)} \int_{r^2}^{r^1} J_0(\gamma^l_{2(j)}r)J_0(\gamma^1_{1(1)}r)dr A^l_{2(j)}$$
$$+ \sum_{j=1}^{K} D^l_{2(j)} \int_{r^2}^{r^1} Y_0(\gamma^l_{2(j)}r)J_0(\gamma^1_{1(1)}r)dr \bar{A}^l_{2(j)}$$
$$+ \sum_{j=1}^{K} D^2_{1(j)} \int_0^{r^2} J_0(\gamma^2_{1(j)}r)J_0(\gamma^1_{1(1)}r)dr A^2_{1(j)}$$
$$+ \sum_{j=1}^{K} D^2_{2(j)} \int_0^{r^2} J_0(\gamma^2_{2(j)}r)J_0(\gamma^1_{1(1)}r)dr A^2_{2(j)}$$

Equation (5.36) represents a single equation with $6K$ unknowns, the coefficients $A^1_{1(j)}$, $\bar{A}^1_{1(j)}$, $A^1_{2(j)}$, $\bar{A}^1_{2(j)}$, $A^2_{1(j)}$ and $A^2_{2(j)}$, $j = 1, \ldots, K$. Another $K - 1$ equations are obtained by equating eqn.(5.31) and (5.33) and taking the inner product with $J_0(\gamma^1_{1(m)}r)$ for $m = 2, \ldots, K$.

There are $6K$ equations for determining the unknown coefficients. The remaining $5K$ equations are obtained as follows:

Rows $K+1$ through $2K$: Replace the second function in all of the integrals of eqn.(5.36) with $Y_0(\gamma^l_{1(m)}r)$, $m = 1$ in row $K+1$, $m = 2$ in row $K+2,\ldots$, $m = K$ in row $2K$.

Rows $2K+1$ through $3K$: Replace the second function in all of the integrals of eqn.(5.36) with $J_0(\gamma^l_{2(m)}r)$, $m = 1$ in row $2K+1$, $m = 2$ in row $2K+2,\ldots$, $m = K$ in row $3K$.

Rows $3K+1$ through $4K$: Replace the second function in all of the integrals of eqn.(5.36) with $Y_0(\gamma^l_{2(m)}r)$, $m = 1$ in row $3K+1$, $m = 2$ in row $3K+2,\ldots$, $m = K$ in row $4K$.

Rows $4K+1$ through $5K$: Replace the second function in all of the integrals of eqn.(5.36) with $J_0(\gamma^2_{1(m)}r)$, $m = 1$ in row $4K+1$, $m = 2$ in row $4K+2,\ldots$, $m = K$ in row $5K$.

Rows $5K+1$ through $6K$: Replace the second function in all of the integrals of eqn.(5.36) with $J_0(\gamma^2_{2(m)}r)$, $m = 1$ in row $5K+1$, $m = 2$ in row $45K+2,\ldots$, $m = K$ in row $6K$.

When the system for the coefficients is constructed, it will be of the form

$$SA = F \tag{5.37}$$

where S is a $6K \times 6K$ matrix, A is a vector of unknown coefficients, and F is a vector that contains the inner products with the input function $f^l_\omega(r)$. The vectors A and F look like:

$$A^l = \begin{bmatrix} A^l_{1(1)} \\ \vdots \\ A^l_{1(K)} \\ \bar{A}^l_{1(1)} \\ \vdots \\ \bar{A}^l_{1(K)} \\ A^l_{2(1)} \\ \vdots \\ A^l_{2(K)} \\ \bar{A}^l_{2(1)} \\ \vdots \\ \bar{A}^l_{2(K)} \\ A^2_{1(1)} \\ \vdots \\ A^2_{1(K)} \\ A^2_{2(1)} \\ \vdots \\ A^2_{2(K)} \end{bmatrix}, \quad F = \begin{bmatrix} \int_{r^2}^{r^1} f^1_\omega(r) J_0(\gamma^1_{1(1)} r)dr + \int_0^{r^2} f^2_\omega(r) J_0(\gamma^1_{1(1)} r)dr \\ \vdots \\ \int_{r^2}^{r^1} f^1_\omega(r) J_0(\gamma^1_{1(K)} r)dr + \int_0^{r^2} f^2_\omega(r) J_0(\gamma^1_{1(K)} r)dr \\ \int_{r^2}^{r^1} f^1_\omega(r) Y_0(\gamma^1_{1(1)} r)dr + \int_0^{r^2} f^2_\omega(r) Y_0(\gamma^1_{1(1)} r)dr \\ \vdots \\ \int_{r^2}^{r^1} f^1_\omega(r) Y_0(\gamma^1_{1(K)} r)dr + \int_0^{r^2} f^2_\omega(r) Y_0(\gamma^1_{1(K)} r)dr \\ \int_{r^2}^{r^1} f^1_\omega(r) J_0(\gamma^1_{2(1)} r)dr + \int_0^{r^2} f^2_\omega(r) J_0(\gamma^1_{2(1)} r)dr \\ \vdots \\ \int_{r^2}^{r^1} f^1_\omega(r) J_0(\gamma^1_{2(K)} r)dr + \int_0^{r^2} f^2_\omega(r) J_0(\gamma^1_{2(K)} r)dr \\ \int_{r^2}^{r^1} f^1_\omega(r) Y_0(\gamma^1_{2(1)} r)dr + \int_0^{r^2} f^2_\omega(r) Y_0(\gamma^1_{2(1)} r)dr \\ \vdots \\ \int_{r^2}^{r^1} f^1_\omega(r) Y_0(\gamma^1_{2(K)} r)dr + \int_0^{r^2} f^2_\omega(r) Y_0(\gamma^1_{2(K)} r)dr \\ \int_{r^2}^{r^1} f^1_\omega(r) J_0(\gamma^2_{1(1)} r)dr + \int_0^{r^2} f^2_\omega(r) J_0(\gamma^2_{1(1)} r)dr \\ \vdots \\ \int_{r^2}^{r^1} f^1_\omega(r) J_0(\gamma^2_{1(K)} r)dr + \int_0^{r^2} f^2_\omega(r) J_0(\gamma^2_{1(K)} r)dr \\ \int_{r^2}^{r^1} f^1_\omega(r) J_0(\gamma^2_{2(1)} r)dr + \int_0^{r^2} f^2_\omega(r) J_0(\gamma^2_{2(1)} r)dr \\ \vdots \\ \int_{r^2}^{r^1} f^1_\omega(r) J_0(\gamma^2_{2(K)} r)dr + \int_0^{r^2} f^2_\omega(r) J_0(\gamma^2_{2(K)} r)dr \end{bmatrix} \tag{5.38}$$

The components of the matrix S are obtained by choosing the correct coefficients of the unknowns from the equations similar to eqn.(5.36). For example, $S_{3K+1,4K+2}$ is the coefficient of the $4K+2^{th}$ variable in row $3K+1$. The $4K+2^{th}$ variable is $A^2_{1(2)}$, its coefficient in row $3K+1$ is given by

$$S_{3K+1,4K+2} = D^2_{1(2)} \int_0^{r^2} J_0(\gamma^2_{1(2)} r) Y_0(\gamma^1_{2(1)} r) dr \tag{5.39}$$

5.2 Dispersion in a Two-Layer Cylinder

In this section the method just described will be employed to generate the dispersion curves of a thick two-layered cylinder. This is the most crucial step in the construction of the displacements or stresses since every subsequent step relies on dispersion data. It will be seen that the number and shape of the dispersion curves will vary significantly with the radius of the pith. This implies that an experimental determination of the dispersion curves alone should be sufficient to determine what percentage of the volume of a SDT sample is composed of pith.

In [64] a method for experimentally determining the dispersion curves is presented and then compared with theoretical curves with some success. Comparison of experimental and theoretical results in the 'dispersion' domain has advantages over comparison of more traditional physical quantities. For instance, the dispersion data is global in the sense that it is independent of the input. Therefore, theoretical results based on dispersion data are free from errors introduced through the approximation of the input. This is another reason why obtaining the dispersion curves is crucial, as more experimental techniques for measuring dispersion curves are created, this domain will provide a more reliable area for comparison of theory and experiments.

The cylinder, in this section, will be a SDT sample composed of Douglas Fir. The radius of pith will be varied. The cylinder under consideration will

have a total radius, r^1, of 20 cm. The radius of the pith, r^2, will be varied to demonstrate the large quantitative differences in the dispersion curves as r^2 is altered. Since these dispersion curves play such a fundamental role in the construction of the model displacements and stresses, varying the inner radius of the cylinder leads to large differences in these quantities.

The properties in Table 5.1 are taken from [53], they represent typical values for Douglas Fir. The pith is given a 40% recuction in all material properties except the density. The density remains the same in both layers.

layer 1		layer 2	
c_{11}^1	4.07 GPa	c_{11}^2	2.44 GPa
c_{12}^1	2.69 GPa	c_{12}^2	1.61 GPa
c_{13}^1	0.24 GPa	c_{13}^2	0.14 GPa
c_{33}^1	6.89 GPa	c_{33}^2	4.13 GPa
c_{44}^1	0.49 GPa	c_{44}^2	0.29 GPa
ρ	800 kg/m^3	ρ	800 kg/m^3

Table 5.1: Material Properties for Douglas Fir with a 40% reduction in the pith.

The following steps were taken in implementing the process described in this chapter to produce the dispersion curves for a two-layered cylinder.

1. Determine the cutoff frequencies.

2. For each cutoff frequency, determine the corresponding dispersion curve.

The cutoff frequencies are values of ω where the dispersion curves (curves in the ωk-plane satisfying the frequency equation $F(\omega, k) = 0$, eqn.(5.27)) intersect the ω-axis, i.e. cutoff frequencies are solutions to

$$F(\omega, 0) = 0. \tag{5.40}$$

The cutoff frequencies are approximated by choosing a frequency step size, $\Delta\omega$, then beginning a secant method, with initial guess $n\Delta\omega$, to solve the equation

$$F(\omega, \delta k) = 0, \tag{5.41}$$

where n takes on the values $1, 2, \ldots, N$, $\omega = N\Delta\omega$ is the largest value of ω of interest and $0 < \delta k \ll 1$. The value of δk is used instead 0 for k to avoid numerical difficulties associated with complex solutions to $F(\omega, k) = 0$ for values of k near zero, but non-positve or non-real.

The details of the algorithm are contained in Appendix B. The Matlab function *freqeqn.m* calculates the value of $F(\omega, k)$ corresponding to the right hand side of eqn.(5.27). The Matlab script *twocylcutoff.m* implements the secant method that finds the solutions to eqn.(5.41) that approximate the cutoff frequencies.

From each cutoff frequency is a dispersion curve in the ωk-plane. The steps to produce these curves are:

For each cutoff frequency

1. Use the cutoff frequency (solution to eqn.(5.41)) as an initial guess to

the equation $F(\omega, \Delta k) = 0$.

2. Use the secant method to find ω_1, the approximation to $F(\omega, \Delta k) = 0$.

3. Store the point $(\omega_1, \Delta k)$ as a point on the dispersion curve.

4. Repeat the process for $k = 2\Delta k, \ldots, M\Delta k$, always using the previous solution, ω_{n-1}, as the initial guess to the solution to $F(\omega, n\Delta k)$.

The Matlab script *dispcurves.m* in Appendix A follows the steps in this algorithm.

Figure 5.3 contains the calculated cutoff frequncies for a two-layered cylinder of varying inner radius, but the total radius of the waveguide remains constant (20 cm). The first and last set of frequencies in Fig. 5.3, inner radii of 0 and 20 cm, correspond to the cutoff frequencies for a solid cylinder. These cutoff frequencies were calculated from the frequency equation for a solid transversely isotropic cylinder. Unlike the frequency equation in eqn.(5.27), the frequency equation for a solid cylinder can be found in closed form and is free from many of the numerical difficulties (such as inverting poorly conditioned matrices) hidden in eqn.(5.27).

The frequency equation for the solid cylinder can be found by paralleling the approach used to find the frequency equation for a shell in sections 4.1

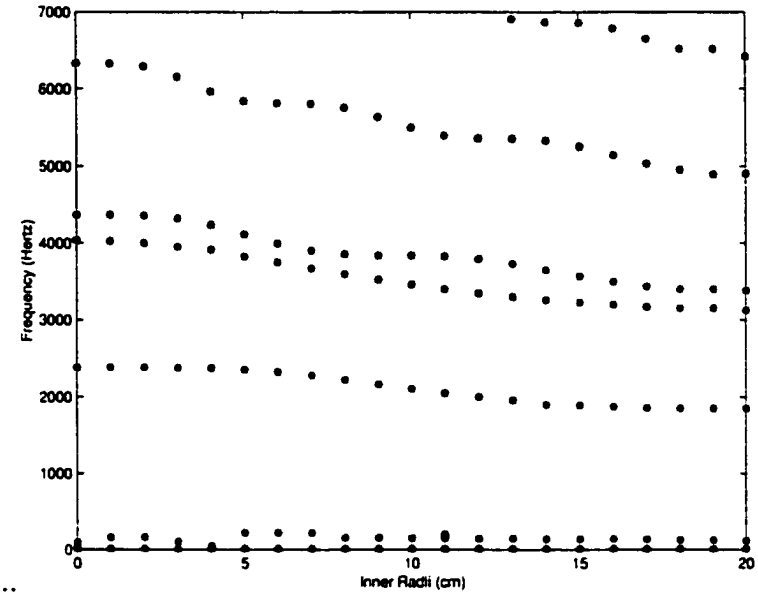

Figure 5.3: Cutoff frequencies for two-layered cylinders of varying inner radii. Inner radius of 0 or 20 cm correpsond to solid cylinders.

through 4.3. The only adjustment to that process is to restrict the form of the displacements, eqn.(4.14) and (4.15), to include Bessel functions of the first kind only. Bessel functions of the second kind take on infinite values at $r = 0$. Therefore, they are physically unreasonable solutions of the displacements in a solid cylinder.

Figure 5.3 shows that the cutoff frequencies calculated for the two-layered cylinder transition smoothly from the solid cylinder composed of a material with the properties of the outer layer (inner radius = 0 cm) to those with the properties of the inner layer (inner radius = 20 cm).

Figures 5.4 through 5.6 are the dispersion curves for two-layered cylinders with inner radii of 5 cm, 10 cm and 15 cm, respectively. As the radius of the

inner layer increases, a larger fraction of the waveguide is composed a less stiff material, see Table 5.1. This results in an reduction of stiffness in the waveguide, allowing more propagating modes at a given frequency.

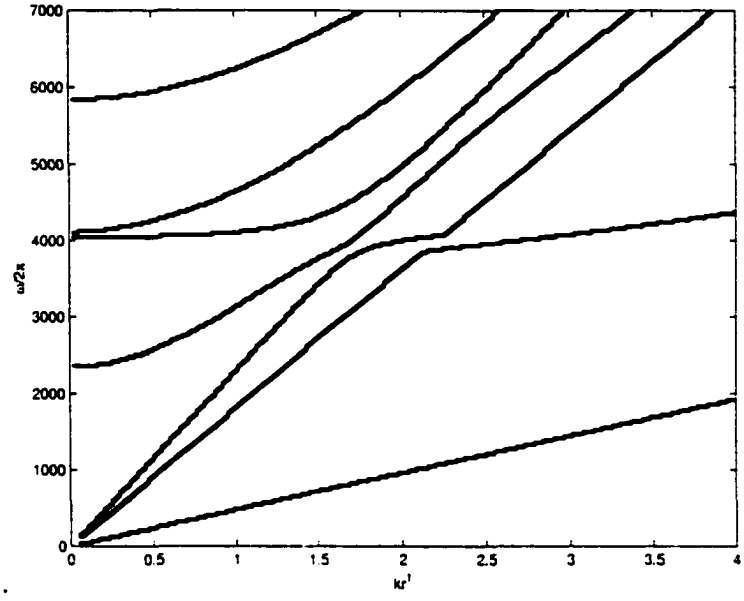

Figure 5.4: Dispersion curves for a two-layered cylinder, $r^1 = 20$ cm, $r^2 = 5$ cm.

These dispersion curves present some interesting phenomenon with regards to determining the properties of a waveguide from the dispersion curves. First, consider the first mode in each of the figures. In each, this curve is a

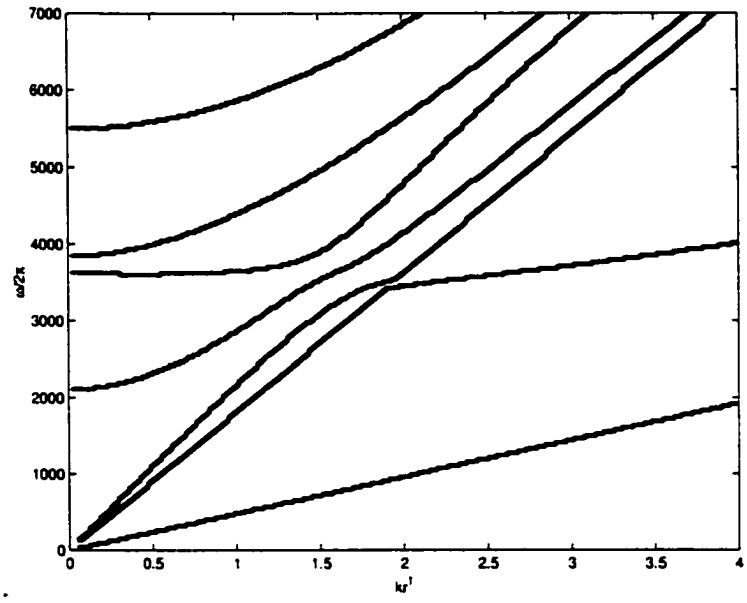

Figure 5.5: Dispersion curves for a two-layered cylinder, $r^1 = 20$ cm, $r^2 = 10$ cm.

straight line through the origin. Therefore, the phase velocity, $c = \frac{\omega}{k}$, is a constant, i.e. this mode is non-dispersive. Furthermore, the ratio of ω to k is the same in each figure. The phase velocity of this mode is independent of the fraction of the waveguide composed of each material. A similar situation occurs in the third mode. It asymptotically approaches a constant phase velocity that does not change with the composition of the waveguide. These two phase velocities depend only on the material properties of the layer, not the amount of each that is present.

A second observation is that the cutoff frequency of the fourth mode changes when the fraction of each material in the waveguide changes. This is also apparent in Fig. 5.3. The cutoff frequencies of all of the higher modes

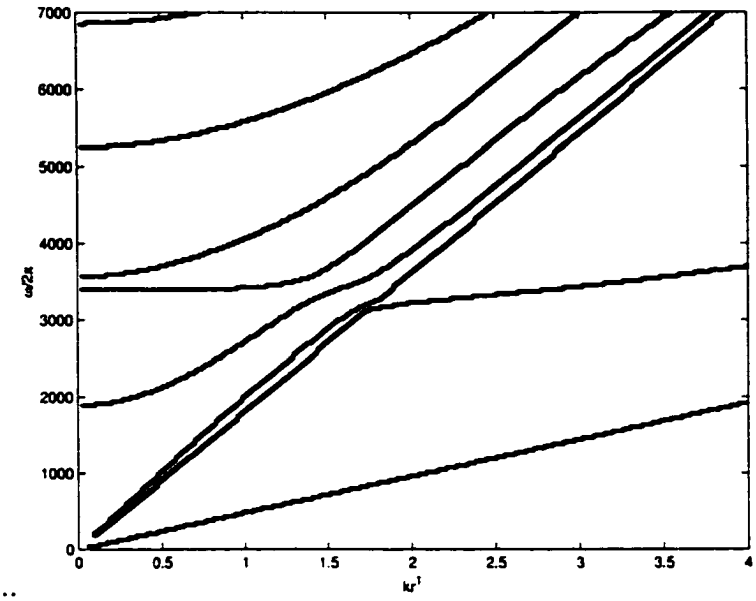

Figure 5.6: Dispersion curves for a two-layered cylinder, $r^1 = 20$ cm, $r^2 = 15$ cm.

change with the inner radius. Therefore, once the material constants are determined from phase velocity measurements of the first and third modes, the fractional composition of the waveguide can also be determined from the cutoff frequencies.

Chapter 6

CONCLUSIONS

The aim of this research was to produce a mechanical model of waves in a semi-infinite cylinder composed of homogeneous, coaxial layers. It was also hoped to be an effective model for use in an experimental or in-situ environment for nondestructive testing of materials, in particular, small diameter timber. As it is, the method for constructing the solution to the fundamental problem may be too computationally burdensome to be practical for some real time applications. However, the primary goal of constructing an analytic or hybrid analytic-numerical solution to the fundamental problem was achieved. The solution constructed also provides information about the mechanical response of the waveguide that would be impossible to extract from a purely numerical approach. This method also seems to be particularly well suited for high frequency calculations.

The steps in this method that contribute to make it computationally troublesome are evaluation of the frequency equation, and solution of the mode coeffieciets. The first step to solving any particular problem with this method

is to determine the values of k that are appropriate at any given frequency. This amounts to finding the roots of the frequency equation. Even for the much simpler problem of an isotropic shell the roots of the frequency equation are difficult to obtain because of the transcendental nature of its terms, i.e. Bessel functions. The transversely isotropic shell is slightly more difficult because of the increased number of parameters, but can be treated the same numerically. Finding the roots of the frequency equation for the layered cylinder represents a significant increase in computational complexity. The frequency equation for the layered cylinder, eqn.(5.27), is the determinant of the global transfer matrix. The global transfer matrix itself is a product of local transfer matrices, eqn.(5.20). Each local transfer is a product that contains a matrix inverse, eqn.(5.14). Therefore, each evaluation of the frequency equation requires at least one matrix inversion. When numerically solving for the roots of the frequency equation, the equation must be evaluated over and over. It is this repeated need to invert matrices that makes finding the appropriate k values much more difficult in the layered case.

A second source of computational burden is solving the system of eqn.(5.37). If there are K wave numbers at a given frequency then this system is $6K \times 6K$. Therefore, even when a small number of modes are propagating there is a significant effort expended in constructing and solving this system. Also, a different system must be constructed and solved for each frequency considered in the applied pressure, σ_{zz}. In practical problems where σ_{zz} will be approxiamated with a high number of frequencies, the construction and evaluation of this system of equations contributes a significant amount to the overall computations needed to implement this method.

Perhaps the most attractive aspect of this approach is its broad applicability. The form of the solution given for the shell in eqn.(4.14) and (4.15) is determined by the geometry of the shell and not it's material properties. This fact is what made it possible to conjecture this form for the solution based on the form of the Pochhammer-Chree solution, eqn.(3.35) and (3.37). Not being limited by the material in the shell allows use of this method for shells of more general anisotropy than merely transversely isotropic. The difference for more general material symmetries will be seen only in the coefficients of the quartic equation that determines γ_1 and γ_2, eqn.(4.17). Otherwise the approach is identical to the transversely isotropic case. Construction of the solution for the layered cylinder then proceeds exactly as described for the transversely isotropic case. Thus, even though only transversely isotropic shells and layered cylinders were considered here, only a small modification is required to apply this method to the most general anisotropic materials.

This method also seems best suited for high frequency applications for a couple of reasons. First, consider a typical dispersion curve such as Fig. 4.1 and 5.3 through 5.6. It is clear that higher frequencies have more propagating modes, with some exceptions, Fig. 5.6. This implies that equations such as eqn.(4.35) and (5.31) will be higher dimensional, therefore, more accurate approximations of the applied stress, σ_{zz}. A better approximation of σ_{zz} will then result in better overall results. A second reason to consider this method most appropriate for high frequencies is the condition of the system in eqn.(5.37). When this system is constructed and evaluated for each frequency considered, a pattern emerges from the condition number of that system with regards to frequency. Consider Fig. 6.1.

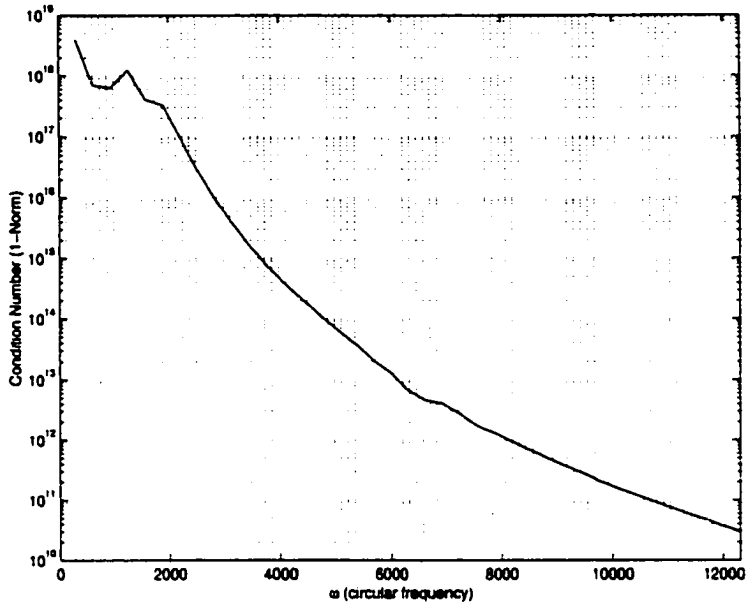

Figure 6.1: Condition number of S in eqn.(5.37) vs. frequency.

Here, the vertical axis is scaled as a log plot and the condition numbers seem to fall off at least linearly with frequency. This means that the condition numbers decrease exponentially with frequency. Therefore, at higher frequencies the system determining the coefficients will be extremely well conditioned, while at low frequencies it is poorly conditioned.

A final observation on the benefits of this method when compared to purely numerical methods is that with numerical methods some interesting mechanical phenomenon will be overlooked. In particular, consider the dispersion curves in Fig. 5.6. Here, it is seen that the second and third modes actually combine to form a single mode. The same phenomenon occurs to the fourth and fifth modes. This behavior of the layered cylinder would be com-

pletely inextractable from a numerical solution to the differential equations that govern the model. Only by attempting to constuct analytical solutions can such behavior be observed.

Chapter 7

REFERENCES

Bibliography

[1] J.D. Achenbach, **Wave Propagation in Elastic Solids**, North Holland Publishing Company, Amsterdam, 1984.

[2] Arfken, George B., **Mathematical Methods for Physicists, 4^{th} ed.**, Academic Press, New York, 1995, 92-97.

[3] D. Bancroft, *The Velocity of Longitudinal Waves in Cylindrical Bars*, Physical Review, 1941, 588-593.

[4] Bertholf, *Numerical Solution for two-dimensional elastic wave propagation in finitel bars*, J. Appl.Mech., 34, 1967, 725-734.

[5] Brian Pavlakovic. Mike Lowe, David Alleyne and Peter Cawley, *Disperse: A General Purpose Program for Creating Dispersion Curves*, Review of Progress in Quantitative Nondestructive Evaluation, Vol. 16, Plenum Press, New York, 1997, 185-192.

[6] C. Chree Trans. Cambridge Phil. Soc. 14, 1889, 250-369.

[7] R.M. Davies, *A Critical Study of the Hopkinson Pressure Bar*, Philosophical Transactions A, 240, 1948, 375-457.

[8] G.F.D. Duff, *The Cauchy Problem for Elastic Waves in an Anisotropic Medium*, Quarterly Journal of Mechanics and Applied Mathematics, 252, 1960, 249-273.

[9] M. Fama, *Radial Eigenfunctions for the Elastic Circular Cylinder*, Q. J. Mech. and Appl. Math., 25, 1972, 479- 495.

[10] Ch. Fiedler and W. Wenzel, *Analytical approximate 3D solution for the longitudinally vibrating cylinder*, Arch. Appl. Mech., 66, 1996, 447-459.

[11] Folk, Fox, Shook and Curtis, *Elastic Strain Produced by Sudden Application of Pressure to One End of a Cylndrical Bar. I. Theory*, J. Appl. Mech., 1969, 552-653.

[12] R. Folk and A. Herczynski, *Solutions of elastodynamic slab problems using a new orthogonality condition*, JASA, 80, 1986, 1103-1110.

[13] A. Herczynski and R. Folk, *Orthogonality Condition for the Pochhammer-Chree Modes*, Q. J. Mech. and Appl. Math., 1989, 523-536.

[14] G. Fox, and C.W. Curtis, *Elastic Strain Produced by Sudden Application of Pressure to One End of a Cylindrical Bar, I. Experimental Observations*, Journal of the Acoustical Society of America 30, 1958, 559-563.

[15] W.B. Fraser, *An Orthogonality Relation for the Modes of Wave Propagation in an Elastic Circular Cylinder*, J. Sound and Vib., 43, 1975, 568-571.

[16] General Technical Report FPL-GTR-113, **Wood Handbook-Wood as an Engineering Material**, USDA Forest Service, Forest Products Laboratory, Madison, WI., 1999, 4-2.

[17] Gieske and Frost, Review of Progress in QNDE, 9, 1982.

[18] I.S. Goldberg and R.T. Folk, *Solutions to Time-Dependent Pure-End-Condition Problems of Elasticity: Pressure-Step Wave Propagation and End-Resonance Effects*, SIAM J. Appl. Math., 53, 1993, 1264-1291.

[19] K.F. Graff, **Wave Motion in Elastic Solids** Oxford University Press, London, 1975.

[20] R.D. Gregory, *A not on bi-orthogonality relations for elastic cylinders of general cross section*, J. Elasticity, 13, 1983, 351-355.

[21] J.L. Habberstad, *A Two-Dimensional Numerical Solution for Elastic Waves in Variously Configured Rods*, J. Appl. Mech., 38(1), 1971, 62-70l.

[22] D.S. Hughes, W.L. Pondrom and R.L. Mims. *Transmission of Elastic Pulses in Metal Rods*, Physical Review 75 (No. 10), 1987, 1552-1556.

[23] C.K. Jen, L. Piche and J.F.Bussiere *Long Isotropic Buffer Rods*, Journal of the Acoustical Society of America 88(1), 1990 23-25.

[24] C.K. Jen, Z. Wang, A. Nicolle, J.F. Bussiere, E.L. Adler and K. Abe, *Acoustic Waveguiding rods with Graded Velocity Profiles*, Ultrasonics 30, 1992, 91-94.

[25] C.K. Jen, B. Cao, K.T. Nguyen, C.A. Loong and J.G. Legoux, *On line ultrasonic monitoring of a die casting process using buffer rods*, Ultrasonics, 35, 1997, 335-344.

[26] L.W. Kennedy and O.E. Jones, *Longitudinal Wave Propagation in a Circular Bar Loaded Suddenly by a Radially Distributed End Stress*, J. Appl. Mech., 1969, 470-478.

[27] J.A. Kainz, X. Le, M.L. Peterson and E.N. Landis, to appear in Review of Progress in QNDE, Vol. 25, 1999.

[28] H. Kolsky, **Stress Waves in Solids**, Dover Publications, Inc., New York, 1963.

[29] E.N. Landis, S.F. Selleck, M.L. Peterson, S.P. Shah and J.D. Achenbach, *Ultrasonic Investigation of Concrete with Distributed Damage*, ACI Materials Journal, Vol. 95, No. 1, 1998, 27-36.

[30] R. Laverty and M. Peterson, *Elastic Response of Thick Isotropic Cylinders with Arbitrary Pressure Applied at One End*, Review of Progress in Quantitative Nondestructive Evaluation, Vol. 18, Kluwer Academic/Plenum Press, 1999, 255-262.

[31] X. Le, J. Kainz , M. L. Peterson, and E. N. Landis, *Smart Timber Bridges for In-Situ Evaluation*, SPIE International Symposium on Nondestructive Evaluation Techniques for Again Infrastructure and Manufacturing. March 30-April 2, 1998, San Antonio Texas.

[32] A.E.H. Love, **A Treatise on the Mathematical Theory of Elasticity**, Reprint. Dover, New York, 1944.

[33] L. Lynnworth, U.S. Patent No. 5,159,838, Nov. 3, 1992.

[34] W. P. Mason, and H.J. McSkimin, *Attenuation and Scattering of High Frequency Sound Waves in Metals and Glasses*, Journal of the Acoustical Society of America, 19, 1947, 464-473.

[35] , H. J. McSkimin, *Propagation of Longitudinal Waves and Shear Waves in Cylindrical Rods at High Frequencies*, Journal of the Acoustical Society of America, 28, 1956, 484-494.

[36] H. J. McSkimin, *Measurement of Ultrasonic Wave Velocities and Elastic Moduli for Small Solid Specimens at High Temperatures*, Journal of the Acoustical Society of America, 31, 1959, 287-295.

[37] J. Miklowitz, *The Propagation of Compressional Waves in a Dispersive Elastic Rod, Part I Results From the Theory*, Journal of Applied Mechanics, 1957, 231.

[38] J. Miklowitz and C.R. Nisewanger, *The Propagation of Compressional Waves in a Dispersive Elastic Rod, Part II Experimental Results and Comparison With Theory*, Journal of Applied Mechanics, 24(2), 1957, 240-244.

[39] I. Mirsky, *Vibrations of Orthotropic, Thick, Cylindrical Shells*, Journal of the Acoustical Society of America, 36(1), 1964, 41-51.

[40] I. Mirsky, *Wave Propagation in Transversely Isotropic Circular Cylinders Part I: Theory*, Journal of the Acoustical Society of America, 37, 1965, 1016-1021.

[41] I. Mirsky, *Wave Propagation in Transversely Isotropic Circular Cylinders Part II: Numerical Results*, Journal of the Acoustical Society of America, 37, 1965, 1022-1026.

[42] P. B. Nagy, *Longitudinal Guided Wave Propagation in a Transversely Isotropic Rod Immersed in Fluid*, Journal of the Acoustical Society of America, 98(1), 1995, 454-457.

[43] A.H. Nayfeh and P.B. Nagy, *General Study of axisymmetric waves in layered anisotropic fibers and their composites*, JASA, 99, 1996, 931-941.

[44] M. Onoe, H.D. McNiven and R.D. Mindlin, *Dispersion of Axially Symmetric Waves in Elastic Rods*, Journal of Applied Mechanics, 1972, 729-734.

[45] L. Pochhammer, J. reine angew. Math., 81, 1876, 324-336.

[46] L.D. Power and S.B. Childs, *Axisymmetric Stresses and Displacements in a Finite Circular Bar*, Int. J. Eng. Sci., 9, 1971, 241-255.

[47] M. L. Peterson, **High Temperature Ultrasonic Monitoring**, Ph.D. Dissertation, Northwestern University, Evanston, IL.

[48] M. L. Peterson, *A Signal Processing Technique for Measurement of Multi-Mode Waveguide Signals: An Application to Monitoring of Reaction Bonding in Silicon Nitride*, Research in Nondestructive Evaluation, Springer Verlag New York Inc., 5, 1994, 239-256.

[49] M. L. Peterson, *A Method for Increased Accuracy of the Measurement of Phase Velocity*, Ultrasonics, 35, 1997, 17-29.

[50] M. L. Peterson, *Prediction of Longitudinal Disturbances in a Multi-Mode Cylindrical Waveguide*, Experimental Mechanics, 39, 1999, 1-7.

[51] M. Redwood, *Velocity and Attenuation of a Narrow Band, High-Frequency Compressional Pulse in a Solid Waveguide*, Journal of the Acoustical Society of America, 31, 1959, 442-448.

[52] M. Redwood, **Mechanical Waveguides**, Pergamon, New York, 1960.

[53] Michael A. Ritter, **Timber Bridges Design, Construction, Inspection and Maintenance**, U.S. Forest Service Document EM 7700-8, 1992.

[54] M. Robert and L.M. Keer, *An Elastic Circular Cylinder with Displacement Prescribed at the Ends-Axially Symmetric Case*, Q. J. Mech. and Appl. Math., 40, 1987, 339-363.

[55] M. Robert and L.M. Keer, *An Elastic Circular Cylinder with Displacement Prescribed at the Ends- Asymmetric Case*, Q. J. Mech. and Appl. Math., 40, 1987, 365-381.

[56] R. J. Ross and R. F. Pellerin, *Nondestructive Testing for Assessing Wood Members in Structures*, Forest Product Laboratory, General Technical Report FPL-GTR-70, 1994.

[57] John. A. Simmons, E. Drescher-Krasicka and H.N.G. Wadley, *Leaky axisymmetric modes in infinite clad rods. I*, Journal of the Acoustical Society of America, 92(2), 1992, 1061-1090.

[58] R. Skalak, *Longitudinal Impact of a Semi-Infinite Circular Elastic Bar*, Journal of Applied Mechanics, 24(1), 1957, 59-64.

[59] M. Spies, *Elastic Waves in homogeneous and layered transversely isotropic media: Plane waves and Gaussian wave packets. A general approach*, Journal of the Acoustical Society of America, 95, 1994, 1748-1760.

[60] R.N. Thurston, *Waves in rods and clad rods*, JASA, 64(1), 1978, 1-37.

[61] L. Y. Tu, J. N. Brennan and J. A. Sauer, *Dispersion of Ultrasonic Pulses in Cylindrical Rods*, Journal of the Acoustical Society of America, 27, 1955, 550-553.

[62] A. Vary, *The Acousto-Ultrasonics Approach* in Acousto-Ultrasonics, Theory and Application, Ed. By J. C. Duke, Plenum Press, 1988.

[63] J. Vollman and J. Dual, *High-resolution analysis of the complex wave spectrum in a cylindrical shell containing a viscoelastic medium. Part I. Theory and Numerical Results.*, Journal of the Acoustical Society of America, 102(2), 1997, 896-908.

[64] J. Vollman, R. Breu and J. Dual, *High-resolution analysis of the complex wave spectrum in a cylindrical shell containing a viscoelastic medium. Part II. Experimental results versus theory.*, Journal of the Acoustical Society of America, 102(2), 1997, 909-920.

[65] G. Wengert and P. Bois, *Evaluation of Electric Moisture Meters on Kiln-Dried Lumber*, Forest Products Journal, 47(7), 1997, 60-62.

[66] Zemanek, Joseph, *An Experimental and Theoretical Investigation of Elastic Wave Propagation in a Cylinder*, Journal of the Acoustical Society of America, 51, 1972, 265-283.

Appendix A

SHELL CODES

This appendix contains all of the Matlab M-files used to create the output included in section 4.5. The first section contains the function *freqeqn.m*. It relates the circular frequency with the axial wavenumber. This function is used in obtaining the dispersion curves. The next two sections contain the scripts *shellcutoff.m* and *dispcurves.m*. The first of these finds the cut-off frequencies below a certain maximum frequency of interest. The script *dispcurves.m* uses the cutoff frequencies already found to construct the dispersion curves.

All of the remaining m-files are devoted to generating the radial displacements and axial displacements. The script *coefficiets.m* uses data already obtained about the dispersion curves and uses that to compute the modal coefficients. The last two m-files use these coefficients to produce graphs of the output. The script *raddisp.m* produces a graph of the radial displacements vs. z. The script *xsection.m* produces graphs of the cross-sectional shapes of the axial displacements of the different modes.

A.1 The Function *freqeqn.m*

```
function y=freqeqn(w,k)

% this is the frequency equation for longitudinal modes
% traveling in an transversely isotropic shell of inner
% and outer radii of a and b, respectively.
% the elastic constants are c11, c12, c13, c33 and c44.
% p is the density

%*********************************************************
% initialize variables
%*********************************************************

% these numbers are for Douglas Fir.  The units are meters(m),
% Pascals(Pa) and kilograms/meter^3 (kg/(m^3)).

b=20e-2;
a=0.5*b;
c33=6.89e+9;
c11=0.59*c33;
c12=0.39*c33;
c13=0.035*c33;
c44=0.071*c33;
p=800;

%*********************************************************
% the frequency equation
%*********************************************************

% first, the radial wavenumbers g1 and g2

A=c11*c44/2;
B=-c11*(p*w^2-c33*k^2)-c44/2*(p*w^2-c44/2*k^2)-(c13+c44/2)^2*k^2;
C=(p*w^2-c33*k^2)*(p*w^2-c44/2*k^2);
g1=sqrt((-B+sqrt(B^2-4*A*C))/(2*A));
g2=sqrt((-B-sqrt(B^2-4*A*C))/(2*A));
```

```
% second, the factors c1 and c2

c1=(p*w^2-c11*g1^2-c44/2*k^2)/(i*k*g1*(c13+c44/2));
c2=(p*w^2-c11*g2^2-c44/2*k^2)/(i*k*g2*(c13+c44/2));

% last, the coeff. of the 4x4 matrix from the BC's

%\sigma_{rr}=0 at r=a

X(1,1)=(c11*g1+i*k*c13*c1)*besselj(0,g1*a)+(c12-c11)/a*besselj(1,g1*a);
X(1,2)=(c11*g1+i*k*c13*c1)*bessely(0,g1*a)+(c12-c11)/a*bessely(1,g1*a);
X(1,3)=(c11*g2+i*k*c13*c2)*besselj(0,g2*a)+(c12-c11)/a*besselj(1,g2*a);
X(1,4)=(c11*g2+i*k*c13*c2)*bessely(0,g2*a)+(c12-c11)/a*bessely(1,g2*a);

%\sigma_{rr}=0 at r=b

X(2,1)=(c11*g1+i*k*c13*c1)*besselj(0,g1*b)+(c12-c11)/a*besselj(1,g1*b);
X(2,2)=(c11*g1+i*k*c13*c1)*bessely(0,g1*b)+(c12-c11)/a*bessely(1,g1*b);
X(2,3)=(c11*g2+i*k*c13*c2)*besselj(0,g2*b)+(c12-c11)/a*besselj(1,g2*b);
X(2,4)=(c11*g2+i*k*c13*c2)*bessely(0,g2*b)+(c12-c11)/a*bessely(1,g2*b);

%\sigma_{rz}=0 at r=a

X(3,1)=c44/2*(i*k-g1*c1)*besselj(1,g1*a);
X(3,2)=c44/2*(i*k-g1*c1)*bessely(1,g1*a);
X(3,3)=c44/2*(i*k-g2*c2)*besselj(1,g2*a);
X(3,4)=c44/2*(i*k-g2*c2)*bessely(1,g2*a);

%\sigma_{rz}=0 at r=b

X(4,1)=c44/2*(i*k-g1*c1)*besselj(1,g1*b);
X(4,2)=c44/2*(i*k-g1*c1)*bessely(1,g1*b);
X(4,3)=c44/2*(i*k-g2*c2)*besselj(1,g2*b);
X(4,4)=c44/2*(i*k-g2*c2)*bessely(1,g2*b);

% now, we return the frequency equation.
```

```
y=det(X);

%*********************************************************
% end of function
%*********************************************************
```

A.2 The Script *shellcutoff.m*

```
% this script finds the cutoff frequencies for the shell
% whose frequency equation is in the function freqeqn.m
% the cutoff frequencies are written to the vector cutoff
% which will be used by other scripts

%*********************************************************
% initialize variables
%*********************************************************
% wend is the highest circular frequency
% dw is the frequency step size
% success is the number of times in a row that Newton's
%   method must meet tolerance for the iteration to stop
% maxiter is the maximum iterations of Newton's method
% tol is the tolerance on Newton's method
% wstart is a starting frequency close to zero

wend=(7e+3)*2*pi;
dw=wend/150;
success=3;
maxiter=20;
tol=dw/1000;
wstart=tol/10;

%*********************************************************
% main program
%*********************************************************
% find the root of freqeqn, with k=0, closest to w for each w
% write the roots to the array cutoff, then sort cutoff
```

```
counter=1;
for w=wstart:dw:wend
  x=w;
  iter=0;
  newtcount=0;
  while newtcount<success & iter<maxiter
    dfreq=(freqeqn(x+tol,tol)-freqeqn(x,tol))/tol;
    newx=x-freqeqn(x,tol)/dfreq;
    if abs(newx-x)<tol
      newtcount=newtcount+1;
    else
      newtcount=0;
    end
    iter=iter+1;
    x=newx;
  end
  ws(counter)=w;
  wroots(counter)=x;
  iters(counter)=iter;
  counter=counter+1;
end
wroots=sort(wroots);

% eliminate from wroots array all roots not between
% zero and wend

goodcount=1;
for n=1:1:length(wroots)
  if wroots(n)>=0 & wroots(n)<=wend
    goodroots(goodcount)=wroots(n);
    goodcount=goodcount+1;
  end
end

% eliminate repeated roots in array goodroots and write
% to array cutoff
```

```
cutcount=1;
for n=1:1:length(goodroots)
  if n==1
    cutoff(1)=goodroots(1);
    cutcount=2;
  elseif abs(goodroots(n)-cutoff(cutcount-1))>dw
    cutoff(cutcount)=goodroots(n);
    cutcount=cutcount+1;
  end
end

%*******************************************************
% write restults to vector cutoff
%*******************************************************

cutoff=sort(cutoff)


%*******************************************************
% end of script
%*******************************************************
```

A.3 The Script *dispcurves.m*

```
% this script takes the cutoff frequencies contained
% in the vector cutoff and uses them to generate dispersion
% curves for the frequency equation in the function
% freqeqn.m
% the output is a graph.
% vertical axis is frequecny divided by 2*pi.
% horizontal axis is wavenumber times width of shell.


%*************************************************************
% initialize variables
```

```
% ************************************************************
% wend is the highest circular frequency
% dw is the frequency step size
% success is the number of times in a row that Newton's
%   method must meet tolerance for the iteration to stop
% maxiter is the maximum iterations of Newton's method
% tol is the tolerance on Newton's method
% wstart is a starting frequency close to zero
% the inner and outer radii are a and b, respectively.

wend=(7e+3)*2*pi;
dw=wend/300;
success=3;
maxiter=20;
tol=dw/1000;
b=20e-2;
a=1/2*b;

%************************************************************
% main program
%************************************************************
% for each cutoff frequency a dispersion curve is traced
% out in the frequency-wavenumber plane

clear datk
clear datw
for n=1:1:length(cutoff)
  counter=1;
  clear tempdatk
  clear tempdatw
  wstart=cutoff(n)+dw;
  k=tol;
  for w=wstart:dw:wend
    iter=0;
    newtcount=0;
    while iter<maxiter & newtcount<success
      dcyl2=(freqeqn(w,k+tol)-freqeqn(w,k))/tol;
```

```
      newk=k-freqeqn(w,k)/dcyl2;
      if abs(newk-k)<tol
        newtcount=newtcount+1;
      else
        newtcount=0;
      end
      k=newk;
      iter=iter+1;
    end
    tempdatk(counter)=real(k);
    tempdatw(counter)=w;
    counter=counter+1;
 end
 if n==1
    datk=tempdatk;
    datw=tempdatw;
 else
    datk=[datk, tempdatk];
    datw=[datw, tempdatw];
 end
end

% sort the data by w

[newdatw, index]=sort(datw);
for j=1:1:length(index)
   newdatk(j)=datk(index(j));
end

% save data to ouput file

save exampledata newdatk newdatw dw

% produce output

plot(newdatk.*b,newdatw./(2*pi),'.')
  xlabel('kb')
```

```
  ylabel('\omega/2\pi')

%*********************************************************
% end of script
%*********************************************************
```

A.4 The Script *coeffients.m*

```
% this script will produce vectors containing all of
% the constants for the solution to transversely
% isoropic shell.
% the response is at a circular frequency w.
% the material properties of the specimen are in the
% function freqeqn.m


%*********************************************************
%          USER INPUTS
%*********************************************************

w=6000*2*pi;

%*********************************************************
%  MATERIAL INFO.  SAME AS IN freqeqn.m
%*********************************************************

% these numbers are for Douglas Fir.  The units are meters(m),
% Pascals(Pa) and kilograms/meter^3 (kg/(m^3)).

b=20e-2;
a=10e-2;

c33=6.89e+9;
c11=0.59*c33(1);
c12=0.39*c33(1);
```

```
c13=0.035*c33(1);
c44=0.071*c33(1);
p=800;


%*********************************************************
% load the frequency/wavenumber data
%*********************************************************

load exampledata

%*********************************************************
% Determine the k's associated with w
%*********************************************************

ktol=0.1;
clear wcounter
wcounter=1;
while w-newdatw(wcounter)>0
   wcounter=wcounter+1;
end
clear kcounter
kcounter=1;
while abs(w-newdatw(wcounter))<=dw
   firstks(kcounter)=newdatk(wcounter);
   wcounter=wcounter+1;
   kcounter=kcounter+1;
end

% Keep only the k's that correspond to a wave
% propagating to the right.

counter=1;
for j=1:1:length(firstks)
   if firstks(j)>0
      secondks(counter)=firstks(j);
      counter=counter+1;
```

```
   end
end

%Eliminate repeat k's

secondks=sort(secondks);
ks(1)=secondks(1);
counter=1;
for j=2:1:length(secondks)
   if abs(secondks(j)-ks(counter))>ktol
      ks(counter+1)=secondks(j);
      counter=counter+1;
   end
end

% put in order according to mode
for j=1:1:length(ks)
   finalks(j)=ks(length(ks)-j+1);
end
ks=finalks;

%*******************************************************
% Determine the gamma's (radial wavenumbers)
%*******************************************************

% g1(j) is gamma1 corresponding to k=ks(j)
% g2(j) is gamma2 corresponding to k=ks(j)

i=sqrt(-1);
for j=1:1:length(ks)
   k=ks(j);
   A=c11*c44/2;
   B=-c11*(p*w^2-c33*k^2)-c44/2*(p*w^2-c44/2*k^2)-(c13+c44/2)^2*k^2;
   C=(p*w^2-c33*k^2)*(p*w^2-c44/2*k^2);
   g1(j)=sqrt((-B+sqrt(B^2-4*A*C))/(2*A));
   g2(j)=sqrt((-B-sqrt(B^2-4*A*C))/(2*A));
end
```

```
%*********************************************************
% Determine the xi's
%*********************************************************

% xi1(j) is xi1 corresponding to k=ks(j)
% xi2(j) is xi2 corresponding to k=ks(j)

i=sqrt(-1);
for j=1:1:length(ks)
   k=ks(j);
   xi1(j)=(p*w^2-c11*g1(j)^2-c44/2*k^2)/(i*k*g1(j)*(c13+c44/2));
   xi2(j)=(p*w^2-c11*g2(j)^2-c44/2*k^2)/(i*k*g2(j)*(c13+c44/2));
end

%*********************************************************
% Determine the A's (the coefficients)
%*********************************************************

% there are 4 vectors with the coefficients in them.
% A1(j) contains A1 corresponding to k=ks(j)
% A1bar(j) contains A1bar corresponding to k=ks(j)
% A2(j) contains A2 corresponding to k=ks(j)
% A2bar(j) contains A2bar corresponding to k=ks(j)

numint=50;
i=sqrt(-1);

dr=(b-a)/numint;
K=length(ks)
S=zeros(4*K,4*K)
F=zeros(1,4*K)
D1=zeros(1,K)
D2=zeros(1,K)
for j=1:1:K
   D1(j)=c13*g1(j)+i*ks(j)*c33*xi1(j);
   D2(j)=c13*g2(j)+i*ks(j)*c33*xi2(j);
```

```
end

for R=1:1:K
   for j=1:1:numint
      r=a+j*dr;
      F(R)=F(R)+f(w,r)*besselj(0,g1(R)*r);
      F(K+R)=F(K+R)+f(w,r)*bessely(0,g1(R)*r);
      F(2*K+R)=F(2*K+R)+f(w,r)*besselj(0,g2(R)*r);
      F(3*K+R)=F(3*K+R)+f(w,r)*bessely(0,g2(R)*r);
   end
end

for R=1:1:K
   for C=1:1:K
      for j=1:1:numint
         r=a+j*dr;

         S(R,C)=S(R,C)+D1(C)*besselj(0,g1(C)*r)*besselj(0,g1(R)*r);
         S(R+K,C)=S(R+K,C)+D1(C)*besselj(0,g1(C)*r)*
bessely(0,g1(R)*r);
         S(R+2*K,C)=S(R+2*K,C)+D1(C)*besselj(0,g1(C)*r)*
besselj(0,g2(R)*r);
         S(R+3*K,C)=S(R+3*K,C)+D1(C)*besselj(0,g1(C)*r)*
bessely(0,g2(R)*r);

         S(R,C+K)=S(R,C+K)+D1(C)*bessely(0,g1(C)*r)*besselj(0,g1(R)*r);
         S(R+K,C+K)=S(R+K,C+K)+D1(C)*bessely(0,g1(C)*r)*
bessely(0,g1(R)*r);
         S(R+2*K,C+K)=S(R+2*K,C+K)+D1(C)*bessely(0,g1(C)*r)*
besselj(0,g2(R)*r);
         S(R+3*K,C+K)=S(R+3*K,C+K)+D1(C)*bessely(0,g1(C)*r)*
bessely(0,g2(R)*r);

         S(R,C+2*K)=S(R,C+2*K)+D2(C)*besselj(0,g2(C)*r)*
besselj(0,g1(R)*r);
         S(R+K,C+2*K)=S(R+K,C+2*K)+D2(C)*besselj(0,g2(C)*r)*
bessely(0,g1(R)*r);
```

```
        S(R+2*K,C+2*K)=S(R+2*K,C+2*K)+D2(C)*besselj(0,g2(C)*r)*
besselj(0,g2(R)*r);
        S(R+3*K,C+2*K)=S(R+3*K,C+2*K)+D2(C)*besselj(0,g2(C)*r)*
bessely(0,g2(R)*r);

        S(R,C+3*K)=S(R,C+3*K)+D2(C)*bessely(0,g2(C)*r)*
besselj(0,g1(R)*r);
        S(R+K,C+3*K)=S(R+K,C+3*K)+D2(C)*bessely(0,g2(C)*r)*
bessely(0,g1(R)*r);
        S(R+2*K,C+3*K)=S(R+2*K,C+3*K)+D2(C)*bessely(0,g2(C)*r)*
besselj(0,g2(R)*r);
        S(R+3*K,C+3*K)=S(R+3*K,C+3*K)+D2(C)*bessely(0,g2(C)*r)*
bessely(0,g2(R)*r);

      end
   end
end

% solve the linear system

A=S\F';

for j=1:1:K
   A1(j)=A(j);
   A1bar(j)=A(K+j);
   A2(j)=A(2*K+j);
   A2bar(j)=A(3*K+j);
end

save examplecoeffs w ks g1 g2 xi1 xi2 A1 A1bar A2 A2bar

%*************************************************
% end of script
%*************************************************
```

A.5 The Script *raddisp.m*

```
% this script will produce a axially varying picture
% of the radial displacements in a
% cylindrical shell responding to an excitation at
% circular frequency w.
% the material properties of the specimen are in the
% function freqeqn.m


%*********************************************************
%  load data from examplecoeffs.mat
%*********************************************************

load examplecoeffs

%*********************************************************
%  MATERIAL INFO.  SAME AS IN freqeqn.m
%*********************************************************

% these numbers are for Douglas Fir.  The units are meters(m),
% Pascals(Pa) and kilograms/meter^3 (kg/(m^3)).

t=1;
r=0.2;
z1=1.1;
z2=2.9;

b=20e-2;
a=10e-2;
c33=6.89e+9;
c11=0.59*c33;
c12=0.39*c33;
c13=0.035*c33;
c44=0.071*c33;
p=800;
```

```
%*********************************************************
%  Produce Output Data
%*********************************************************

% the output is a graph from z=z1 to z2 of the radial
% displacements at radius r and time t of the propagating modes.

numzsteps=200;
dz=(z2-z1)/numzsteps;

i=sqrt(-1);
zs=[z1:dz:z2];

for j=1:1:length(zs)
   z=zs(j);
   m=1;
      p1=A1(m)*besselj(1,g1(m)*r);
      p2=A1bar(m)*bessely(1,g1(m)*r);
      p3=A2(m)*besselj(1,g2(m)*r);
      p4=A2bar(m)*bessely(1,g2(m)*r);
      p5=exp(i*(ks(m)*z-w*t));
      mode1(j)=real((p1+p2+p3+p4)*p5);
   m=2;
      p1=A1(m)*besselj(1,g1(m)*r);
      p2=A1bar(m)*bessely(1,g1(m)*r);
      p3=A2(m)*besselj(1,g2(m)*r);
      p4=A2bar(m)*bessely(1,g2(m)*r);
      p5=exp(i*(ks(m)*z-w*t));
      mode2(j)=real((p1+p2+p3+p4)*p5);
   m=3;
      p1=A1(m)*besselj(1,g1(m)*r);
      p2=A1bar(m)*bessely(1,g1(m)*r);
      p3=A2(m)*besselj(1,g2(m)*r);
      p4=A2bar(m)*bessely(1,g2(m)*r);
      p5=exp(i*(ks(m)*z-w*t));
      mode3(j)=real((p1+p2+p3+p4)*p5);
```

```
end

% find the maximum element of each mode to use as
% a normalizing constant.

mode1max=max(abs(mode1));
mode2max=max(abs(mode2));
mode3max=max(abs(mode3));

%************************************************************
% Produce Output Pictures
%************************************************************

figure
subplot(2,2,1)
 plot(zs./b,mode1./mode1max)
 title('Mode 1')
 axis([z1/b z2/b -1.1 1.1])
 xlabel('z/b')
 ylabel('Displacement')
subplot(2,2,2)
 plot(zs./b,mode2./mode2max)
 title('Mode 2')
 axis([z1/b z2/b -1.1 1.1])
 xlabel('z/b')
 ylabel('Displacement')
subplot(2,2,3)
 plot(zs./b,mode3./mode3max)
 title('Mode 3')
 axis([z1/b z2/b -1.1 1.1])
 xlabel('z/b')
 ylabel('Displacement')

 %************************************************************
 % end of script
 %************************************************************
```

A.6 The Script *xsection.m*

```
% this script will produce a cross-sectional picture
% of the shape of the propagating axial modes in a
% cylindrical shell responding to an excitation at
% circular frequency w.
% the material properties of the specimen are in the
% function freqeqn.m


%*********************************************************
%  load data from examplecoeffs.mat
%*********************************************************

load examplecoeffs

%*********************************************************
%  MATERIAL INFO.  SAME AS IN freqeqn.m
%*********************************************************

% these numbers are for Douglas Fir.  The units are meters(m),
% Pascals(Pa) and kilograms/meter^3 (kg/(m^3)).

b=20e-2;
a=10e-2;
c33=6.89e+9;
c11=0.59*c33;
c12=0.39*c33;
c13=0.035*c33;
c44=0.071*c33;
p=800;


%*********************************************************
%  Produce Output Data
%*********************************************************
```

```
% the output is a graph from r=a to b of the shape of
% each of the propagating modes.

% the matrices mode1,2 and 3 contains the shapes in each mode.

numrsteps=25;
dr=(b-a)/numrsteps;
[th,r]=meshgrid((0:5:360)*pi/180, a:dr:b);
[x,y]=pol2cart(th,r);
r=sqrt(x.^2+y.^2);

i=sqrt(-1);
m=1;
      p1=A1(m)*xi1(m)*besselj(0,g1(m)*r);
      p2=A1bar(m)*xi1(m)*bessely(0,g1(m)*r);
      p3=A2(m)*xi2(m)*besselj(0,g2(m)*r);
      p4=A2bar(m)*xi2(m)*bessely(0,g2(m)*r);
      mode1=abs(p1+p2+p3+p4);

i=sqrt(-1);
m=2;
      p1=A1(m)*xi1(m)*besselj(0,g1(m)*r);
      p2=A1bar(m)*xi1(m)*bessely(0,g1(m)*r);
      p3=A2(m)*xi2(m)*besselj(0,g2(m)*r);
      p4=A2bar(m)*xi2(m)*bessely(0,g2(m)*r);
      mode2=abs(p1+p2+p3+p4);

i=sqrt(-1);
m=3;
      p1=A1(m)*xi1(m)*besselj(0,g1(m)*r);
      p2=A1bar(m)*xi1(m)*bessely(0,g1(m)*r);
      p3=A2(m)*xi2(m)*besselj(0,g2(m)*r);
      p4=A2bar(m)*xi2(m)*bessely(0,g2(m)*r);
      mode3=abs(p1+p2+p3+p4);

% find the maximum element of each mode to use as
% a nor malizing constant.
```

```
mode1max=0;
mode2max=0;
mode3max=0;
for j=1:1:length(mode1(:,1))
   currmax1=max(mode1(j,:));
   currmax2=max(mode2(j,:));
   currmax3=max(mode3(j,:));
   if currmax1>mode1max
      mode1max=currmax1;
   end
   if currmax2>mode2max
      mode2max=currmax2;
   end
   if currmax3>mode3max
      mode3max=currmax3;
   end
end

%*************************************************************
% Produce Output Pictures
%*************************************************************

figure
mesh(x,y,mode1./mode1max)
colormap(cool)

figure
mesh(x,y,mode2./mode2max)
colormap(cool)

figure
mesh(x,y,mode3./mode3max)
colormap(cool)

figure
subplot(2,2,1)
```

```
mesh(x,y,mode1./mode1max)
colormap(cool)
subplot(2,2,2)
mesh(x,y,mode2./mode2max)
colormap(cool)
subplot(2,2,3)
mesh(x,y,mode3./mode3max)
colormap(cool)

%*************************************************************
% end of script
%*************************************************************
```

Appendix B

TWO-LAYERED CODES

This appendix contains the Matlab M-files for the two layered cylinder that are significantly different than the corresponding codes for the shell. The codes included are the function *freqeqn.m*, which contains the frequency equation for the two layered cylinder. The scripts *twocylcutoff.m* and *dispcurves.m* are used to generate the dispersion curves. These codes are identical to the corresponding codes for the shell, *shellcutoff.m* and *dispcurves.m*, found in Appendix A. Therefore, these codes were not copied again in this appendix.

A primary goal for the two-layered cylinder is to compare theoretical results with experimental data. Since experimental stresses, in particular, the applied σ_{zz}, are not of a single frequency nature it was necessary to include an m-file that would produce a finite frequency approximation of a real input. The script *inputapprox.m* performs this approximation.

The last m-file is the script *sigmazz.m*. Its role is to generate the time domain response of the two-layered cylinder to the multiple frequency excitation. It accomplishes this by summing of modes at each frequency in the approximation of the applied σ_{zz}

B.1 The Function *freqeqn.m*

```
function y=freqeqn(w,k)

% this is the frequency equation for longitudinal modes
% traveling in an transversely isotropic cylinder
% composed of two layers.  The outer layer is layer 1.
% it lies between r=r1 and r=r2.  the inner layer is
% layer 2.  it lies betwwen r=r2 and r=0.
% r1>r2>0
% the elastic constants of each layer are kept in a
% 2-vector with the first entry for layer 1 and the second
% for layer 2.
% the elastic constants are c11, c12, c13, c33 and c44.
% p is the density

%*********************************************************
% initialize variables
%*********************************************************

% these numbers are for Douglas Fir.  The units are meters(m),
% Pascals(Pa) and kilograms/meter^3 (kg/(m^3)).
% the inner layer (layer 2) is chosen with a 40% reduction in
% all the elastic constants.

r1=20e-2;
r2=7e-2;

% layer 1 (outer layer)
c33(1)=6.89e+9;
c11(1)=0.59*c33(1);
c12(1)=0.39*c33(1);
c13(1)=0.035*c33(1);
c44(1)=0.071*c33(1);
p(1)=800;

% layer 2 (inner layer)
```

```
c33(2)=0.6*c33(1);
c11(2)=0.6*0.59*c33(2);
c12(2)=0.6*0.39*c33(2);
c13(2)=0.6*0.035*c33(2);
c44(2)=0.6*0.071*c33(2);
p(2)=p(1);

%*******************************************************
% the frequency equation
%*******************************************************

% first, the radial wavenumbers g1 and g2 in each layer

for j=1:1:2
  A(j)=c11(j)*c44(j)/2;
  B(j)=-c11(j)*(p(j)*w^2-c33(j)*k^2)-c44(j)/2*(p(j)*
w^2-c44(j)/2*k^2)-(c13(j)+c44(j)/2)^2*k^2;
  C(j)=(p(j)*w^2-c33(j)*k^2)*(p(j)*w^2-c44(j)/2*k^2);
  g1(j)=sqrt((-B(j)+sqrt(B(j)^2-4*A(j)*C(j)))/(2*A(j)));
  g2(j)=sqrt((-B(j)-sqrt(B(j)^2-4*A(j)*C(j)))/(2*A(j)));
end

% second, the factors c1 and c2 in each layer

i=sqrt(-1);
for j=1:1:2
  xi1(j)=(p(j)*w^2-c11(j)*g1(j)^2-c44(j)/2*k^2)/(i*k*g1(j)*
(c13(j)+c44(j)/2));
  xi2(j)=(p(j)*w^2-c11(j)*g2(j)^2-c44(j)/2*k^2)/(i*k*g2(j)*
(c13(j)+c44(j)/2));
end

% third, the coeff. matrices

for j=1:1:2
  a1(j)=c11(j)*g1(j)+i*k*c13(j)*g1(j);
```

```
  a2(j)=c11(j)*g2(j)+i*k*c13(j)*g2(j);
  b1(j)=c12(j)-c11(j);
  b2(j)=b1(j);
  c1(j)=c44(j)/2*(i*k-g1(j)*xi1(j));
  c2(j)=c44(j)/2*(i*k-g2(j)*xi2(j));
end


X1out(1,1)=besselj(1,g1(1)*r1);
X1out(1,2)=bessely(1,g1(1)*r1);
X1out(1,3)=besselj(1,g2(1)*r1);
X1out(1,4)=bessely(1,g2(1)*r1);
X1out(2,1)=xi1(1)*besselj(0,g1(1)*r1);
X1out(2,2)=xi1(1)*bessely(0,g1(1)*r1);
X1out(2,3)=xi2(1)*besselj(0,g2(1)*r1);
X1out(2,4)=xi2(1)*bessely(0,g2(1)*r1);
X1out(3,1)=a1(1)*besselj(0,g1(1)*r1)+b1(1)*besselj(1,g1(1)*r1)/r1;
X1out(3,2)=a1(1)*bessely(0,g1(1)*r1)+b1(1)*bessely(1,g1(1)*r1)/r1;
X1out(3,3)=a2(1)*besselj(0,g2(1)*r1)+b2(1)*besselj(1,g2(1)*r1)/r1;
X1out(3,4)=a2(1)*bessely(0,g2(1)*r1)+b2(1)*bessely(1,g2(1)*r1)/r1;
X1out(4,1)=c1(1)*besselj(1,g1(1)*r1);
X1out(4,2)=c1(1)*bessely(1,g1(1)*r1);
X1out(4,3)=c2(1)*besselj(1,g2(1)*r1);
X1out(4,4)=c2(1)*bessely(1,g2(1)*r1);

X1in(1,1)=besselj(1,g1(1)*r2);
X1in(1,2)=bessely(1,g1(1)*r2);
X1in(1,3)=besselj(1,g2(1)*r2);
X1in(1,4)=bessely(1,g2(1)*r2);
X1in(2,1)=xi1(1)*besselj(0,g1(1)*r2);
X1in(2,2)=xi1(1)*bessely(0,g1(1)*r2);
X1in(2,3)=xi2(1)*besselj(0,g2(1)*r2);
X1in(2,4)=xi2(1)*bessely(0,g2(1)*r2);
X1in(3,1)=a1(1)*besselj(0,g1(1)*r2)+b1(1)*besselj(1,g1(1)*r2)/r2;
X1in(3,2)=a1(1)*bessely(0,g1(1)*r2)+b1(1)*bessely(1,g1(1)*r2)/r2;
X1in(3,3)=a2(1)*besselj(0,g2(1)*r2)+b2(1)*besselj(1,g2(1)*r2)/r2;
X1in(3,4)=a2(1)*bessely(0,g2(1)*r2)+b2(1)*bessely(1,g2(1)*r2)/r2;
```

```
X1in(4,1)=c1(1)*besselj(1,g1(1)*r2);
X1in(4,2)=c1(1)*bessely(1,g1(1)*r2);
X1in(4,3)=c2(1)*besselj(1,g2(1)*r2);
X1in(4,4)=c2(1)*bessely(1,g2(1)*r2);

X2out(1,1)=besselj(1,g1(2)*r2);
X2out(1,2)=besselj(1,g2(2)*r2);
X2out(2,1)=xi1(2)*besselj(0,g1(2)*r2);
X2out(2,2)=xi2(2)*besselj(0,g2(2)*r2);
X2out(3,1)=a1(2)*besselj(0,g1(2)*r2)+b1(2)*besselj(1,g1(2)*r2)/r2;
X2out(3,2)=a2(2)*besselj(0,g2(2)*r2)+b2(2)*besselj(1,g2(2)*r2)/r2;
X2out(4,1)=c1(2)*besselj(1,g1(2)*r2);
X2out(4,2)=c2(2)*besselj(1,g2(2)*r2);

% the global transfer matrix and frequency eqn.
% this is actually a 4x2 matrix, but the 3rd and 4th
% equations are homogeneous, so their determinant is
% set to zero for the frequency eqn.

Q=X1out*inv(X1in)*X2out;



y=Q(3,1)*Q(4,2)-Q(3,2)*Q(4,1);

%*********************************************************
% end of function
%*********************************************************
```

B.2 The Script *inputapprox.m*

```
% this m-file will produce a finite frequency approximation
% of the time domain data contained in the file chopdata.

%***************load time domain data**********************

load chopdata2
```

```
%************************************************************

%***************assign program parameters*****************

numint=length(ts);
T=ts(numint);
fundw=pi/(T);
numfreq=40;
delt=T/numint;

%************************************************************

%*****************initialize coefficients****************

for j=1:1:numfreq
   c(j)=0;
end
constantterm=0;

%************************************************************

%************************************************************
% MAIN PROGRAM
%************************************************************

i=sqrt(-1);
for j=1:1:numint
   volt=frontvolts(j);
   t=ts(j);
   constantterm=constantterm+1/(2*T)*volt;
   for m=1:1:numfreq
      c(m)=c(m)+1/(2*T)*(volt*exp(i*m*fundw*t));
   end
end
```

```
for j=1:1:numint
   approx=0;
   t=ts(j);
   for m=1:1:numfreq
      approx=approx+c(m)*exp(-i*m*fundw*t);
   end
   nearsig(j)=approx;
end

normaliser=max(real(nearsig));
coeffs=c./normaliser;
for n=1:1:numfreq
   ws(n)=fundw*n;
end

%******************End Main Program*************************

%****************************************************************
% Produce Output
%****************************************************************
save chopfreqdata2 coeffs ws

maxvolts=max(frontvolts);
minvolts=min(frontvolts);
tinit=0;
tfinal=ts(numint);

subplot(2,2,1)
   plot(ts,frontvolts)
   axis([tinit tfinal minvolts-0.1 maxvolts+0.2])
   title('Time Domain Signal')
subplot(2,2,2)
   plot(ts, real(nearsig./normaliser)+real(constantterm)/(2*normaliser))
   axis([tinit tfinal minvolts-0.1 maxvolts+0.2])
   title('Signal Approximation')
subplot(2,2,3)
   stem(ws,abs(c)./normaliser)
```

```
   title('Complex Modulus of Coefficients')
   xlabel('\omega')
   axis([0 max(ws) 0 max(abs(c))/normaliser+0.02])
subplot(2,2,4)
   stem(ws,angle(c))
   title('Phase Angle of Coefficients')
   xlabel('\omega')
   axis([0 max(ws) -pi-0.1  pi+0.1])

figure
plot(ts, frontvolts, ts, real(nearsig./normaliser)+real(constantterm)/
(2*normaliser))

%*****************************************************************
% END OF SCRIPT
%*****************************************************************
```

B.3 The Script *sigmazz.m*

```
% this script will produce the time domain response
% of a two-layered transversely isotropic cylinder
% to a multiple frequency excitation.
% the material properties of the specimen are in the
% function freqeqn.m


%*********************************************************
%          USER INPUTS
%*********************************************************

r=10e-2;
z=293e-2;

%*********************************************************
%  MATERIAL INFO.  SAME AS IN freqeqn.m
```

```
%*********************************************************

% these numbers are for Ponderosa Pine.  The units are meters(m),
% Pascals(Pa) and kilograms/meter^3 (kg/(m^3)).
% the inner layer (layer 2) is chosen with a reduction in
% all the elastic constants.

r1=10e-2;
r2=3e-2;

% layer 1 (outer layer)
%c33(1)=5e+9; bad try
c33(1)=8.89e+9;
c11(1)=0.476*c33(1);
c12(1)=0.393*c33(1);
c13(1)=0.369*c33(1);
c44(1)=0.064*c33(1);
%p(1)=650; bad try
p(1)=448;

% layer 2 (inner layer)

reduxfactor=0.40;
c33(2)=(1-reduxfactor)*c33(1);
c11(2)=(1-reduxfactor)*c11(1);
c12(2)=(1-reduxfactor)*c12(1);
c13(2)=(1-reduxfactor)*c13(1);
c44(2)=(1-reduxfactor)*c44(1);
p(2)=p(1);


%*********************************************************
% load the frequency/wavenumber data
% load the frequency approx. data
%*********************************************************

load dispersiondata
```

```
load chopdata2
load chopfreqdata2

%*********************************************************
% set up solution vector
%*********************************************************

condtol=5e+16;
endtime=ts(length(ts))*1;
dt=endtime/length(ts);
time=[dt:dt:endtime];

for j=1:1:length(time)
   press(j)=0;
end

%*********************************************************
%  BEGIN MAIN LOOP OVER w
%*********************************************************

for n=1:1:length(ws)
   w=ws(n)

%*********************************************************
% Determine the k's associated with w
%*********************************************************

if w<newdatw(1)

   % if w is too low for dispersion data, then interpolate
   % k from an average of the non-dispersive mode
   temp=0;
   for j=1:1:10
      temp=temp+w*newdatk(j)/newdatw(j);
   end
   ks(1)=temp/10;
else
```

```
ktol=0.1;
clear wcounter
wcounter=1;
while w-newdatw(wcounter)>0
   wcounter=wcounter+1;
end
clear kcounter
kcounter=1;
while abs(w-newdatw(wcounter))<=dw
   firstks(kcounter)=newdatk(wcounter);
   wcounter=wcounter+1;
   kcounter=kcounter+1;
end

% Keep only the k's that correspond to a wave
% propagating to the right.

counter=1;
for j=1:1:length(firstks)
   if firstks(j)>0
      secondks(counter)=firstks(j);
      counter=counter+1;
   end
end

%Eliminate repeat k's

secondks=sort(secondks);
ks(1)=secondks(1);
counter=1;
for j=2:1:length(secondks)
   if abs(secondks(j)-ks(counter))>ktol
      ks(counter+1)=secondks(j);
      counter=counter+1
   end
end
```

```
   % put in order according to mode
   for j=1:1:length(ks)
      finalks(j)=ks(length(ks)-j+1);
   end
   ks=finalks;
end

%*********************************************************
% Determine the gamma's (radial wavenumbers)
%*********************************************************

% g1(l,j) is gamma1 in layer l corresponding to k=ks(j)
% g2(l,j) is gamma2 in layer l corresponding to k=ks(j)

i=sqrt(-1);
for l=1:1:2
   C11=c11(l);
   C12=c12(l);
   C13=c13(l);
   C33=c33(l);
   C44=c44(l);
   P=p(l);
   for j=1:1:length(ks)
    k=ks(j);
    A=C11*C44/2;
    B=-C11*(P*w^2-C33*k^2)-C44/2*(P*w^2-C44/2*k^2)-(C13+C44/2)^2*k^2;
    C=(P*w^2-C33*k^2)*(P*w^2-C44/2*k^2);
    g1(l,j)=sqrt((-B+sqrt(B^2-4*A*C))/(2*A));
    g2(l,j)=sqrt((-B-sqrt(B^2-4*A*C))/(2*A));
  end
end
%*********************************************************
% Determine the xi's
%*********************************************************

% xi1(l,j) is xi1 in layer l corresponding to k=ks(j)
% xi2(l,j) is xi2 in layer l corresponding to k=ks(j)
```

```
i=sqrt(-1);
for l=1:1:2
   C11=c11(l);
   C13=c13(l);
   C33=c33(l);
   C44=c44(l);
   P=p(l);
   for j=1:1:length(ks)
      k=ks(j);
      G1=g1(l,j);
      G2=g2(l,j);
      xi1(l,j)=(P*w^2-C11*G1^2-C44/2*k^2)/(i*k*G1*(C13+C44/2));
      xi2(l,j)=(P*w^2-C11*G2^2-C44/2*k^2)/(i*k*G2*(C13+C44/2));
  end
end

%*********************************************************
% Determine the A's (the coefficients)
%*********************************************************

% there are 4 matrices with the coefficients in them.
% A1(l,j) contains A1 of layer l corresponding to k=ks(j)
% A1bar(l,j) contains A1bar of layer l corresponding to k=ks(j)
% A2(l,j) contains A2 of layer l corresponding to k=ks(j)
% A2bar(l,j) contains A2bar of layer l corresponding to k=ks(j)

  numint=50;
  i=sqrt(-1);

% in layer 1 (outer layer)

dr1=(r1-r2)/numint;
dr2=r2/numint;
K=length(ks);
S=zeros(6*K,6*K);
F1=zeros(1,6*K);
```

```
F2=zeros(1,6*K);
D1=zeros(2,K);
D2=zeros(2,K);
for j=1:1:K
   k=ks(j);
   for l=1:1:2
      C13=c13(l);
      C33=c33(l);
      G1=g1(l,j);
      G2=g2(l,j);
      XI1=xi1(l,j);
      XI2=xi2(l,j);
      D1(l,j)=C13*G1+i*k*C33*XI1;
      D2(l,j)=C13*G2+i*k*C33*XI2;
   end
end

% the right hand side vector

for R=1:1:K
   for j=1:1:numint
      R1=r2+j*dr1;
      F1(R)=F1(R)+f(n,R1)*besselj(0,g1(1,R)*R1);
      F1(K+R)=F1(K+R)+f(n,R1)*bessely(0,g1(1,R)*R1);
      F1(2*K+R)=F1(2*K+R)+f(n,R1)*besselj(0,g2(1,R)*R1);
      F1(3*K+R)=F1(3*K+R)+f(n,R1)*bessely(0,g2(1,R)*R1);
      F1(4*K+R)=F1(4*K+R)+f(n,R1)*besselj(0,g1(2,R)*R1);
      F1(5*K+R)=F1(5*K+R)+f(n,R1)*besselj(0,g2(2,R)*R1);

      R2=j*dr2;
      F2(R)=F2(R)+f(n,R2)*besselj(0,g1(1,R)*R2);
      F2(K+R)=F2(K+R)+f(n,R2)*bessely(0,g1(1,R)*R2);
      F2(2*K+R)=F2(2*K+R)+f(n,R2)*besselj(0,g2(1,R)*R2);
      F2(3*K+R)=F2(3*K+R)+f(n,R2)*bessely(0,g2(1,R)*R2);
      F2(4*K+R)=F2(4*K+R)+f(n,R2)*besselj(0,g1(2,R)*R2);
      F2(5*K+R)=F2(5*K+R)+f(n,R2)*besselj(0,g2(2,R)*R2);
   end
```

```
end

F=F1+F2;

% the coefficient matrix

for R=1:1:K
   for C=1:1:K
      for j=1:1:numint
         R1=r2+j*dr1;
         S(R,C)=S(R,C)+D1(1,C)*besselj(0,g1(1,C)*R1)*
besselj(0,g1(1,R)*R1);
         S(R+K,C)=S(R+K,C)+D1(1,C)*besselj(0,g1(1,C)*R1)*
bessely(0,g1(1,R)*R1);
         S(R+2*K,C)=S(R+2*K,C)+D1(1,C)*besselj(0,g1(1,C)*R1)*
besselj(0,g2(1,R)*R1);
         S(R+3*K,C)=S(R+3*K,C)+D1(1,C)*besselj(0,g1(1,C)*R1)*
bessely(0,g2(1,R)*R1);
         S(R+4*K,C)=S(R+4*K,C)+D1(1,C)*besselj(0,g1(1,C)*R1)*
besselj(0,g1(2,R)*R1);
         S(R+5*K,C)=S(R+5*K,C)+D1(1,C)*besselj(0,g1(1,C)*R1)*
besselj(0,g2(2,R)*R1);

         S(R,C+K)=S(R,C+K)+D1(1,C)*bessely(0,g1(1,C)*R1)*
besselj(0,g1(1,R)*R1);
         S(R+K,C+K)=S(R+K,C+K)+D1(1,C)*bessely(0,g1(1,C)*R1)*
bessely(0,g1(1,R)*R1);
         S(R+2*K,C+K)=S(R+2*K,C+K)+D1(1,C)*bessely(0,g1(1,C)*R1)*
besselj(0,g2(1,R)*R1);
         S(R+3*K,C+K)=S(R+3*K,C+K)+D1(1,C)*bessely(0,g1(1,C)*R1)*
bessely(0,g2(1,R)*R1);
         S(R+4*K,C+K)=S(R+4*K,C+K)+D1(1,C)*bessely(0,g1(1,C)*R1)*
besselj(0,g1(2,R)*R1);
         S(R+5*K,C+K)=S(R+5*K,C+K)+D1(1,C)*bessely(0,g1(1,C)*R1)*
besselj(0,g2(2,R)*R1);

         S(R,C+2*K)=S(R,C+2*K)+D2(1,C)*besselj(0,g2(1,C)*R1)*
```

```
besselj(0,g1(1,R)*R1);
        S(R+K,C+2*K)=S(R+K,C+2*K)+D2(1,C)*besselj(0,g2(1,C)*R1)*
bessely(0,g1(1,R)*R1);
        S(R+2*K,C+2*K)=S(R+2*K,C+2*K)+D2(1,C)*besselj(0,g2(1,C)*R1)*
besselj(0,g2(1,R)*R1);
        S(R+3*K,C+2*K)=S(R+3*K,C+2*K)+D2(1,C)*besselj(0,g2(1,C)*R1)*
bessely(0,g2(1,R)*R1);
        S(R+4*K,C+2*K)=S(R+4*K,C+2*K)+D2(1,C)*besselj(0,g2(1,C)*R1)*
besselj(0,g1(2,R)*R1);
        S(R+5*K,C+2*K)=S(R+5*K,C+2*K)+D2(1,C)*besselj(0,g2(1,C)*R1)*
besselj(0,g2(2,R)*R1);

        S(R,C+3*K)=S(R,C+3*K)+D2(1,C)*bessely(0,g2(1,C)*R1)*
besselj(0,g1(1,R)*R1);
        S(R+K,C+3*K)=S(R+K,C+3*K)+D2(1,C)*bessely(0,g2(1,C)*R1)*
bessely(0,g1(1,R)*R1);
        S(R+2*K,C+3*K)=S(R+2*K,C+3*K)+D2(1,C)*bessely(0,g2(1,C)*R1)*
besselj(0,g2(1,R)*R1);
        S(R+3*K,C+3*K)=S(R+3*K,C+3*K)+D2(1,C)*bessely(0,g2(1,C)*R1)*
bessely(0,g2(1,R)*R1);
        S(R+4*K,C+3*K)=S(R+4*K,C+3*K)+D2(1,C)*bessely(0,g2(1,C)*R1)*
besselj(0,g1(2,R)*R1);
        S(R+5*K,C+3*K)=S(R+5*K,C+3*K)+D2(1,C)*bessely(0,g2(1,C)*R1)*
besselj(0,g2(2,R)*R1);

        R2=j*dr2;
        S(R,C+4*K)=S(R,C+4*K)+D1(2,C)*besselj(0,g1(2,C)*R2)*
besselj(0,g1(1,R)*R2);
        S(R+K,C+4*K)=S(R+K,C+4*K)+D1(2,C)*besselj(0,g1(2,C)*R2)*
bessely(0,g1(1,R)*R2);
        S(R+2*K,C+4*K)=S(R+2*K,C+4*K)+D1(2,C)*besselj(0,g1(2,C)*R2)*
besselj(0,g2(1,R)*R2);
        S(R+3*K,C+4*K)=S(R+3*K,C+4*K)+D1(2,C)*besselj(0,g1(2,C)*R2)*
bessely(0,g2(1,R)*R2);
        S(R+4*K,C+4*K)=S(R+4*K,C+4*K)+D1(2,C)*besselj(0,g1(2,C)*R2)*
besselj(0,g1(2,R)*R2);
        S(R+5*K,C+4*K)=S(R+5*K,C+4*K)+D1(2,C)*besselj(0,g1(2,C)*R2)*
```

```
besselj(0,g2(2,R)*R2);

        S(R,C+5*K)=S(R,C+5*K)+D2(2,C)*besselj(0,g2(2,C)*R2)*
besselj(0,g1(1,R)*R2);
        S(R+K,C+5*K)=S(R+K,C+5*K)+D2(2,C)*besselj(0,g2(2,C)*R2)*
bessely(0,g1(1,R)*R2);
        S(R+2*K,C+5*K)=S(R+2*K,C+5*K)+D2(2,C)*besselj(0,g2(2,C)*R2)*
besselj(0,g2(1,R)*R2);
        S(R+3*K,C+5*K)=S(R+3*K,C+5*K)+D2(2,C)*besselj(0,g2(2,C)*R2)*
bessely(0,g2(1,R)*R2);
        S(R+4*K,C+5*K)=S(R+4*K,C+5*K)+D2(2,C)*besselj(0,g2(2,C)*R2)*
besselj(0,g1(2,R)*R2);
        S(R+5*K,C+5*K)=S(R+5*K,C+5*K)+D2(2,C)*besselj(0,g2(2,C)*R2)*
besselj(0,g2(2,R)*R2);
      end
   end
end

condition(n)=condest(S);

if condition(n)<condtol
   % solve the system

   A=S\F';
   freqnum=n
   for j=1:1:K
      A1(1,j)=A(j);
      A1bar(1,j)=A(K+j);
      A2(1,j)=A(2*K+j);
      A2bar(1,j)=A(3*K+j);
      A1(2,j)=A(4*K+j);
      A1bar(2,j)=0;
      A2(2,j)=A(5*K+j);
      A2bar(2,j)=0;
   end

   % add to sigmazz
```

```
   for j=1:1:length(time)
      wpress(j)=0;
   end
   for m=1:1:K
      k=ks(m);
      G1=g1(1,m);
      G2=g2(1,m);
      XI1=xi1(1,m);
      XI2=xi2(1,m);
      arrivetime=z*k/w;
      for j=1:1:length(time)
         t=time(j);
         if t>arrivetime & t<arrivetime+ts(length(ts))

            C13=c13(1);
            C33=c33(1);

            p1=(C13*G1+i*K*C33*XI1)*besselj(0,G1*r)*A1(1,m);
            p2=(C13*G1+i*K*C33*XI1)*bessely(0,G1*r)*A1bar(1,m);
            p3=(C13*G2+i*K*C33*XI2)*besselj(0,G2*r)*A2(1,m);
            p4=(C13*G2+i*K*C33*XI2)*bessely(0,G2*r)*A2bar(1,m);
            p5=exp(i*k*z)*exp(-i*w*t);

            wpress(j)=wpress(j)+real((p1+p2+p3+p4)*p5);
         end
      end
   end

   press=press+wpress;
end
%*************************************************
% END MAIN LOOP OVER w
%*************************************************

end
```

```
%*************************************************
% Produce output
%*************************************************

% normalize sigmazz

normalizer=max(abs(press));
normpress=press./normalizer;

figure
plot(time, normpress, ts, endvolts)
figure
plot(ws,condition)
%*************************************************
% end of script
%*************************************************
```

Appendix C

MULTIPLE FREQUENCY EXAMPLE

The single frequency input and response model is insufficient for most applications. Most inputs will, in general, be the superposition of an infinite number of harmonic stresses. These can be approximated within an arbitrary accuracy by the sum of a finite number of frequenies. This is the approach used here.

In the shell example, section 4.5, the input was assumed to be at a single frequency, ω. At this frequency, K modes were found to propagate and these modes were used to approximate the input, σ_{zz}.

$$\sigma_{zz}\,|_{z=0} = \sum_{j=1}^{K} \sigma_{zz}(r, 0, t; k_{(j)}) \tag{C.1}$$

Taking advantage of the linearity of the model, multiple frequencies can be considered by summing over the response to each frequency. If the multiple

frequency approximation contains the frequencies $\{\omega_1, \omega_2, \ldots, \omega_N\}$, then the approximation of the input takes the form

$$\sigma_{zz}\,|_{z=0} = \sum_{m=1}^{N}\sum_{j=1}^{K} \sigma_{zz}(r, 0, t; k_{(j)}, \omega_m), \qquad \text{(C.2)}$$

where the response to each individual frequency is treated exactly as before and the sum of all these responses is considered the response to the multiple frequency input.

This method, superposition of propagating modes at a single frequency then superposition of frequencies will be employed to compare the theoretical response of this model to the response actually observed in a SDT experiment.

C.1 SDT Experiment

This section is intended to describe the experiment from which data was taken to compare with the results obtained by the method developed in this chapter. Figure C.1 is a diagram of the experimental setup.

In the experiment a SDT sample was subject to an excitation from a hammer strike on one end. The elastic waves produced were measured at two points on the surface of the sample. One was made 100mm from the end where the hammer struck. This measurement is intended ot record the incident wave. The second measurement was made 1250mm from the opposite end of the sample. This measurement was to record the propagating wave before a reflection off the end could interfere.

The measurements were made by two single axis pinducer DC -12.MHz

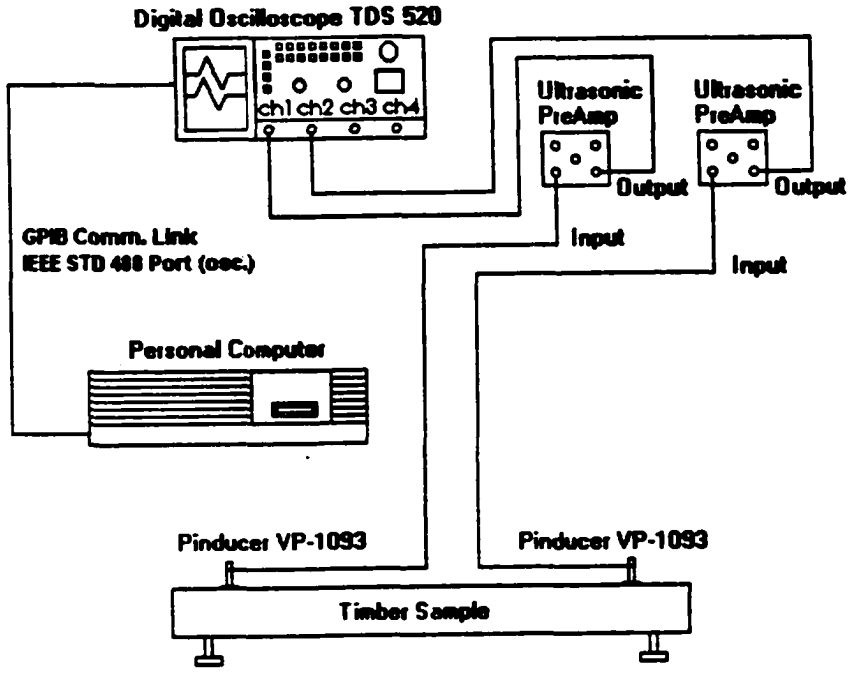

Figure C.1: Diagram of SDT experiment

(-3dB) model VP-1093 (Vapley-Fisher, Hopkinton, MA.) ultrasonic transducers with a sensitivity of 50 dB relative to 1 volt/meter/sec. These transducers were attached to the SDT sample by gluing them to a lag bolt drilled into the sample. The data was taken from the transducers with a TDS 520A digital oscilloscope at a rate of 250 kHz.

C.2 Results

The first step in implementing the model is to convert the experimental input into a form that can be written as a sum of single frequency inputs. This sum will necessarily be an approximation since an infinite number of frequencies are present in the real input. The Matlab script *inputapprox.m*, in Appendix B, was used to find this approximation. The script was run to produce a 40 frequency approximation. The results of this approximation are plotted in Fig. C.2 along with the signal being approximated.

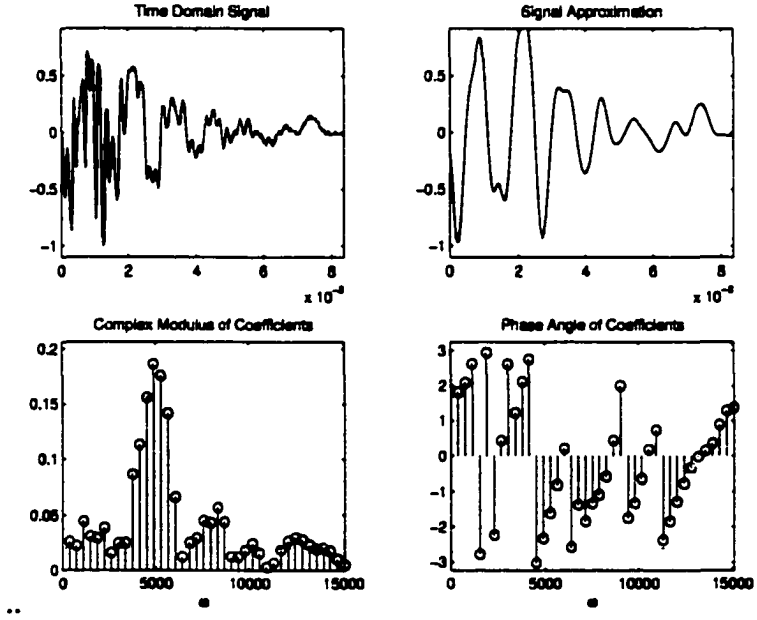

Figure C.2: The measured input and information about the finite frequency approximation.

From this graphical representation of the data it is clear that frequencies

centered around $\omega = 5$ kHz contribute the most to the signal. Figure C.3 is a plot of the experimental signal and the 40 frequency approximation on the same axes.

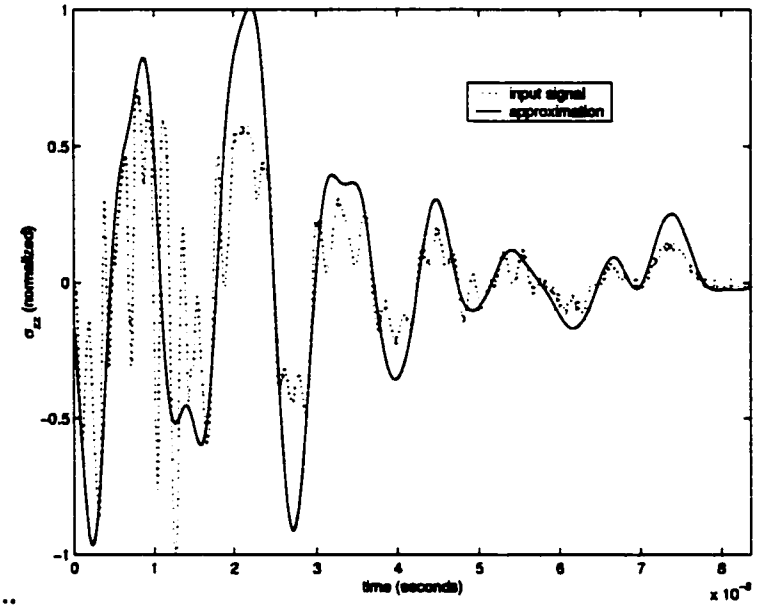

Figure C.3: The measured input and finite frequency approximation.

The information contained in this approximation is implemented in the model in the following way. For each frequency considered, a complex coefficient, B_m, was found that represents the magnitude and phase of the frequency in the approximation. Therefore, at $z = 0$ the normal stress was approximated by

$$\sigma_{zz} \mid_{z=0} \approx \sum_{m=1}^{40} B_m e^{-i\omega_m t}. \tag{C.3}$$

the Matlab script *dispcurves.m*, in Appendix A, along with the function *freqeqn.m*, in Appendix B. Figure C.4 contains the output from these programs. Compared with the previous example, very few modes propagate in the experimental model at the frequencies being considered. This is mostly because the experimental model is considerably thinner, i.e. r^1 for the sample in the experiment is much smaller that r^1 in the previous example.

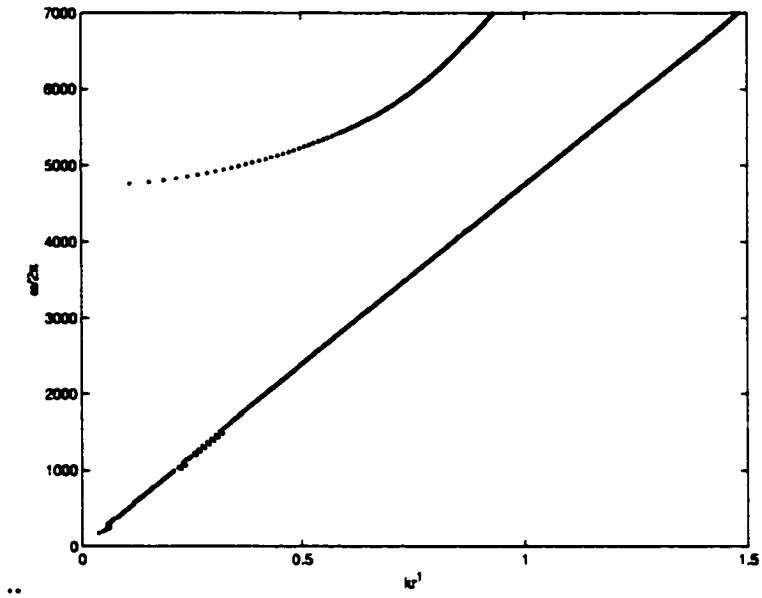

Figure C.4: Dispersion curves for experiment.

For most of the frequencies included in the model the SDT being considered will respond as a single mode waveguide. Only at the highest frequencies considered is a second mode present.

The time domain response of the model is constructed using the matlab script *sigmazz.m*, in Appendix B. The results are plotted in Fig. C.5 with

the experimental measurements.

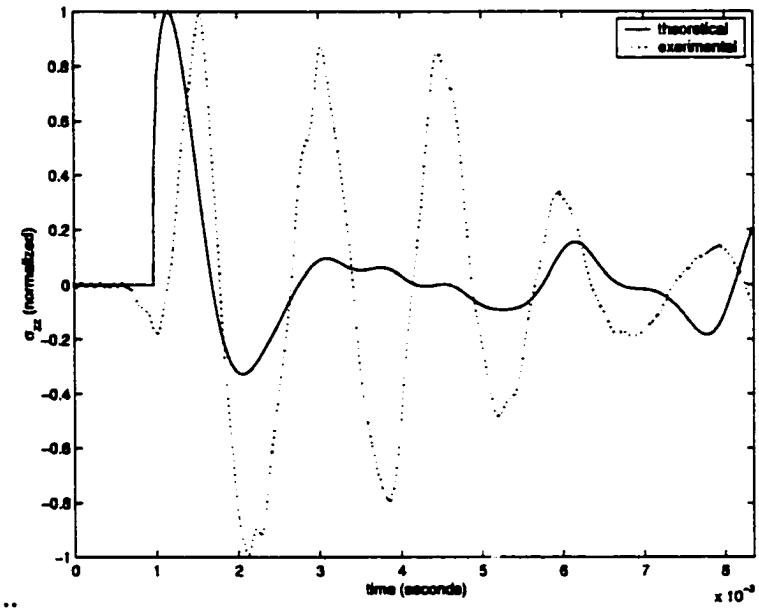

Figure C.5: Theoretical and experimental responses.

The theoretical model predicts the arrival of the wave at the correct time and the initial shape fairly accurately. The shape of the experimental and theoretical waves differ considerably afterwards.